

AN INVESTIGATION INTO RELIABILITY BASED METHODS TO INCLUDE RISK OF FAILURE IN LIFE CYCLE COST ANALYSIS OF REINFORCED CONCRETE BRIDGE REHABILITATION

A thesis submitted in fulfillment of the requirements
for the degree of Master of Engineering

Weiqi Zhu

**School of Civil, Environmental and Chemical Engineering
Science, Engineering and Technology Portfolio
RMIT University
July, 2008**

DECLARATION

I certify that except where due acknowledgement has been made, this work is that of myself alone. The content of the thesis is the result of work that has been carried out since the official commencement date of the approved research program under the supervision of Associate Professor Sujeeva Setunge of the School of Civil, Environmental and Chemical Engineering, RMIT. This work has not been submitted previously, in whole or part, to qualify for any other academic award. Any editorial work, paid or unpaid, carried out by a third party is acknowledged.

Name: Weiqi Zhu

Sign:

Date:

ABSTRACT

Reliability based life cycle cost analysis is becoming an important consideration for decision-making in relation to bridge design, maintenance and rehabilitation. An optimal solution should ensure reliability during service life while minimizing the life cycle cost. Risk of failure is an important component in whole of life cycle cost for both new and existing structures.

Research work presented here aimed to develop a methodology for evaluation of the risk of failure of reinforced concrete bridges to assist in decision making on rehabilitation. Methodology proposed here combines fault tree analysis and probabilistic time-dependent reliability analysis to achieve qualitative and quantitative assessment of the risk of failure. Various uncertainties are considered including the degradation of resistance due to initiation of a particular distress mechanism, increasing load effects, changes in resistance as a result of rehabilitation, environmental variables, material properties and model errors. It was shown that the proposed methodology has the ability to provide users two alternative approaches for qualitative or quantitative assessment of the risk of failure depending on availability of detailed data. This work will assist the managers of bridge infrastructures in making decisions in relation to optimization of rehabilitation options for aging bridges.

ACKNOWLEDGEMENT

First of all, I would like to express my deep sense of appreciation to my supervisor Associate Professor Sujeeva Setunge for her consistent support and warm-hearted guidance for my research. This work would not have been completed without her patience and understanding.

I would like to extend my gratitude to CRC research team comprising of QDMR, BCC, RMIT and QUT. Thanks in particular to Dr. Rebecca Gravina and Dr. Srikanth Venkatesan, who helped me kindly during several stages of this research. QDMR is greatly appreciated for providing data and materials for case study of this research.

Finally a special thanks goes to my parents, who have given sustainable financial support and great encouragement to ensure the completion of my research.

LIST OF PUBLICATIONS

Zhu, W, Setunge, S, Gravina, R & Venkatsan, S (2007), 'Use of fault tree analysis in risk assessment of reinforced concrete bridges exposed to aggressive environments', in *Proceedings of the 4th International Structural Engineering and Construction Conference*, Melbourne, pp. 387-393.

Zhu, W, Setunge, S, Gravina, R & Venkatsan, S (2007), 'Use of fault tree analysis in risk assessment of reinforced concrete bridges exposed to aggressive environments', *Concrete in Australia*, vol. 34, no. 1, pp. 50-54.

Zhu, W, Setunge, S, Gravina, R & Venkatsan, S (2008), 'Estimation of residual capacity and time-dependent reliability of reinforced concrete bridges after initiation of a deterioration mechanism and subsequent rehabilitation', *Australian Structural Engineering Conference*. Melbourne (Accepted for publication).

TABLE OF CONTENT

ABSTRACT	III
ACKNOWLEDGEMENT	IV
LIST OF FIGURES.....	X
LIST OF TABLES.....	XIV
CHAPTER 1 INTRODUCTION.....	1
1.1 STATEMENT OF THE PROBLEM.....	1
1.2 RESEARCH OBJECTIVES	3
1.3 THESIS OUTLINE	4
CHAPTER 2 LITERATURE REVIEW	7
2.1 PERFORMANCE ASSESSMENT AND DETERIORATION MODELING	7
2.1.1 <i>Time-dependent reliability analysis</i>	7
2.1.2 <i>Markov chain deterioration model</i>	11
2.1.3 <i>Deterioration modeling based on fault tree analysis</i>	13
2.2 RISK ASSESSMENT	16
2.3 CONCLUSION	19
CHAPTER 3 QUALITATIVE RISK ASSESSMENT OF REINFORCED CONCRETE BRIDGES USING FAULT TREE ANALYSIS	22
3.1 INTRODUCTION.....	22
3.2 FAULT TREE MODEL	24
3.2.1 <i>Overall fault tree frame</i>	25
3.2.2 <i>Major sub-tree: deterioration of pier</i>	27
3.2.2.1 Identification of failure modes	27

3.2.2.2 Fault tree decomposition of major failure modes	30
3.2.2.2.1 Plastic shrinkage	31
3.2.2.2.2 Carbonation	32
3.2.2.2.3 Alkali-silica reaction.....	33
3.2.2.2.4 Chloride induced corrosion.....	35
3.3 RISK ASSESSMENT USING FAULT TREE MODEL.....	36
3.3.1 Input likelihood ratings.....	36
3.3.2 Input consequence ratings	38
3.3.3 Fault tree calculation.....	39
3.3.4 Output risk ratings.....	42
3.4 CASE STUDY	43
3.4.1 Case description	43
3.4.2 Inputs	43
3.4.3 Results.....	46
3.4.4 Sensitivity analysis.....	46
3.5 CONCLUSION	49

CHAPTER 4 PROBABILISTIC TIME-DEPENDENT RELIABILITY ANALYSIS OF DETERIORATED REINFORCED CONCRETE BRIDGE COMPONENTS50

4.1 INTRODUCTION.....	50
4.2 PROBABILISTIC ANALYSIS OF TIME-DEPENDENT RESISTANCE.....	52
4.2.1 Chloride induced corrosion	53
4.2.1.1 Chloride concentration.....	53
4.2.1.1.1 Surface chloride concentration-- C_o	54
4.2.1.1.2 Diffusion coefficient-- D	56
4.2.1.1.3 Critical chloride concentration-- C_{cr}	57
4.2.1.1.4 Comparison of chloride concentration	58
4.2.1.1.5 Probabilistic modeling of distribution of corrosion initiation time	60
4.2.1.2 Corrosion propagation.....	66
4.2.1.2.1 Area loss of steel reinforcement.....	69
4.2.1.2.2 Comparison of area loss.....	72
4.2.1.2.3 Probabilistic modeling of area loss	74

4.2.2 Resistance degradation.....	79
4.3 TIME-DEPENDENT STRUCTURAL RELIABILITY	81
4.3.1 Time-dependent live load model	81
4.3.2 Probability of failure and reliability index.....	82
4.3.3 Service life prediction	83
4.4 ILLUSTRATIVE EXAMPLE.....	83
4.4.1 Example description	83
4.4.2 Structural resistance	86
4.4.3 Structural reliabilities.....	87
4.4.3.1 Basic results	87
4.4.3.2 Comparative results	89
4.4.4 Analysis of rehabilitation options	93
4.5 CONCLUSION	95
CHAPTER 5 LIFE CYCLE COST ANALYSIS AND INTEGRATION MODEL.....	96
5.1 LIFE CYCLE COST ANALYSIS.....	97
5.1.1 Modeling of the initial cost.....	98
5.1.2 Modeling of the maintenance (repair) cost.....	99
5.1.3 Modeling of user cost.....	100
5.1.4 Modeling of expected failure costs.....	100
5.2 AN INTEGRATED MODEL	101
5.2.1 VOTING gate model	102
5.2.2 Integration	106
5.3 ILLUSTRATIVE EXAMPLE.....	107
5.4 CONCLUSION	111
CHAPTER 6 CONCLUSION AND RECOMMENDATIONS	113
6.1 CONCLUSION	113
6.1.1 Qualitative risk assessment based on fault tree analysis	113
6.1.2 Probabilistic time-dependent reliability analysis.....	115
6.1.3 Life cycle cost analysis and integrated model	117
6.1.4 Summary	118

6.2 RECOMMENDATIONS.....	119
REFERENCES.....	121
APPENDIX A SPECIFIC RULES FOR ASSIGN LIKELIHOOD RATINGS.....	127
APPENDIX B MODELING CORROSION INITIATION TIME.....	131
APPENDIX C MODELING TIME-DEPENDENT AREA LOSS OF A STEEL BAR.....	133
APPENDIX D ILLUSTRATIVE EXAMPLE CALCULATION OF TIME-DEPENDENT RELIABILITY ANALYSIS.....	139

LIST OF FIGURES

Figure 2.1	Effect of mean critical chloride concentration on corrosion initiation time.....	9
Figure 2.2	Time-dependent cumulative probabilities of failure for de-icing salts and no deterioration.	10
Figure 2.3	Main fault tree diagram for scour and channel instability at bridges.....	14
Figure 2.4	Top-level fault tree for accelerated concrete deck deterioration.	14
Figure 2.5	Generic representation of the flow of risk-based decision analysis.	17
Figure 3.1	General process of using fault tree analysis in risk assessment.	23
Figure 3.2	Typical fault tree used in risk assessment.	23
Figure 3.3	Top level fault tree frame.....	26
Figure 3.4	Major sub-system fault tree of piers deterioration.	27
Figure 3.5	Secondary sub-system fault tree of headstocks deterioration.	29
Figure 3.6	Secondary sub-system fault tree of columns deterioration.	29
Figure 3.7	Secondary sub-system fault tree of pilecaps deterioration.....	30
Figure 3.8	Secondary sub-system fault tree of piles deterioration.	30
Figure 3.9	Fault tree of plastic shrinkage.....	31
Figure 3.10	Fault tree of carbonation.	33
Figure 3.11	Fault tree of Alkali-silica reaction.	34
Figure 3.12	Fault tree of chloride induced corrosion	35
Figure 3.13	Example of calculation of the probability of top event of plastic shrinkage.....	40
Figure 3.14	Example of calculation of the probability of top event of ASR on piles.....	41
Figure 3.15	Munna Point bridge.....	44
Figure 3.16	Cracks observed on pilecaps	44
Figure 3.17	Cracks observed on piles.	45

Figure 3.18 Result of risk ratings of case piles and pilecaps.....	47
Figure 3.19 General procedure of using fault tree analysis on qualitative risk assessment of reinforced concrete bridges.	48
Figure 4.1 Realizations of time-dependent resistance and time various load effects.	51
Figure 4.2 Management process of structural assessment and decision making.....	52
Figure 4.3 Chloride concentrations at a depth 50mm from the surface for ordinary concrete mix.	59
Figure 4.4 Chloride concentrations at a depth 50mm from the surface for coastal zone structures.	59
Figure 4.5 Probability density function fit of corrosion initiation time of RC elements located 50m from coast with ordinary concrete mix ($w/c=0.55$) and concrete cover depth $x=50$ mm.	62
Figure 4.6 Probability density function of corrosion initiation time of de-icing salts affected RC elements with ordinary concrete mix ($w/c=0.55$).	62
Figure 4.7 Probability density function of corrosion initiation time of de-icing salts affected RC elements with cover depth $x=50$ mm.	63
Figure 4.8 Probability density function of corrosion initiation time of onshore splash zone RC elements with ordinary concrete mix ($w/c=0.55$).	63
Figure 4.9 Probability density function of corrosion initiation time of onshore splash zone RC elements with cover depth $x=50$ mm.	64
Figure 4.10 Probability density function of corrosion initiation time of RC elements located 50m from coast with ordinary concrete mix ($w/c=0.55$).	64
Figure 4.11 Probability density function of corrosion initiation time of RC elements located 50m from coast with cover depth $x=50$ mm.	65
Figure 4.12 Effect of coefficient of variation of surface chloride concentration $COV(C_0)$ on distribution of corrosion initiation time.....	65
Figure 4.13 Influence of water-cement ratio and cover on initial corrosion current.	67
Figure 4.14 Reduction of corrosion current over time.	67
Figure 4.15 Area loss function comparison of different corrosion types for the sample steel bar..	72

Figure 4.16 Area loss function comparison of different quality of concrete with cover=50mm.	73
Figure 4.17 Area loss function comparison of different concrete cover depth with ordinary quality of concrete.	73
Figure 4.18 Histogram of residual area of steel reinforcement of the sample structural component after 50 years exposure under general corrosion.	75
Figure 4.19 Histogram of residual area of steel reinforcement of the sample structural component after 50 years exposure under localized corrosion.	76
Figure 4.20 Histogram of residual area of steel reinforcement of the sample structural component after 50 years exposure under combination corrosion.	76
Figure 4.21 Probability density function of residual area of steel reinforcement of the sample structural component under general corrosion.	77
Figure 4.22 Probability density function of residual area of steel reinforcement of the sample structural component under localized corrosion.	77
Figure 4.23 Probability density function of residual area of steel reinforcement of the sample structural component under localized corrosion.	78
Figure 4.24 Histogram of residual area of steel reinforcement of the sample structural component after 10 years corrosion.	78
Figure 4.25 General description of changes of resistance of rehabilitated structure.	80
Figure 4.26 Cross-section of case pier column.	84
Figure 4.27 Mean structural resistances as a function of time.	86
Figure 4.28 Probability density function of structural resistance.	87
Figure 4.29 Probability of failure as a function of time.	88
Figure 4.30 Reliability index as a function of time.	88
Figure 4.31 Variations of reliability index for different load and resistance scenarios.	90
Figure 4.32 Variations of reliability index for different corrosion types.	91
Figure 4.33 Variations of reliability index for different exposure environment.	91
Figure 4.34 Variations of reliability index for concrete cover depth.	92
Figure 4.35 Variations of reliability index for different water-cement ratio.	92
Figure 4.36 Time-dependent reliability indexes for rehabilitation options.	94

Figure 5.1	Cash flow for the rehabilitation of bridges.	98
Figure 5.2	VOTING gate.	104
Figure 5.3	Illustrate the meaning of VOTING gate.	104
Figure 5.4	Changes of system probability of failure with M (N=5).....	105
Figure 5.5	Changes of system probability of failure with N (M=2).....	105
Figure 5.6	Flow chart of qualitative and quantitative risk assessment of bridge system.	106
Figure 5.7	Overview of case pier.	108
Figure 5.8	Calculation of components probability of failure of case headstocks.....	109
Figure 5.9	Calculation of components probability of failure of case columns.....	109
Figure 5.10	Calculation of components probability of failure of case pilecaps.	110
Figure 5.11	Calculation of components probability of failure of case piles.....	110
Figure 5.12	Calculation of probability of failure of case pier.....	110
Figure C.1	Distribution of A(50) under general corrosion.....	135
Figure C.2	Distribution of A(50) under localized corrosion.	137
Figure C.3	Distribution of A(50) under combination corrosion.....	138

LIST OF TABLES

Table 2.1	Typical transition matrix	12
Table 2.2	Basic event probabilities.	15
Table 2.3	Typical risk matrix for qualitative risk analysis.	17
Table 2.4	Typical risk matrix for risk ranking.....	18
Table 2.5	Advantages and disadvantages of identified methodologies.	20
Table 3.1	Common symbolic notation used in fault trees.	25
Table 3.2	Major bridge components.....	26
Table 3.3	Events table of plastic shrinkage.	32
Table 3.4	Events table of carbonation.	33
Table 3.5	Events table of ASR.	34
Table 3.6	Events table of chloride induced corrosion.	35
Table 3.7	Likelihood ratings.	36
Table 3.8	Suggested specification and detailing requirements for concrete exposed to various environments.	37
Table 3.9	Likelihoods of A2 and CHL2 according to exposure classification.	38
Table 3.10	Consequence ratings.	39
Table 3.11	Consequences ratings for failure modes of piles.	39
Table 3.12	Normalization of likelihoods.	41
Table 3.13	Risk matrix according to likelihoods and consequences.	42
Table 3.14	Risk ratings.....	42
Table 3.15	Inputs table of case pier piles.	45
Table 3.16	Inputs table for case pier pilecaps.....	46
Table 3.17	Importance of variability of parameters on variability of total scaled risk ratings.	48
Table 4.1	Statistical characteristics of chloride concentration variables.	61

Table 4.2	Calculation of area loss of steel reinforcement cross section under general corrosion.	69
Table 4.3	Calculation of area loss of steel reinforcement cross section under localized corrosion.	70
Table 4.4	Calculation of area loss of steel reinforcement cross section under combination corrosion.....	71
Table 4.5	Statistical characteristics of chloride propagation variables.....	75
Table 4.6	Statistical characteristics of resistance and load variables of case column.....	84
Table 5.1	Loss of lives in everyday life.	101
Table 5.2	Case inputs.	108
Table 5.3	Case outputs.	111
Table 6.1	Distribution of modeling results of important variables associated with chloride induced corrosion.....	116
Table A.1	Rules for assign likelihood ratings of each basic events.....	127
Table A.2	ASR sensitive aggregates.	128
Table A.3	Likelihood of A2 according to exposure classification.....	128
Table A.4	Concrete details in marine conditions.....	129
Table A.5	Concrete details in marine conditions category 4.....	130
Table A.6	Likelihood of CHL1 according to environment classification.....	130
Table A.7	Likelihood of CHL7.	130
Table B.1	Statistics characteristics of inputs for modeling corrosion initiation time.	131
Table B.2	Statistics characteristics of modeling results of corrosion initiation time of ordinary quality of concrete structures with different concrete cover depth.....	131
Table B.3	Statistics characteristics of modeling results of corrosion initiation time of x=5cm concrete structures with different concrete qualities.	132
Table B.4	Sensitivity of Statistics characteristics of modeling result of corrosion initiation time with $COV(C_0)$	132
Table C.1	Probabilistic characteristics of corrosion variables.....	133
Table C.2	Mean values of initial corrosion current.	133
Table C.3	Modeling result of time-dependent cross-sectional area of case steel bar under general corrosion.....	134

Table C.4	Modeling result of time-dependent cross-sectional area of case steel bar under localized corrosion.....	136
Table C.5	Modeling result of time-dependent cross-sectional area of case steel bar under combination corrosion.	138
Table D.1	Probabilistic characteristics of live load.	140
Table D.2	Probabilistic characteristics of resistance of structures under combination corrosion, general corrosion and localized corrosion.	141
Table D.3	Probabilistic characteristics of resistance of structures under different exposure environment.....	141
Table D.4	Probabilistic characteristics of resistance of structures with different concrete cover depth.	142
Table D.5	Probabilistic characteristics of resistance of structures with different water-cement ratio.	142
Table D.6	Probabilistic characteristics of probability of failure and reliability index of structures under combination corrosion, general corrosion and localized corrosion.	144
Table D.7	Probabilistic characteristics of probability of failure and reliability index of structures under different exposure environments.	145
Table D.8	Probabilistic characteristics of probability of failure and reliability index of structures with different concrete cover depth.	146
Table D.9	Probabilistic characteristics of probability of failure and reliability index of structures with different water-cement ratio.	147

CHAPTER 1 INTRODUCTION

1.1 Statement of the problem

Authorities managing concrete bridge structures face a significant challenge of dealing with increasing demand on load-carrying capacity, observed fast rates of deterioration and limited budgets for rehabilitation and strengthening of older structures. In Australia, more than 60% bridges of local roads are over 50 years old (Stewart, 2001). More than 24,000 Australian bridges were constructed prior to 1976 and are in need of strengthening/rehabilitation due to increase in traffic loading, premature deterioration and inadequate maintenance. It is obvious that rehabilitation and maintenance of those bridges is a strong financial commitment.

Options of rehabilitation available to the authorities have been expanded over the years with new developments in materials and structural technology. However, a lack of availability of complete information, which facilitates estimation of risk of failure, makes it difficult for the decision maker to make an informed decision. The broad range of high-level options identified by the authorities is given below:

- do nothing;
- restrict use;
- maintain and monitor;
- rehabilitate;

- strengthen/widen;
- replace super-structure;
- replace entire bridge.

Since most parameters influencing bridge performance are based on uncertain or incomplete information, a probabilistic reliability analysis of these bridges is important in decisions related to bridge design, assessment and rehabilitation. Estes and Frangopol (1999) developed a general methodology for optimizing rehabilitation options based on minimum expected cost. It is summarized as follows:

- “Identify the relevant failure modes of the bridge. Decide which variables are random and find the parameters (e.g. mean, standard deviation) associated with these random variables. Develop limit state equations in terms of these random variables for each failure mode. Compute the reliability with respect to the occurrence of each failure mode.
- Develop a system model of the overall bridge as a series-parallel combination of individual failure modes. Compute the system reliability of the bridge.
- Develop deterioration and live-load models which describe how the structure and its environment are expected to change over time. This will inevitably introduce new random variables. Compute the system reliability of the structure over time.
- Establish a repair or replacement criterion. Develop repair options and their associated costs.
- Using all feasible combinations of the repair options and the expected service life of the structure, optimize the repair strategy by minimizing total lifetime

repair cost while maintaining the prescribed level of reliability.

- Develop a lifetime inspection program to provide the necessary information to update the optimum repair strategy over time.”

Whilst the general methodology is quite useful, application of it requires many input parameters and data which are not readily available.

Previous work at RMIT (Nezamian et al., 2004) has led to the development of an overall framework for life cycle cost analysis of rehabilitation options of bridge structures. This framework requires a number of input parameters for effective application by the industry. The input parameters for the analysis are identified as initial cost, maintenance, monitoring and repair cost, user cost and expected failure cost. In this framework, expected failure cost of a bridge as part of the life cycle analysis is measured as:

$$\text{Failure cost} = \text{probability of failure} \times \text{cost of failure}.$$

However, the method to estimate probability of failure is not identified, which is an extremely essential input parameter for the life cycle costing model as decision support tools.

1.2 Research objectives

To address the gap in knowledge identified in 1.1, the aim of this research is to develop a methodology of estimating the risk of failure and probability of failure of reinforced concrete bridges, which can be used as input parameters for the life cycle costing. The work completed will assist the managers of bridge infrastructure

in making decisions in relation to different rehabilitation options for managing aging bridges. Detailed objectives of this study are:

- to analyze the risk of failure and probability of failure of existing reinforced concrete bridges qualitatively and quantitatively;
- to consider the effects of interactions among various deterioration parameters and among bridge components on system failure;
- to identify major durability related distress mechanisms of deterioration of reinforced concrete bridges and model the subsequent risk of failure of bridge system;
- to analyze the time-dependent reliability of reinforced concrete bridge components due to initiation of a distress mechanism using recent corrosion models and test data collected from literature;
- to predict future performance of bridge components after rehabilitation and estimate corresponding failure cost;
- to study the sensitivity of parameters relating to exposed environment, durability design, construction and load effects on probability of failure of components and overall risk of failure of entire bridges;
- to illustrate the application of the models developed using case studies.

1.3 Thesis outline

The thesis consists of six chapters. The background and motivation of this research along with the objectives have been presented in previous sections. In Chapter 2, a literature review associated with deterioration of reinforced concrete bridges,

performance assessment and risk analysis is carried out. This review includes commonly used methodologies in this area such as probabilistic reliability analysis, Markov chain deterioration model and fault tree analysis.

Chapter 3 provides a risk analysis model of reinforced concrete bridges based on fault tree analysis which can be applied as a qualitative assessment tool. This chapter will examine four major distress mechanisms of bridge piers exposed to aggressive environments. Rules for assigning inputs of likelihoods and consequences for basic events will be presented in detail. A case study will be demonstrated as an illustrative example to show the usage of the model in estimating and predicting potential hazards and risk of failure of both existing bridges and new bridges affected by durability issues.

In Chapter 4, probabilistic time-dependent reliability analysis for bridge components will be discussed. This is a component level model aimed at major components of reinforced concrete bridges exposed to aggressive environment. Chloride induced corrosion is selected as the major distress mechanism concerned in this research. A recent corrosion model will be identified as well as various influencing parameters covered in literature. Time-dependent reliability is then analyzed by simulation of resistance degradation and increasing load effects. Results obtained from sensitivity analysis of effects of environmental and design variables on time-dependent reliability will be presented. Possible performance and changes of safety index after rehabilitation can be predicted.

Life cycle cost model will be presented in Chapter 5, as well as a process to

integrate the qualitative risk assessment model based on fault tree analysis and the quantitative time-dependent reliability analysis model. VOTING gate model is added in order to estimate the system probability of failure of existing reinforced concrete bridges, which in turn is employed in life cycle cost analysis and evaluation of failure cost associated with maintenance and rehabilitation decision making.

Finally, summary and recommendations are given in Chapter 6.

CHAPTER 2 LITERATURE REVIEW

In order to fulfill the research objectives outlined in 1.3, a review of literature was necessary to gain the state of the art knowledge in this area. After a preliminary review, it was decided that in order to develop a methodology for evaluation the risk of failure of existing reinforced concrete bridges, information in three major areas are needed. First, a deterioration model for a given distress mechanism should be identified, which covers the range of parameters influencing the particular mechanism. Then, a method of analyzing the probability of failure of structural components due to the occurrence of the mechanism is needed. Finally, to estimate risk of failure, a method to compute systemic probability of failure and associated cost is required. This chapter covers recent published work and methodologies in these areas related to deterioration models, risk assessment and reliability analysis of reinforced concrete bridges.

2.1 Performance assessment and deterioration modeling

2.1.1 Time-dependent reliability analysis

Analysis of the time-dependent reliability of existing structures is increasingly gaining importance as decision support tools in civil engineering applications in the

last decade. Consequently, many researchers attempted to model the parameters associated with corrosion mechanisms, material properties and exposed environment, which further lead to structural deterioration and resistance degradation. Deterioration models for major distress mechanisms of reinforced concrete structures such as alkali-silica reaction, chloride induced corrosion of reinforcement are investigated by laboratory tests, statistical analysis and mathematical modeling (Gonzalez et al., 1995, Leira and Lindgard, 2000, McGee, 2000, Papadakis et al., 1996, Patev et al., 2000, Rendell et al., 2002).

Since corrosion of reinforcement is a major reason of structural deterioration, many researchers attempted to evaluate the effect of chloride induced corrosion on reinforced concrete structures and time-dependent reliability. General approach of these researches is to identify resistance degradation models based on chloride induced corrosion, which is further combined with load effect model to assess time-dependent reliability and probability of failure. However, these researches contain are not consistent on emphases in concepts of failure, corrosion modeling, limit states and reliability analysis methodologies.

Based on Fick's second law of diffusion, Enright and Frangopol (1998b) performed sensitivity analysis on effect of mean and coefficient of variation of four parameters, concrete cover depth, chloride diffusion coefficient, surface chloride concentration and critical chloride concentration on corrosion initiation time, as shown in Figure 2.1. The model of cross-sectional area loss of reinforcement as a function of time under general corrosion has been provided. Stewart and Rosowsky (1998) proposed probabilistic models to represent the structural deterioration of

reinforced concrete bridge decks and time dependent reliability. The characteristics of various exposed environments and their influence on corrosion have been identified. Flexural cracking limit state has also been considered by Stewart and Rosowsky. Val et al. (1998) presents a model which includes a non-linear finite element structural model and probabilistic models for analysis of reliability of high-way bridges considering chloride corrosion and bond strength loss. Based on this model, Vu and Stewart (2000) promoted an improved chloride induced corrosion model and a time-dependent load model. This research examined the degradation of both flexural capacity and shear capacity under localized corrosion. Changes of time dependent reliability of a simply reinforced concrete slab bridge with different durability design specifications were compared by these researchers (see Figure 2.2).

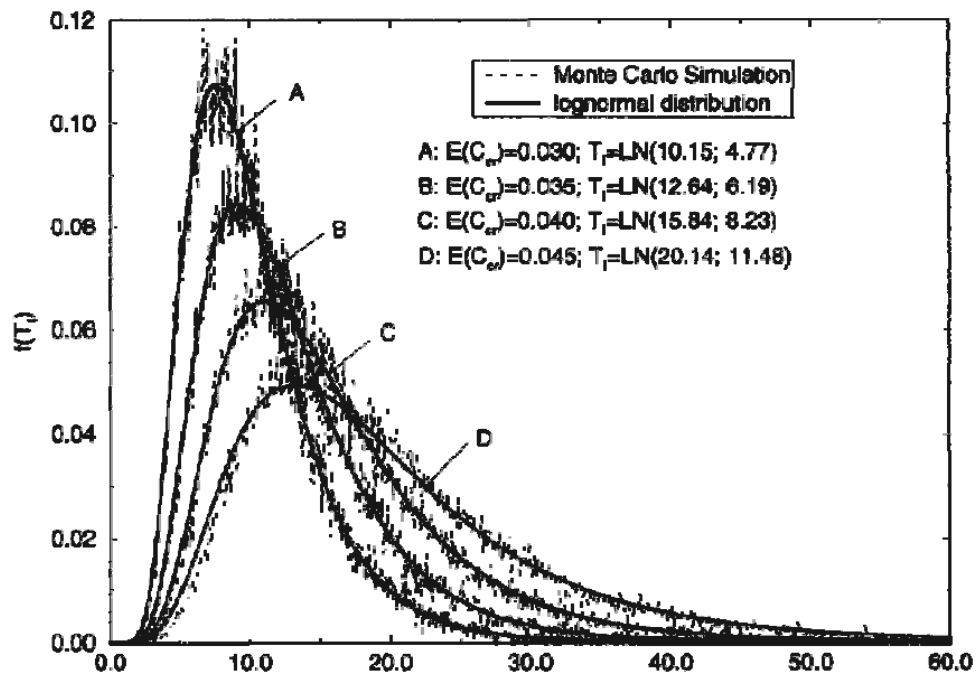


Figure 2.1 Effect of mean critical chloride concentration on corrosion initiation time.

Reliability is considered as an important indicator of structural performance. The ultimate objective of time-dependent reliability analysis is to link with inspection, maintenance and rehabilitation to offer management with an integrated decision support tool. Cheung and Kyle (1996) present a framework for reliability-based analysis of bridge performance and service life prediction. Five limit state functions of concrete slabs are defined and modeled, they are flexural strength, punching shear, deflection, delamination and surface wearing.

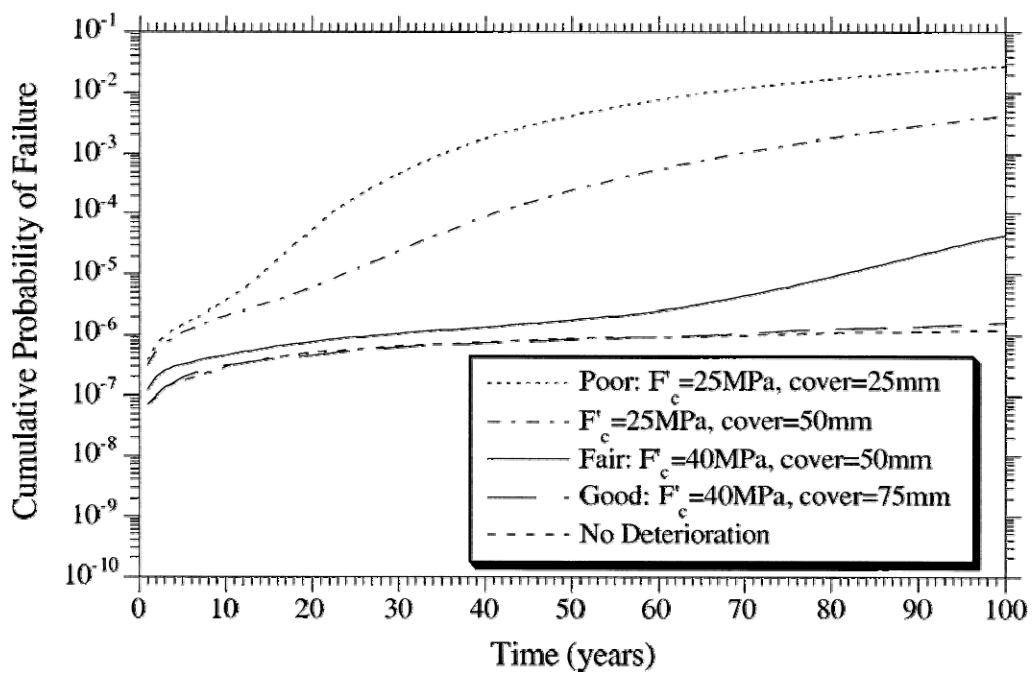


Figure 2.2 Time-dependent cumulative probabilities of failure for de-icing salts and no deterioration.

Recently, many researchers have used reliability based life cycle cost analysis in decision-making. Val and Stewart (2003) indicate that the time-dependent reliability analysis can be conducted with a probabilistic life cycle cost model to provide criteria for optimizing repair strategies. They compared expected maintenance and repair costs associated with cracking and spalling (failure of serviceability) of different durability designs and exposed environments of marine

structures. Failure cost of ultimate failure (collapse) is neglected. In other life cycle cost models, failure cost is formulated as the product probability of failure P_f and cost of failure C_F (Branco and Brito, 2004b, Nezamian et al., 2004, Stewart, 2001):

$$C_{failure} = P_f \cdot C_F \quad (2.1)$$

These researches provide a broad overview of the concepts, methodologies and applications of a reliability based approach for bridge performance assessment and decision optimization. However, existing models for assessing life cycle cost is not fully consistent and various limited states are examined. Most of these researches fail to mention the effect of intervention due to repair or rehabilitation on time-dependent reliability.

2.1.2 Markov chain deterioration model

Markov chain is a stochastic approach that is widely used for modeling deterioration of highway bridges and infrastructure assets. Most Markov chain deterioration models use discrete condition rating systems (Maheswaran et al., 2005, Sharabah et al., 2006, Zhang et al., 2003). It can be used to predict the probability that a given structural element in a given environment and a certain initial condition will continue to remain in its current condition state, or change to next or another condition state. In these models, time can be either discrete (Sharabah et al., 2006) or continuous (Maheswaran et al., 2005).

Markov chain deterioration models assume that the future probabilistic behavior of the process depends only on the present state regardless of the past. Assume there are four ratings A, B, C and D where A represents new or nearly new state and D represent a condition which indicates the element has to be replaced. The deterioration model is built based on transition matrix which shows the probability of the performance of structural element passing from one state to another state. Transition matrix is then multiplied by initial distribution to obtain a new performance distribution for the next time period.

A typical transition matrix is shown in Table 2.1 below (Sharabah et al., 2006). The identification of transition matrix should be based on analysis of large amount of performance and inspection data of similar structures. Maheswaran (2005) used inspection records from 1996 to 2001 of approximately 1000 bridges from VicRoads database. Zhang et al. (2003) analyzed the historical ratings generated during the past 20 years for all state on-system bridges in National Bridge Inventory of Louisiana, USA.

State	A	B	C	D	Sum
A	0.4	0.3	0.2	0.1	1
B	0	0.2	0.4	0.4	1
C	0	0	0.2	0.8	1
D	0	0	0	1	1

Table 2.1 Typical transition matrix

The main advantage of Markov chain deterioration models is that they have the ability to capture the time dependence and uncertainty of deterioration process and

applicability to both components and systems because of computation efficiency and simplicity (Morcous et al., 2003). However, compared to probabilistic reliability analysis, the results obtained from Markov chain deterioration models are much less precise.

2.1.3 Deterioration modeling based on fault tree analysis

Fault tree analysis is a system analysis technique used to determine the root causes and probability of occurrence of a specified undesired event. It is one of the important techniques for hazard identification that has been developed from various engineering areas. Fault tree analysis is used on reinforced concrete bridges in several research projects to assess the deterioration and predict probability of failure of entire bridges or certain bridge sub-systems. Johnson (1999) applied fault tree model in analysis of bridge failure due to scour and channel instability. As scour at bridges is a very complex process, fault tree model is used to examine possible interactions of scour processes and their effect on bridge piers and abutments, see Figure 2.3. The probabilities of basic events in the fault tree were evaluated by simulation of scour equations presented in literature. Sianipar and Adams (1997) demonstrated a method of using fault tree analysis to quantify the interaction phenomena in a bridge system. The top level fault tree developed is shown in Figure 2.4, which examined the effect of malfunction of bearings and expansion joints on deterioration of a concrete deck. The research drew a conclusion that the probability of acceleration of concrete deck deterioration is 0.4 if all basic events exist. Another fault tree model of bridge deterioration has been

developed to calculate the probability of bridge deterioration by LeBeau and Wadia-Fascetti (2000). The probabilities of basic events were obtained by assigning questionnaires to seven bridge engineers and inspectors. The probabilities of basic events used in this research are shown in Table 2.2. A comparison between the efficiency of different rehabilitation alternatives also has been evaluated.

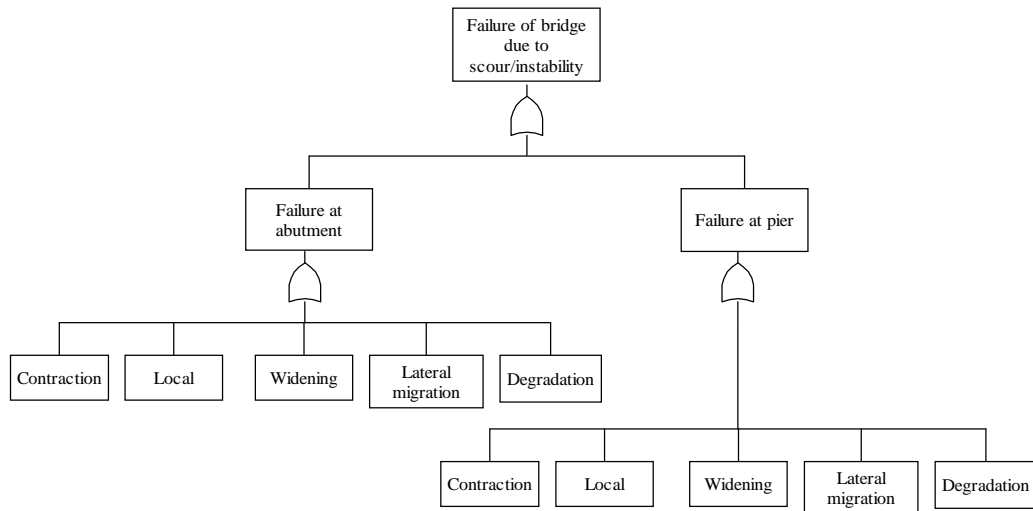


Figure 2.3 Main fault tree diagram for scour and channel instability at bridges.

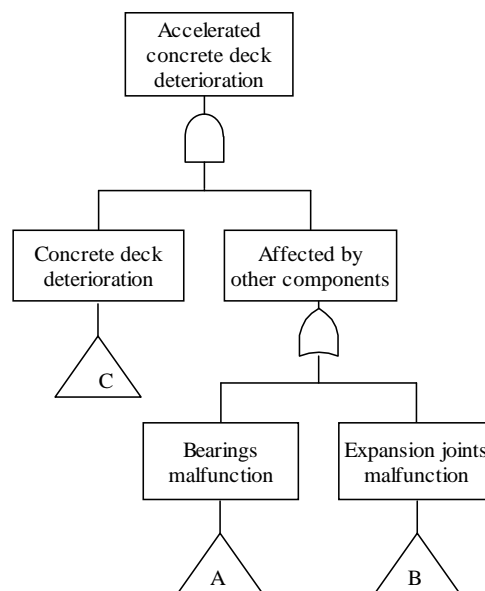


Figure 2.4 Top-level fault tree for accelerated concrete deck deterioration.

These researches prove that it is possible to develop a fault tree model to represent the various interactions involved in possible events that would lead to a bridge failure. Fault trees in above researches are analyzed quantitatively by identifying numerical probability of occurrence of basic events as inputs and result in a quantitative probability of occurrence of top events. However, the inputs of basic events are subjective to some extent. Under certain assumptions, the results are adoptable on those bridges with the similar structure, but fail to show the difference due to different age, exposed environment, load effect, etc.

Basic Event		Probability	Basic Event		Probability
1	Paving over expansion joint	0.06	17	Corrosion of girder	0.16
2	Improper alignment of expansion joint	0.13	18	Fatigue cracking	0.05
3	Abutment settlement	0.07	19	Poor alignment of girder	0.14
4	Excessive dirt and debris	0.21	20	Corrosion damage of girder	0.07
5	Traffic impact damage of joints	0.12	21	Worn bearing elements	0.36
6	Clogged deck drains	0.44	22	Incomplete bearing assemblies	0.07
7	Leakage	0.18	23	Corroded bearings	0.15
8	Corrosion of joints	0.14	24	Deteriorated concrete pedestals	0.14
9	Improper installation of joint	0.18	25	Differential vertical movement (abutment)	0.03
10	Deck cracking	0.14	26	Rotational movement (abutment)	0.03
11	Deck spalls	0.15	27	Cracks in abutment	0.05
12	Corroding reinforcement in deck	0.16	28	Spalls in abutment	0.13
13	Delamination (deck)	0.10	29	Corroded reinforcement of abutment	0.11
14	Poor condition of wearing surface	0.25	30	Delamination (abutment)	0.09
15	Efflorescence (deck)	0.12	31	Efflorescence (abutment)	0.06
16	Damaged drainage outlet pipes	0.43	32	Severe environmental exposure	0.57

Table 2.2 Basic event probabilities.

2.2 Risk assessment

Risk is a measure of the potential loss occurring due to natural or human activities. Such potential losses may be formed as loss of human life, adverse health effects, loss of property and damage to the natural environment (Modarres, 2005). Risk is measured by multiplying the consequences of an event by their probability of occurrence (AS/NZS 4360, 2004). Consequence is the outcome or impact of the occurrence of a failure event. Considering an activity with only one event with potential consequences C , the risk R equals to the probability that this event will occur P multiplied by the consequences, that is:

$$R = P \cdot C \quad (2.2)$$

Thus, it can be concluded that, in life cycle cost model, failure cost (see Equation 2.1) actually is the quantitative form of risk of failure with cost of failure C_F as consequences of failure events. Figure 2.5 shows a generic representation of process of risk assessment and management. The individual steps in the flow chart are described in Stewart and Melchers (1997a).

Qualitative risk assessment is easy to perform when precise data is not required. In this approach, rank-ordered approximations are sufficient and often quickly estimated the risk (Modarres, 2005). Table 2.3 shows a typical qualitative risk assessment matrix. It can be used to assess the risk of identified risk scenarios of a system failure. Another way is to assign numerical values to represent frequencies and consequences ratings to arrive at numerical results of risk ratings and risk rankings (see Table 2.4). These methods are simple to apply and easy to use and

understand, but is extremely subjective.

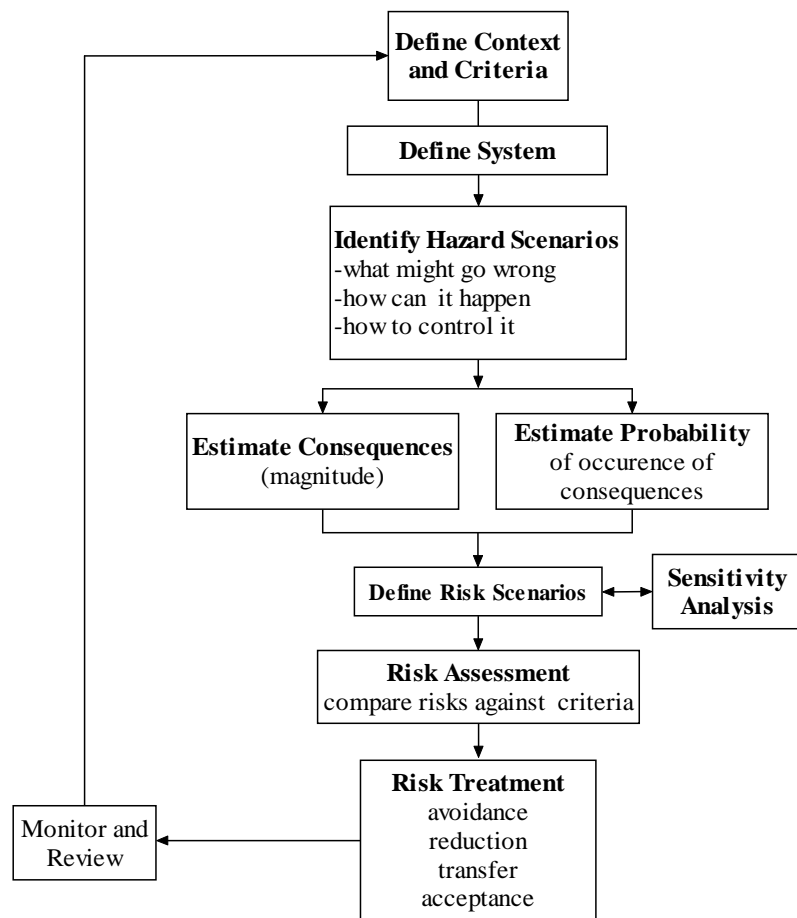


Figure 2.5 Generic representation of the flow of risk-based decision analysis.

	Severity of consequence			
Frequency of occurrence	Catastrophic	Critical	Marginal	Negligible
Frequent	High risk	High risk	High risk	Intermediate risk
Probable	High risk	High risk	Intermediate risk	Low risk
Occasional	High risk	High risk	Low risk	Low risk
Remote	High risk	High risk	Low risk	Low risk
Improbable	High risk	Intermediate risk	Low risk	Trivial risk
Incredible	Intermediate risk	Intermediate risk	Trivial risk	Trivial risk

Table 2.3 Typical risk matrix for qualitative risk analysis.

Frequency of occurrence	Severity of consequence			
	4	3	2	1
6	24	18	12	6
5	20	15	10	5
4	16	12	8	4
3	12	9	6	3
2	8	6	4	2
1	4	3	2	1

Table 2.4 Typical risk matrix for risk ranking.

In quantitative risk analysis, the uncertainty associated with the estimation of the probability of the occurrence of the undesirable events and the consequences are characterized by using the probabilistic concepts. It is obvious that quantitative risk analysis is the preferred approach when adequate field data, test data and other evidence exist to estimate the probability (or frequency) and magnitude of consequences (Modarres, 2005). Failure data collection and analysis is essential which consists of collecting and assessing generic data, statistically evaluating system data and developing failure distributions using test or simulation. Quantitative risk analysis can provide integrated and systematic examination of risks of a complex system and quantitative safety of overall system as criteria for future management. However, the application of quantitative risk analysis methods in practice is limited because it is complicated, time-consuming and expensive. Also, human performance models and interaction with the system are highly uncertain and difficult to quantify.

Risk analysis may also use a mix of qualitative and quantitative approaches since

some decision making criteria only rely on results of qualitative analysis. Fault trees may be employed for overall, generalized system risk assessment (Stewart and Melchers, 1997b). Williams et al. (2001) use fault tree analysis to assess the risk involved in Bowen basin spoil rehabilitation. Creagh et al. (2006) developed a risk assessment model based on fault tree analysis for the performance of unbound granular paving materials. Both of above fault tree models uses qualitative and likelihood and consequence ratings as inputs and obtain risk ratings which ensure decision making based on risk ranking. This method is systematic and structured, it allows the assessment of a large range of variables and their interaction involved in causing potential losses. Comparing to quantitative risk analysis, it is much easier and require less data. The subjectivity involved in modeling result is greatly reduced as well.

2.3 Conclusion

The literature review on deterioration modeling, reliability analysis and risk assessment of reinforced concrete bridges provides detailed knowledge and methodology which can be generalized and applied on aging reinforced concrete bridges and their rehabilitation. Methods used by previous researchers can be summarized as follow, their advantages and disadvantages are summarized in Table 2.5:

- Use of Markov process to evaluate element probability of failure and future performance;
- Probabilistic time-dependent reliability analysis methods using deterioration

model of a mechanism to calculate probability of failure;

- Fault tree analysis to analyze the systemic probability of failure based on probability of occurrence of basic events.

Methods Description	Advantage	Disadvantage
Markov process	<p>Be able to consider the time dependence and uncertainty of deterioration process;</p> <p>Can be applied on both components and systems.</p>	<p>Require large amount of historical data;</p> <p>Lack of precision;</p> <p>Failed to link with environmental variables.</p>
Probabilistic time-dependent reliability methods	<p>Success in considering time dependence and uncertainty associated with various factors;</p> <p>Be able to achieve reliable compute results with practical meanings;</p> <p>Suitable for both new and existing structures;</p> <p>Be able to used in reliability based design and management.</p>	<p>Not easy to compute, requires access to powerful software;</p> <p>Requires precise probabilistic distribution of various uncertain parameters based on laboratory test or statistics;</p>
Fault tree analysis	<p>Visual model clearly displays cause-effect relationships;</p> <p>Structured methods to consider complexity involved in causing system failure;</p> <p>Can be analyzed qualitatively and quantitatively;</p>	<p>Difficult to identify the occurrence of basic events (probability of components failure);</p>

Table 2.5 Advantages and disadvantages of identified methodologies.

After considering the published work, it was identified that one single method can not provide all the answers needed by a management decision maker. As depicted in Table 2.5, lack of data often makes one single method impractical. Therefore it was decided to examine prediction of probability of failure using two approaches; one qualitative and one quantitative, which could result in qualitative risk of failure and quantitative failure cost respectively. Following chapters will present a qualitative risk assessment method of reinforced concrete bridges based on fault

tree analysis, a probabilistic analysis method of time-dependent reliability of reinforced concrete bridges components based on improved corrosion model and an integration model to combine these two models to quantitatively estimate probability of failure and failure cost.

CHAPTER 3 QUALITATIVE RISK ASSESSMENT OF REINFORCED CONCRETE BRIDGES USING FAULT TREE ANALYSIS

3.1 Introduction

Reinforced concrete bridges can deteriorate before the end of service life if the design does not satisfy the requirement of the environment to which it is exposed. However, deterioration of reinforced concrete structures does not necessarily imply structural collapse but could lead to loss of structural serviceability, such as poor durability and poor appearance with cracking, spalling, and so on. Evaluation of the risk of failure of serviceability is important in decision making in relation to identifying different rehabilitation options for managing aging bridges.

Fault tree analysis is a system analysis technique adopted to determine the root cause and the probability of occurrence of a specified undesired event (Ericson, 2005). It is often used in evaluating large complex dynamic systems to identify and prevent potential problems. Fault tree analysis can be used for risk assessment based on the likelihood and consequence ratings of various events of fault tree (Williams et al., 2001). The process of using fault tree analysis in risk assessment is shown in Figure 3.1. Likelihoods are assigned to basic events of the fault tree while

consequence ratings are assigned to each failure mode (Creagh et al., 2006, Vick, 2002, Williams et al., 2001). Fault tree analysis is employed to estimate the likelihoods of major failure modes, therefore, overall risk can be assessed by multiplying likelihoods and consequences. Figure 3.2 shows a typical fault tree used in this process.

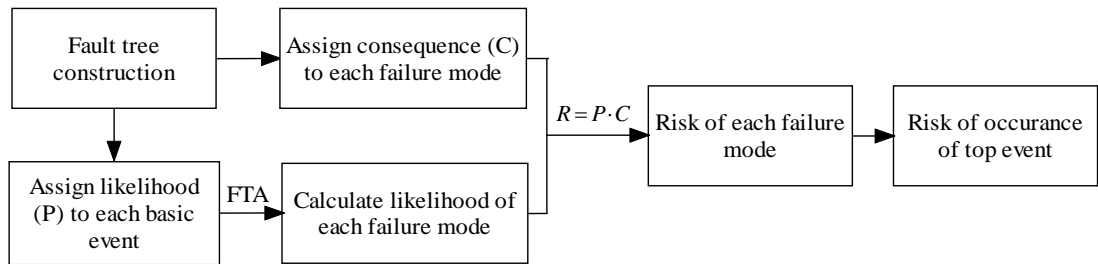


Figure 3.1 General process of using fault tree analysis in risk assessment.

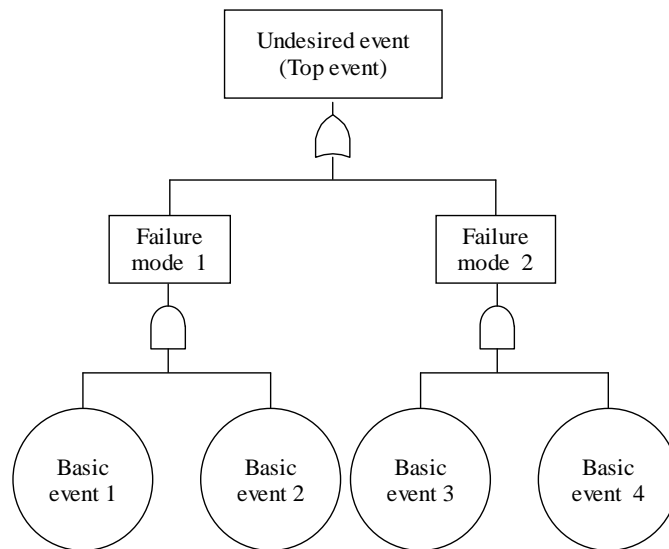


Figure 3.2 Typical fault tree used in risk assessment.

This chapter presents a frame of a fault tree model to qualitatively analyze the risk of failure of reinforced concrete bridges due to poor durability (serviceability limit state). The fault tree method considers all possible events that could lead to the

occurrence of major distress mechanisms. The output risk ratings can be regarded as a prediction of the performance of the bridge or bridge component during future service life. It can also be used to rank the ratings of risk of failure of a number of bridges based on sufficient construction and inspection data. For the purposes of qualitative analysis of risk of failure, likelihoods and consequences are rated using logarithmic, three point scale.

3.2 Fault tree model

A fault tree is a graphical model which uses logic gates and fault events to model the interrelations involved in causing the undesired event. Common symbolic notations used in fault trees are shown in Table 3.1 (Ericson, 2005, Mahar and Wilbur, 1990). A logic gate may have one or more input events but only one output event. AND gate means the output event occur if all input events occur simultaneously while the output event of OR gate occurs if any one of the input events occurs.

The fault tree model can be converted into a mathematical model to compute the failure probabilities and system importance measures (Ericson, 2005, Mahar and Wilbur, 1990). The equation for an AND gate is

$$P = \prod_{i=1}^n p_i \quad (3.1)$$

and the equation for an OR gate is

$$P = 1 - \prod_{i=1}^n (1 - p_i) \quad (3.2)$$

where n is the number of input events to the gate, p_i are the probabilities of failure of the input events and it is assumed that the input events are independent (Faber,2006).

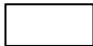
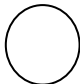

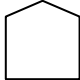
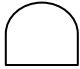

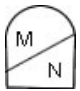
Symbol	Name	Usage
	Rectangle	Event at the top and intermediate positions of the tree
	Circle	Basic event at lowest positions of the tree
	Triangle	Transfer
	House	Input Event
	AND Gate	Output event occurs if all input events occur simultaneously
	OR Gate	Output event occurs if any one of the input events occurs
	Voting Gate	M of N combinations of inputs causes output to occur.

Table 3.1 Common symbolic notation used in fault trees.

3.2.1 Overall fault tree frame

A reinforced concrete bridge comprises of superstructure and substructure, which can be further divided into several components. Table 3.2 lists main bridge components considered in this research (Tonias and Zhao, 2007). By dividing the

structure into several sub-systems, the top level of the fault tree model is constructed, as shown in Figure 3.3. The top event of this fault tree is defined as bridge failure due to poor durability. The deterioration of major components of a bridge may attribute to the overall performance of the whole structure. Failure of each component A-E can be further decomposed. By examining the failure of each component, the overall risk of failure of a bridge can be assessed.

Bridge components		Description
Superstructure	Deck	The deck is the physical extension of the roadway across the obstruction to be bridged. The main function of deck is to distribute loads transversely along the bridge cross section.
	Girder	Girders distribute loads longitudinally and resist flexure and shear.
Substructure	Abutment	Abutments are earth-retaining structures which support the superstructure and overpass roadway at the beginning and end of a bridge.
	Pier	Piers are structures which support the superstructure at intermediate points between the end supports (abutments).
	Bearing	Bearings are mechanical systems which transmit the vertical and horizontal loads of the superstructure to the substructure, and accommodate movements between the superstructure and the substructure.

Table 3.2 Major bridge components.

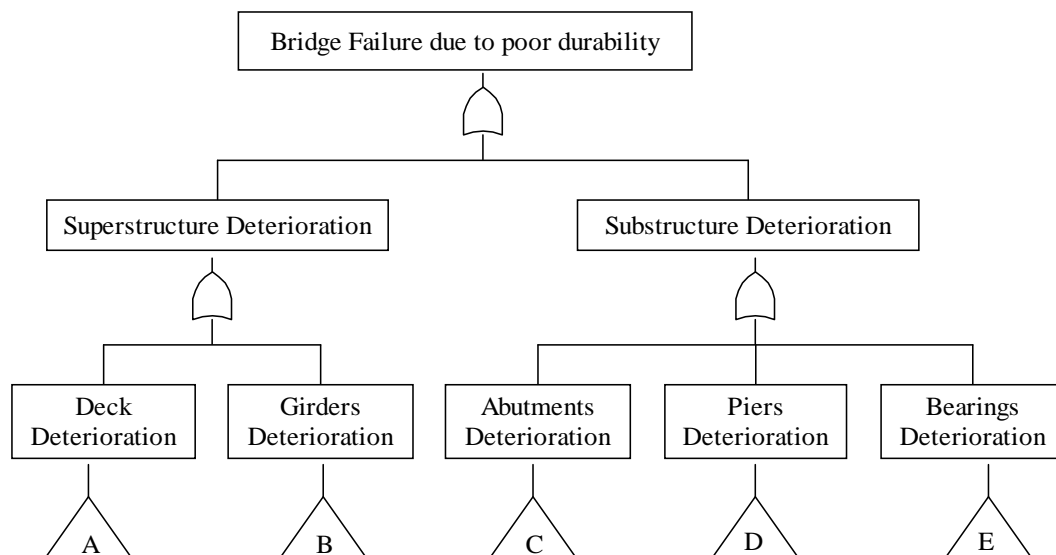


Figure 3.3 Top level fault tree frame.

3.2.2 Major sub-tree: deterioration of pier

This chapter mainly demonstrates the application of proposed methodology using pier deterioration as an example sub-tree. Piers are crucial components in reinforced concrete structures. They are usually located in a tidal, splash or submerged zone which is directly exposed to an aggressive environment. Thus the problem of pier deterioration is considered as a major issue. By examining the branch of pier, the analysis of pier conditions can be accomplished which might reflect the effect of pier deterioration due to the durability of the bridge at a certain extent. Failure of other components can be evaluated using a similar method to obtain the overall risk of an entire bridge. Figure 3.4 shows the sub-tree of piers mentioned in this research.

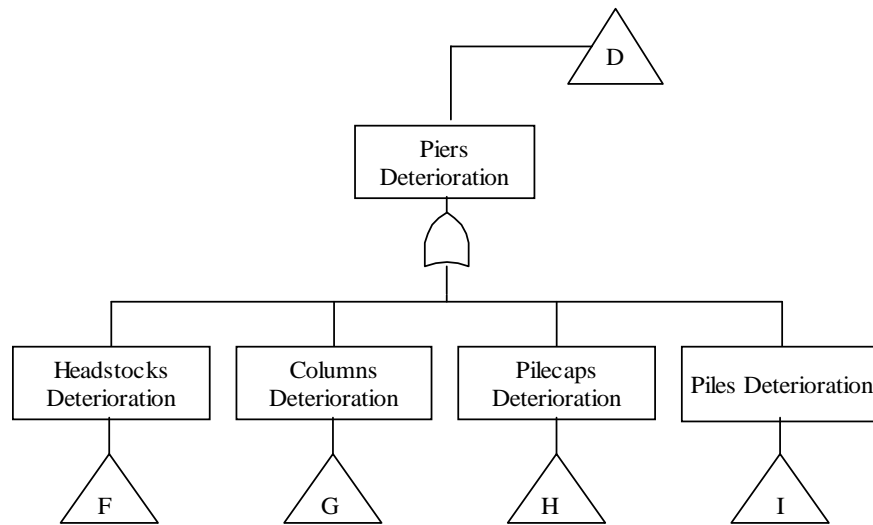


Figure 3.4 Major sub-system fault tree of piers deterioration.

3.2.2.1 Identification of failure modes

Generally speaking, problems with concrete structures can be grouped into

following aspects (Rendell et al., 2002):

- Initial design errors: either structural or in the assessment of environmental exposure.
- Built-in problems: the concrete itself can have built-in problems. A good example of this is alkali-silica reaction (ASR).
- Construction defects: poor workmanship and site practice can create points of weakness in concrete that may cause acceleration in the long-term deterioration of the structure. A common defect of this type is poor curing of the concrete.
- Environmental deterioration: a structure has to satisfy the requirement of resistance against the external environment. Problems may occur in the form of physical agents such as abrasion, and biological or chemical attack such as sulfate attack from ground water.

For piers, deterioration may arise from environmental attack, overload and scour.

As the top event is bridge failure due to poor durability, in this research, following distress mechanisms were selected as major failure modes:

- Chloride induced corrosion
- Alkali-Silica reaction
- Carbonation
- Plastic shrinkage

These distress mechanisms were selected as key failure modes because they obviously indicate deficiencies in material durability of reinforced concrete bridges.

They can often lead to cracking, spalling, honeycombing of concrete and

significant reduction of structural safety (Venkatesan et al., 2006). Figure 3.5 to 3.8 presents the sub-system fault trees for headstocks, columns, pilecaps and piles deterioration respectively.

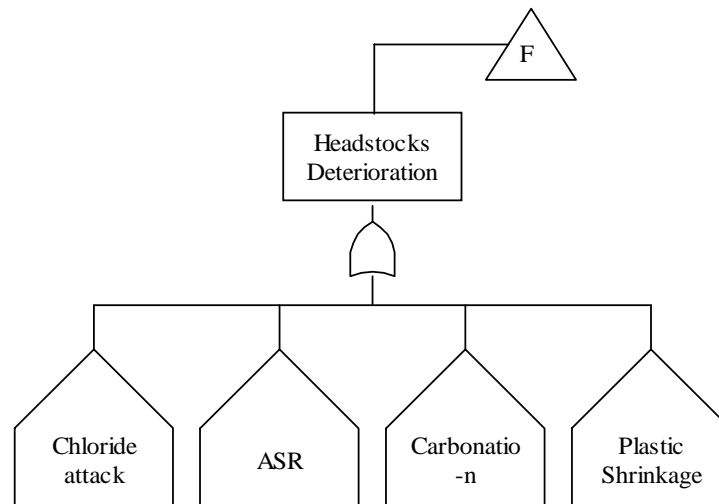


Figure 3.5 Secondary sub-system fault tree of headstocks deterioration.

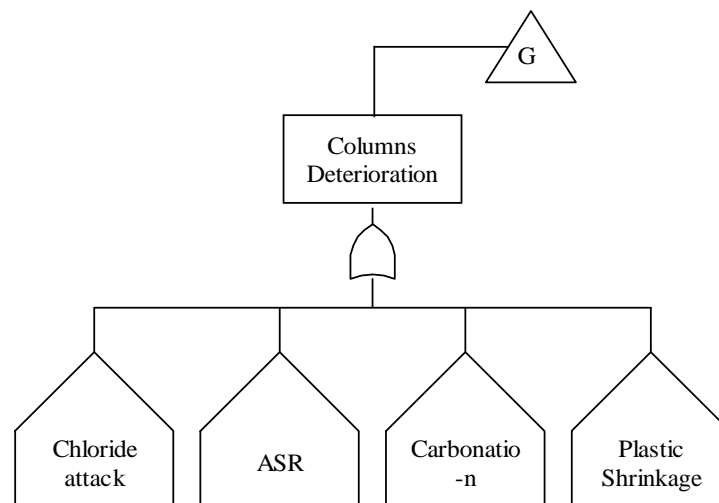


Figure 3.6 Secondary sub-system fault tree of columns deterioration.

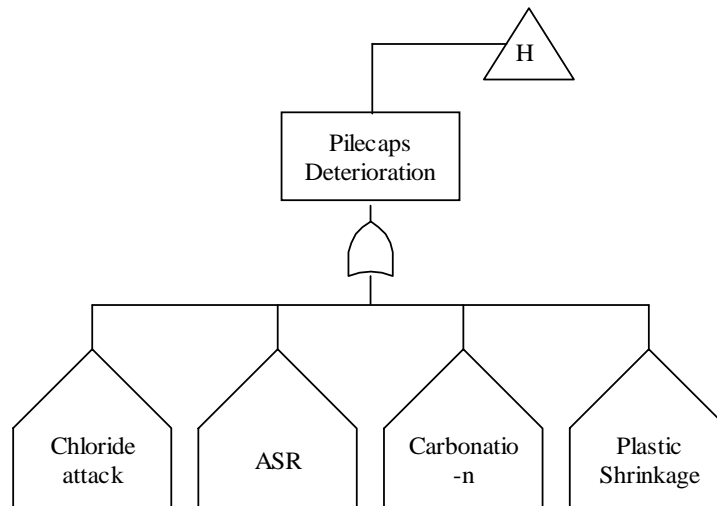


Figure 3.7 Secondary sub-system fault tree of pilecaps deterioration.

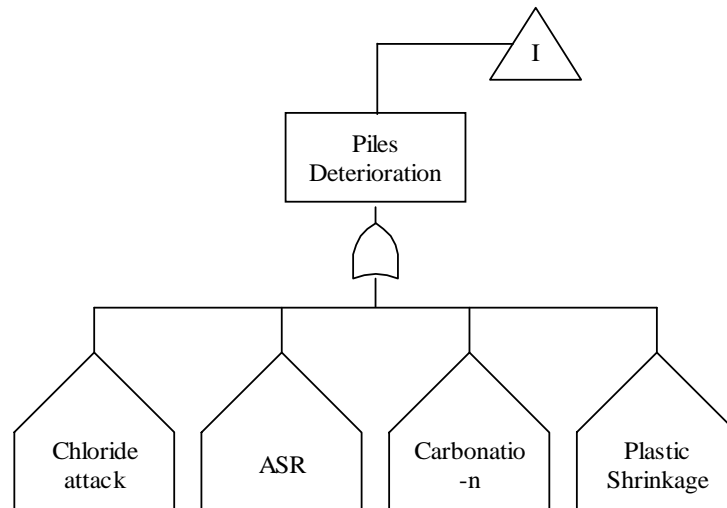


Figure 3.8 Secondary sub-system fault tree of piles deterioration.

3.2.2.2 Fault tree decomposition of major failure modes

The occurrence of major failure modes are related to complex interactions of various factors. These variables can be grouped into (Rendell et al., 2002, Ropke, 1982):

- Applied loads;

- Material variables, such as aggregates, water-cement ratio, admixture ,compaction, permeability;
- Design variables, such as, depth of concrete cover, concrete strength;
- Exposed environment, such as climatic condition, aggressive sources, relative humidity;
- Construction and curing.

3.2.2.2.1 Plastic shrinkage

Plastic shrinkage results from rapid evaporation of water from the surface of the concrete in plastic state. The consequent cracks could provide pathways that will open the concrete to external attack. It easily occurs in hot, dry climates and windy atmosphere especially where inadequate attention has been paid to protection and curing (Rendell et al., 2002). Fault tree of plastic shrinkage is shown in Figure 3.9 with basic events shown in Table 3.3.

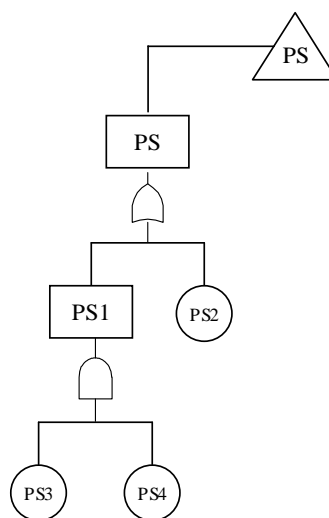


Figure 3.9 Fault tree of plastic shrinkage

Events	Description
PS	Plastic Shrinkage
PS1	Arid environment
PS2	Improper curing
PS3	High wind speed
PS4	Low relative humidity

Table 3.3 Events table of plastic shrinkage.

3.2.2.2.2 Carbonation

Carbonation of concrete occurs when carbon dioxide penetration in the concrete surface and leads to a change from the initial pH value of around 12 to lower values (Branco and Brito, 2004a). It is often observed in urban areas where there are high levels of carbon dioxide. The occurrence of carbonation requires the presence of water and carbon dioxide gas in the pore structure (Rendell et al., 2002). If the carbonation reaches the surface of reinforcement, depassivation of the steel will take place and a corrosion process initiates if sufficient oxygen and moisture are available. Thus, carbonation can be presented by the fault tree shown in Figure 3.10.

Basic events of fault tree of carbonation are shown in Table 3.4.

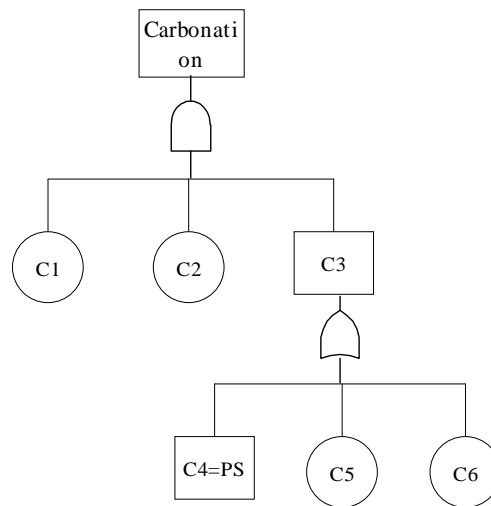


Figure 3.10 Fault tree of carbonation.

Events	Description	Events	Description
C1	High Carbon dioxide in the environment	C4	Crazing due to plastic shrinkage (PS)
C2	High relative humidity	C5	Improper concrete mix in design (water cement ratio)
C3	Permeable concrete	C6	Improper construction and curing

Table 3.4 Events table of carbonation.

3.2.2.2.3 Alkali-silica reaction

ASR is the reaction between alkali in the cement and reactive silica in certain types of aggregates that occurs in the presence of water (Rendell et al., 2002). The reaction produces a gel which occupies more volume and induces expansion and cracks. It is believed that the most expansive reaction is associated with poorly organized silica forms such as opal and chert. However, there are certain admixtures, such as fly ash, which have the ability to reduce expansion due to alkali-silica reactivity. Thus, reactive aggregate, poor concrete quality and

excessive moisture are the necessary events to cause ASR. After identification of these necessary events which cause ASR, fault tree can be constructed as shown in Figure 3.11 with basic events shown in Table 3.5.

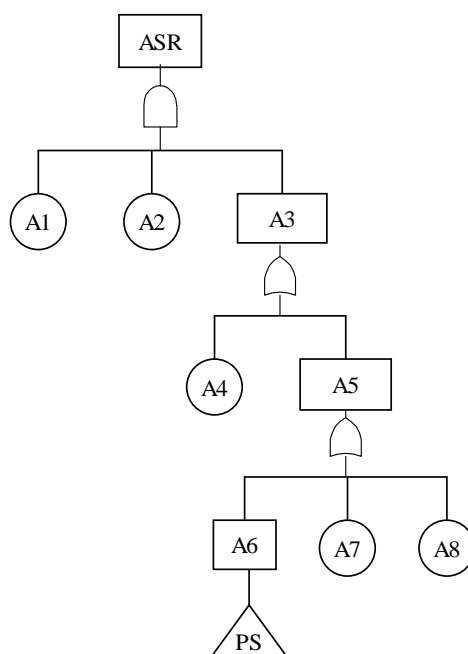


Figure 3.11 Fault tree of Alkali-silica reaction.

Events	Description	Events	Description
ASR	Alkali-silica reaction	A5	Permeable concrete
A1	Reactive aggregate	A6	Crazing due to plastic shrinkage
A2	Presence of excessive moisture	A7	Improper water cement ratio in design
A3	Poor material	A8	Improper construction and curing
A4	Improper admixture		

Table 3.5 Events table of ASR.

3.2.2.2.4 Chloride induced corrosion

Chlorides in the external environment may diffuse in the concrete and finally arrive on the surface of steel bars. Structures with permeable concrete with excessive pores and carbonated concrete cover are particularly at risk. The corrosion of steel reinforcement initiate when the concentration of chloride ions on the surface of steel bar reaches a critical value. Corrosion of steel could cause severe cracking and even spalling. Thus, fault tree of chloride induced corrosion can be constructed as shown in Figure 3.12. Basic events of this fault tree are shown in Table 3.6.

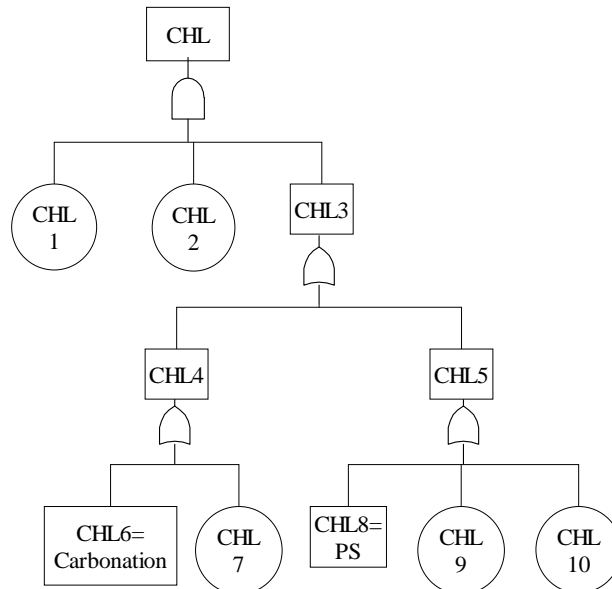


Figure 3.12 Fault tree of chloride induced corrosion

Events	Description	Events	Description
CHL	Chloride attack	CHL6	Carbonation
CHL1	High chloride environment	CHL7	Insufficient depth of concrete cover in design
CHL2	Moisture and oxygen	CHL8	Plastic Shrinkage
CHL4	Insufficient depth of concrete cover	CHL9	Improper water cement ratio design
CHL5	Permeable concrete	CHL10	Improper construction and curing

Table 3.6 Events table of chloride induced corrosion.

3.3 Risk assessment using fault tree model

3.3.1 Input likelihood ratings

Ideally, the probability of basic events should be estimated from available data. However, real data to estimate a probability distribution is not available. Therefore it was decided to utilize semi-quantitative inputs to define likelihood ratings. These can be estimated with industry consultation. In converting the likelihood ratings to a numerical value, a three point logarithmic scale is used to obtain a quantitative difference between ratings, see Table 3.7. This approach has been used by Williams et al. (2001).

Load, environment, construction, material and design data are needed to assess the likelihood ratings of basic events. Likelihood is assigned by examining whether the load, design, construction and material of the bridge are compatible with external environment which it is exposed to. The judgment can be made according to either experts' opinions or corresponding design codes and specifications, see Table 3.8 (Guirguis, 1980).

Likelihood Rating	Description	Log Scale
1-Low	Low likelihood of occurrence	0.001
2-Medium	Moderate likelihood of occurrence	0.01
3-High	High likelihood of occurrence	0.1

Table 3.7 Likelihood ratings.

Environmental Category	Specification		Detailing Requirements
Category 1 <ul style="list-style-type: none"> Low humidity (25-50% throughout year) Temperature range 10-35 °C Large daily temperature range Low rainfall Low atmospheric pollution 	Maximum w/c	0.6	Minimum cover 30 mm
	Minimum cement content	280 kg / m ³	
Category 2 <ul style="list-style-type: none"> High humidity throughout year High rainfall Moderate atmospheric pollution Running water (not soft) 	Maximum w/c	0.55	Minimum cover 40 mm
	Minimum cement content	300 kg / m ³	
Category 3 <ul style="list-style-type: none"> Wind driven rain 1-5km of coast Heavy condensation Soft water action Freeze-thaw action High atmospheric pollution 	Maximum w/c	0.5	Minimum cover 50 mm
	Minimum cement content	330 kg / m ³	
Category 4 <ul style="list-style-type: none"> Abrasion Corrosive atmosphere Corrosive water Marine conditions: wetting and drying sea spray within 1km of sea coast Application of de-icing salt 	Maximum w/c	0.45	Minimum cover 65 mm
	Minimum cement content	400 kg / m ³	

Table 3.8 Suggested specification and detailing requirements for concrete exposed to various environments.

No.	Exposure classification	Likelihood of A2	Likelihood of CHL2
1	Below low water level (submerged)	High	Low
2	In tidal zone (also wetting and drying zone)	Medium	High
3	In Splash Zone	Medium	High
4	In Splash - Spray zone (also wetting and drying zone)	Medium	High
5	In splash-tidal zone	Medium	Medium
6	Above Splash zone	Low	Medium
7	Well above splash zone (nearly top deck)	Low	Low
8	Benign Environment	Low	Low

Table 3.9 Likelihoods of A2 and CHL2 according to exposure classification.

For example, high moisture is essential in the occurrence of ASR. A supply of water may come from high humidity (Relative Humidity > 75%) or ground water (Rendell et al., 2002). For chloride induced corrosion, high moisture, high chloride and oxygen should be available. Table 3.9 shows likelihoods of A2 and CHL2 according to the exposure classification. Note that for other bridge components, such as deck, the event of excessive moisture could also be associated with climatic conditions including humidity and rainfall. Details of rules for assigning likelihoods ratings for each basic event are attached in Appendix A.

3.3.2 Input consequence ratings

Consequence ratings of each failure modes are required to be assigned by experts, considering the effects on load carrying capacity, the severity of expenditure of retrofitting or rehabilitation, and so on, as shown in Table 3.10. The model converts

these ratings into numerical ratings based on the same logarithmic, three point scale as likelihood ratings. Table 3.11 shows the opinion of a CRC research team comprising of QDMR, BCC, RMIT and QUT on the consequences ratings for the failure modes of piles malfunction. The value of consequence can be determined by assigning questionnaires to a group of experts and bridge inspectors, using weight factors to achieve a more reasonable result.

Consequence Rating	Description	Log Scale
1-Low	Deal with routinely, negligible expenditure	0.001
2-Medium	Requires significant maintenance expenditure	0.01
3-High	Greatly reduced durability, requires major maintenance expenditure	0.1

Table 3.10 Consequence ratings.

Failure modes	Consequence ratings
ASR	High
Chloride induced corrosion	High
Carbonation	Medium
Plastic shrinkage	Low

Table 3.11 Consequences ratings for failure modes of piles.

3.3.3 Fault tree calculation

The overall likelihood of failure modes can be calculated using the AND gate and OR gate equations. The approach starts with the basic events and goes through the fault tree to the top event. The probability of occurrence of ASR can be evaluated

by following steps:

$$P(PS_1) = P(PS_3) \cdot P(PS_4) \quad (3.3)$$

$$P(A_6) = 1 - [1 - P(PS_1)] \cdot [1 - P(PS_2)] \quad (3.4)$$

$$P(A_5) = 1 - [1 - P(A_6)] \cdot [1 - P(A_7)] \cdot [1 - P(A_8)] \quad (3.5)$$

$$P(A_3) = 1 - [1 - P(A_4)] \cdot [1 - P(A_5)] \quad (3.6)$$

$$P(ASR) = P(A_1) \cdot P(A_2) \cdot P(A_3) \quad (3.7)$$

Figure 3.13 and 3.14 shows the bottom-up calculation of the likelihood of occurrence of ASR with hypothetic inputs.

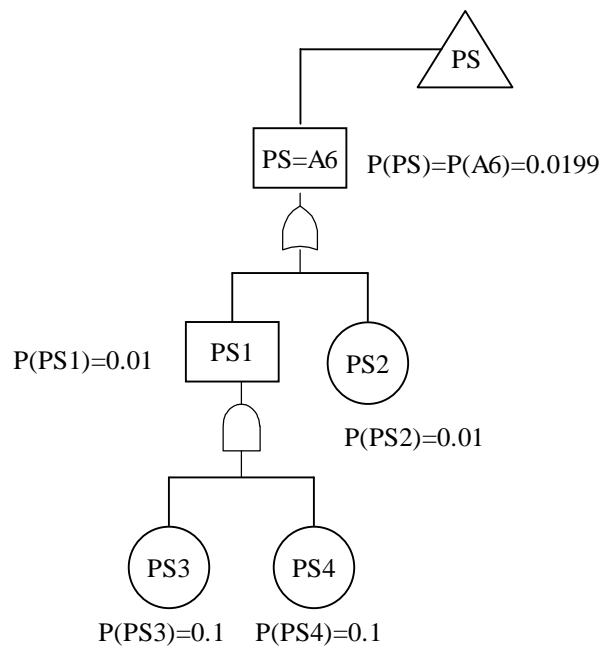


Figure 3.13 Example of calculation of the probability of top event of plastic shrinkage.

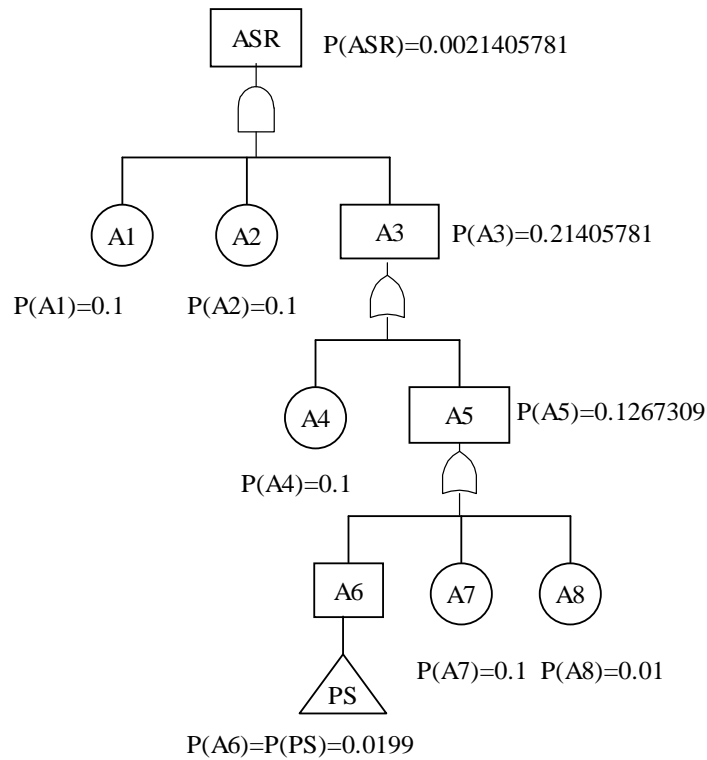


Figure 3.14 Example of calculation of the probability of top event of ASR on piles.

In order to exclude the difference resulting from disparate fault tree structures and to achieve more comparable results, in later calculations, likelihood of each failure mode calculated using logarithm scales have been normalized by assigning 0.1 to the one with the highest inputs and apportioning other results relative to this highest value, see Table 3.12.

Failure modes	Maximum likelihoods (Log scale)		
	Calculation results	Normalized results	Multiple
ASR	0.00350461	0.1	28.533845
Chloride induced corrosion	0.003522686	0.1	28.387429
Carbonation	0.0027829	0.1	35.933738
Plastic shrinkage	0.109	0.1	0.9174312

Table 3.12 Normalization of likelihoods.

3.3.4 Output risk ratings

Given that all the likelihoods and consequences are available, the risk of failure is calculated by multiplying likelihood and consequence. Table 3.13 shows the matrix of qualitative analysis of risk ratings according to the likelihoods and consequences ratings. In semi-quantitative analysis, the numerical risk calculated by logarithm scale is converted back into risk ratings on a scale from 0.0 (very low risk) to 3.0 (highest risk), shown in Table 3.14.

	Consequence		
Likelihood	Low	Medium	High
Low	Low	Low	Moderate
Medium	Low	Moderate	High
High	Moderate	High	High

Table 3.13 Risk matrix according to likelihoods and consequences.

Risk rating	Risk level	Description
0-1	Low	Acceptable risk, dealt with routine maintenance
1-2	Moderate	Questionable, requires significant review
2-3	High	Unacceptable high risk, harmful to the durability of structure, requires high maintenance costs

Table 3.14 Risk ratings.

3.4 Case study

3.4.1 Case description

The methodology proposed is validated using a case study bridge provided by Queensland Department of Main Roads, see Figure 3.15. It is the pier of a 25 years old seven span reinforced concrete bridge located in coastal zone. Each pier consists of a headstock supported by two cylindrical columns, which in turn is supported by a pilecap. The headstocks, columns and pilecaps are all cast insitu concrete. Below each pilecap are ten 450mm driven pre cast concrete piles. The location of the bridge is vital to the tourists, council and to the community. The pilecaps are located within the tidal zone. Cracking defects of the piles and pilecaps of the bridge were observed of which cores were undertaken for laboratory analysis. The result of visual inspection and laboratory testing shows that the pier pilecaps were suffering from chloride induced corrosion, see Figure 3.16. While the primarily reason for cracks on piles was ASR, as shown in Figure 3.17.

3.4.2 Inputs

The report of condition review mainly described problems with piles and pilecaps. Most inputs were identified from the condition review report. For example, piles are submerged below water level, according to Table 3.9, A2 for piles is “High” and CHL1 for piles is “Low”. While the pilecaps are located in tidal zone, so A2 for pilecaps is “Medium” and CHL1 for pilecaps is “High”. The remainder of

unspecified likelihoods were assumed to be “Medium”. Table 3.15 and 3.16 lists the inputs for the case pier piles and pilecaps respectively. Headstocks and columns were not assessed because the report does not mention any details for them.



Figure 3.15 Munna Point bridge.

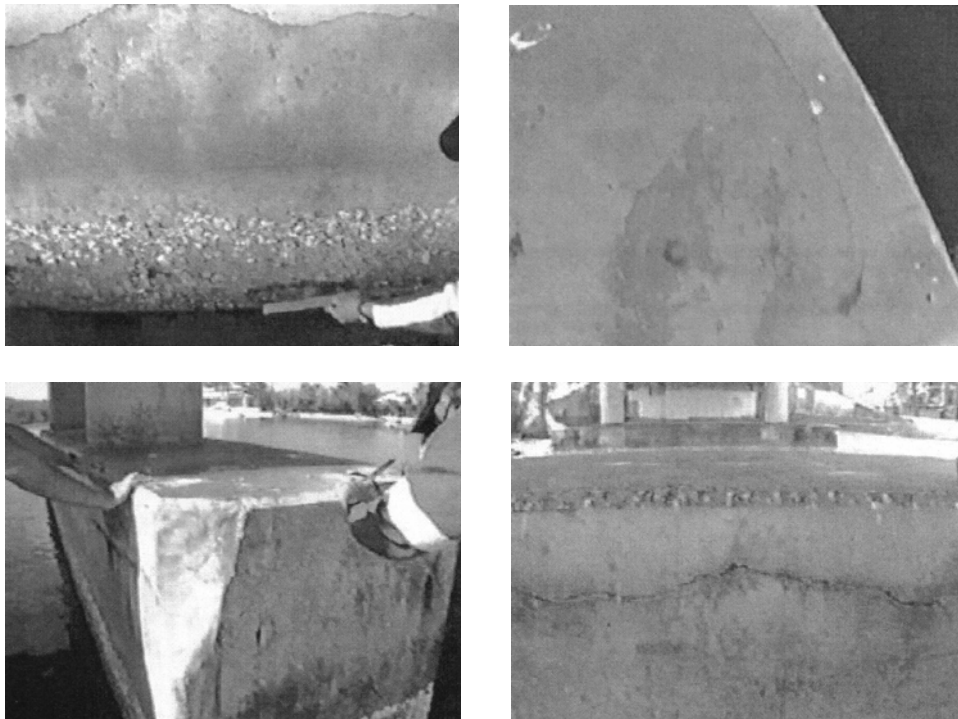


Figure 3.16 Cracks observed on pilecaps

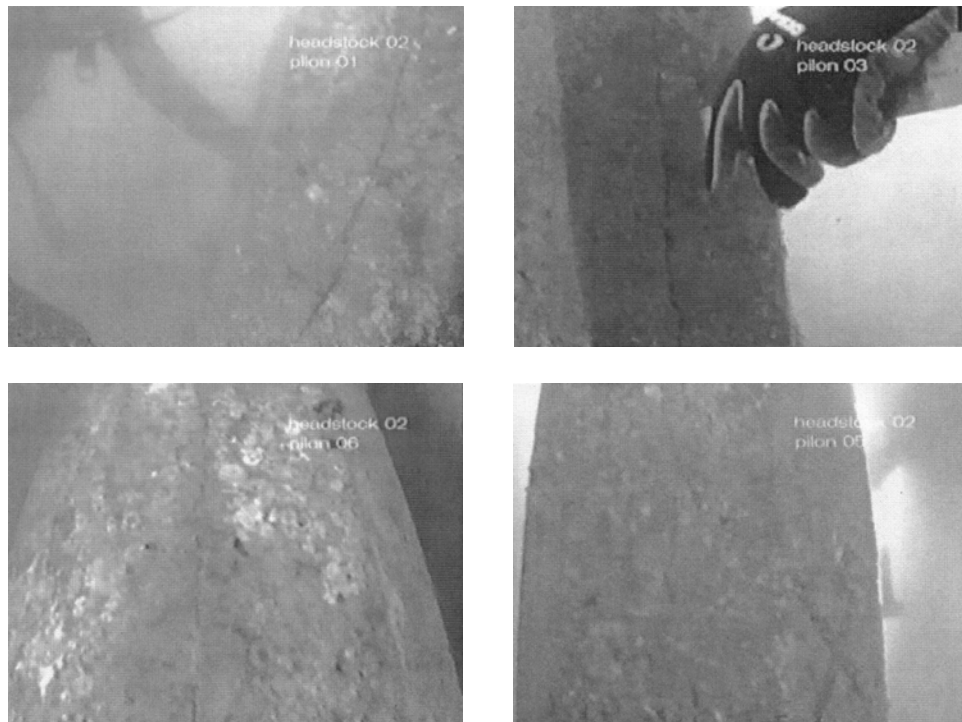


Figure 3.17 Cracks observed on piles.

Alkali-Silica Reaction	A1= High	A2= High	A4= High	A7= Medium	A8= Medium
Chloride induced corrosion	CHL1= High	CHL2= Low	CHL7= Medium	CHL9= Medium	CHL10= Medium
Carbonation	C1= Low	C2= High	C5= Medium	C6= Medium	
Plastic Shrinkage	PS2= Medium	PS3= Medium	PS4= Medium		

Table 3.15 Inputs table of case pier piles.

Alkali-Silica Reaction	A1= High	A2= Medium	A4= High	A7= Medium	A8= Medium
Chloride induced corrosion	CHL1= High	CHL2= High	CHL7= Medium	CHL9= Medium	CHL10= Medium
Carbonation	C1= Medium	C2= High	C5= Medium	C6= Medium	
Plastic Shrinkage	PS2= Medium	PS3= Medium	PS4= Medium		

Table 3.16 Inputs table for case pier pilecaps.

3.4.3 Results

To avoid overlooking high risks of individual failure modes, both the individual risk ratings and the total scaled risk ratings are required when comparing between projects or bridge components. As presented in Figure 3.18, the primary failure mode of the piles is ASR with a “High” risk and other failure modes all have acceptable risks. For the pilecaps, chloride induced corrosion is the major problem, followed by ASR with a questionable risk. The result of total scaled ratings indicates that the pilecaps has higher risk of failure than the piles. The result has general agreement with the result of investigation presented in the report.

3.4.4 Sensitivity analysis

Sensitivity analysis of the likelihoods and consequences mainly focuses on their

contribution to total scaled risk rating when vary each variables from “Medium” to “High”, see Table 3.17. It was found that varying the consequence rating will result in a notable difference on the total risk ratings. Changing the consequence rating of one failure mode would result in a 32.2% increment of the total scaled risk ratings. In the likelihoods of various basic events, water-cement ratio and the moisture in external environment related variables are the most sensitive ones. The total scaled risk ratings would increase by 52% if improper water-cement ratio is used in design. The use of poor material will produce a significant risk of poor performance and durability. The risk will be more severe if the bridge element is exposed to aggressive environment.

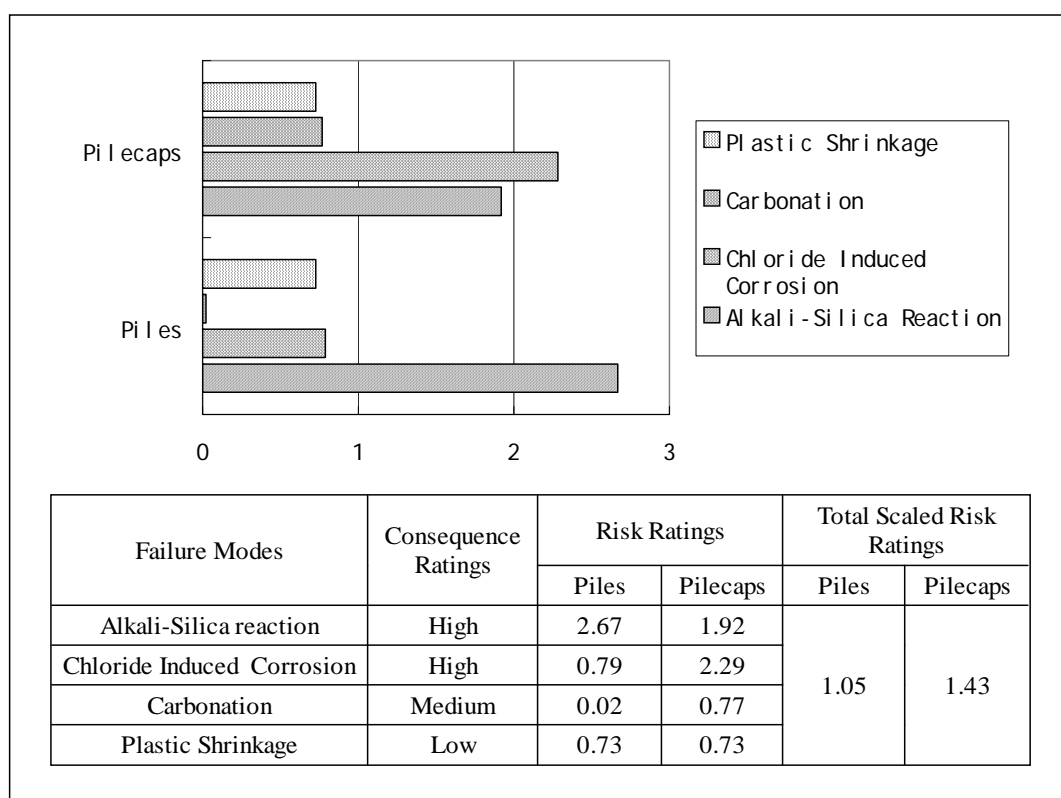


Figure 3.18 Result of risk ratings of case piles and pilecaps.

Variables			Variation of total scaled risk ratings
Likelihood ratings	Environment	Moisture	64.5%
		Chloride	32.2%
		Relative humidity	32.2%
		Carbon dioxide	32.2%
	Material	Water-cement ratio	52.0%
		Aggregates	32.2%
		Admixture	16.3%
		Cover depth	16.3%
	Construction		32.7%
Consequence ratings			32.2%

Table 3.17 Importance of variability of parameters on variability of total scaled risk ratings.

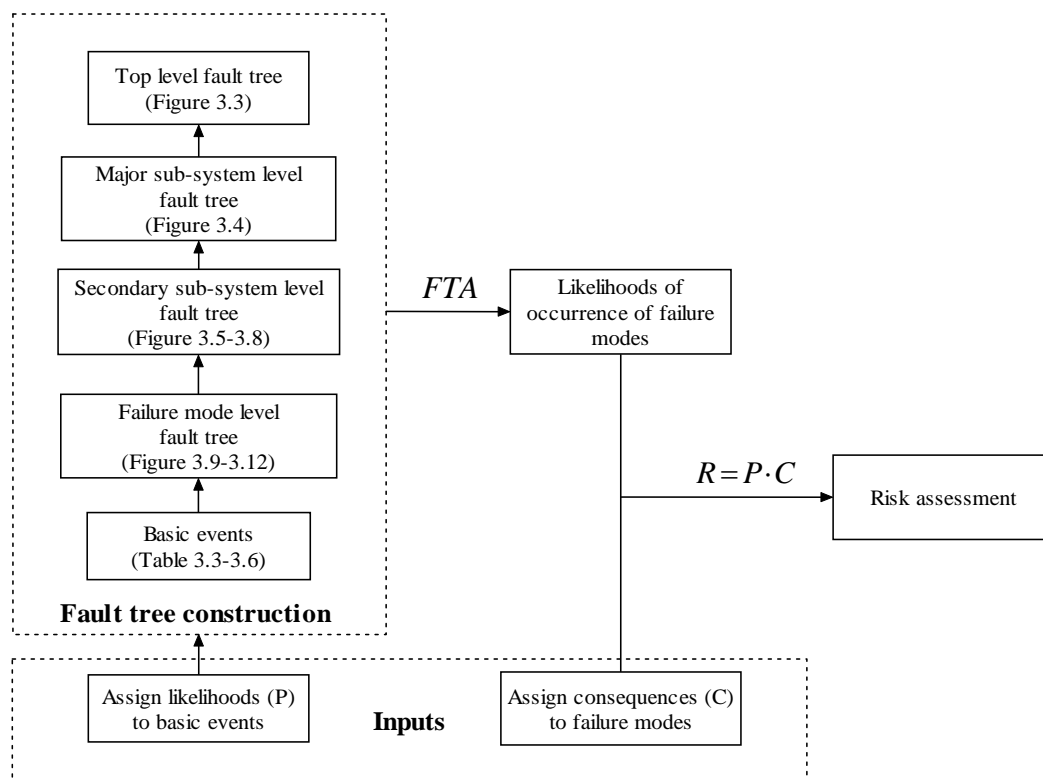


Figure 3.19 General procedure of using fault tree analysis on qualitative risk assessment of reinforced concrete bridges.

3.5 Conclusion

Using fault tree analysis on risk assessment of reinforced concrete bridges could lead to a qualitative assessment of the system risk of failure and risk ranking of bridge components affected by durability issues. The presented methodology of fault tree based risk assessment model can be concluded as shown in Figure 3.19. For reinforced concrete bridges, four common but important distress mechanisms were identified, they are chloride induced corrosion, alkali-silica reaction, carbonation and plastic shrinkage. Necessary and sufficient events involved in inducing these mechanisms related to design, material construction and exposed environment were identified as well as the logical relationships among them. The fault tree model was constructed incorporating these varieties. In this research, three scaled ratings of likelihoods and consequences are assigned to basic events and failure modes respectively as inputs. These inputs are converted into numerical ratings using logarithmic scales for further calculation. Outcomes of the total risk of failure are also scaled in ratings. A case pier column is studied to illustrate the procedure and calibrate the presented methodology. Risk ranking shows that the most severe failure modes for the case pier piles and pilecaps is ASR and chloride induced corrosion respectively, which is consistent with performance reports based on inspection and laboratory test. However, it is found in sensitivity analysis that the modeling results are sensitive to some parameters. The total scaled risk rating would increase by 52% when improper water-cement ratio is used compares to the normal situation. Consequences are one of the most sensitive parameters as well, which induce a 32.2% change of total scale risk rating when changing from “Medium” to “High”.

CHAPTER 4 PROBABILISTIC TIME-DEPENDENT RELIABILITY ANALYSIS OF DETERIORATED REINFORCED CONCRETE BRIDGE COMPONENTS

4.1 Introduction

Reliability is an important index to represent the performance of a structure. For existing bridges, service load might increase with time and the resistance capacity might degrade due to corrosion or fatigue. Failure occurs when the load effect exceeds the resistance. Thus the estimation of time-dependent reliability for structures or structural components should be based on probabilistic modeling of both the time-dependent resistances and the load effects. Generally, the time-dependent reliability can be expressed as the probability of failure p_f or reliability index β , as,

$$p_f(t) = \phi[-\beta(t)] = P[R(t) \leq S(t)] \quad (4.1)$$

where $R(t)$ is the resistance at time t , $S(t)$ is the load effect at time t and ϕ is the standard normal distribution function. Typical relationship between load effects and resistance over the service life of a bridge is shown in Figure 4.1.

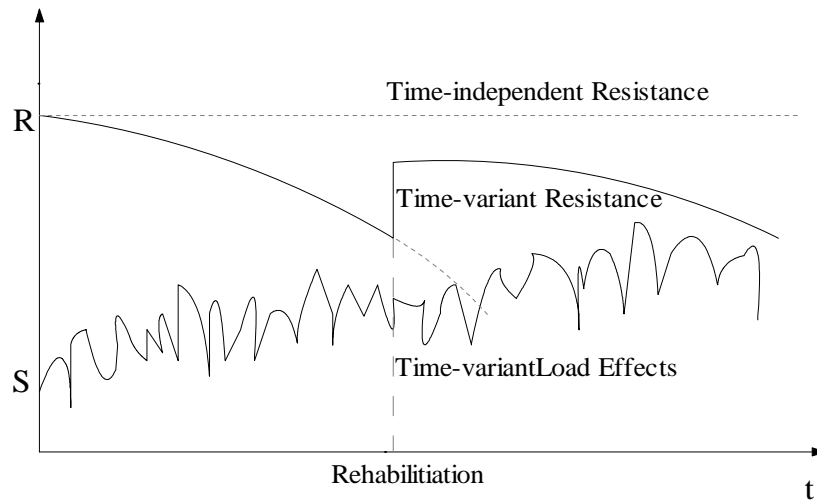


Figure 4.1 Realizations of time-dependent resistance and time various load effects.

Figure 4.2 presents a process for rehabilitation decision making of aging bridges. Reliability-based life cycle cost analysis was used here as the criterion for selecting and optimizing rehabilitation plans. Updating the reliability over the life cycle of a structure is of significance in the following aspects (Stewart, 2001):

- bridge assessment by comparing the reliability-based acceptance criteria and prediction of possible service life,
- determining maintenance priority of a groups of bridges up for repair or maintenance by ranking the reliabilities,
- estimating the effectiveness of different maintenance strategies based on life cycle cost analysis.

The major focus of this work was to establish a generic methodology which can be applicable to many possible modes of failure. In achieving this objective, it was decided that one failure mechanism related to durability of reinforced concrete bridge components would be considered. The method developed is therefore based on the durability failure of reinforcement due to occurrence of one

failure mode. This can be applicable to other failure modes upon validation. As chloride induced corrosion is one of the major causes of deterioration of reinforced concrete structures, especially for the ones located in a marine environment, this chapter will present development of a methodology to quantitatively estimate the time-dependent reliability and probability of failure of reinforced concrete bridge components due to chloride induced corrosion.

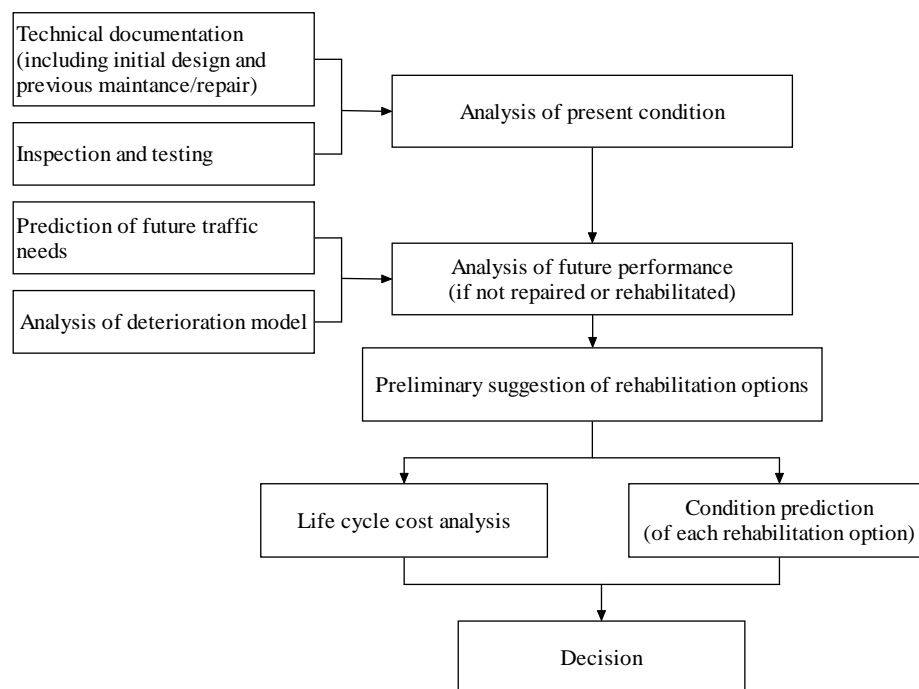


Figure 4.2 Management process of structural assessment and decision making

4.2 Probabilistic analysis of time-dependent resistance

The resistance of reinforced concrete structures can degrade in service due to complicated combinations of various reasons. The degradation is an irreversible process unless appropriate repair or rehabilitation work is done. Parameters which

can affect the resistance of RC structures might include changes of material properties, area loss of steel reinforcement and the bond strength loss due to carbonation and corrosion of steel reinforcement. At present, analysis in this research has been performed at an element level considering that the primary reason for degradation of resistance is only the area loss of steel reinforcement due to corrosion of steel. Changes of mechanical properties of materials and the bond strength loss result from corrosion are not considered.

4.2.1 Chloride induced corrosion

4.2.1.1 Chloride concentration

Most present models assume that chloride induced corrosion is initiated by the diffusion of chloride ions, in other words, the process of chloride ingress into concrete is generally assumed to obey the Fick's second law of diffusion (Enright and Frangopol, 1998b, Thoft-Christensen, 1998). The corrosion of reinforcement commence when the surface concentration of chloride ions reaches a critical threshold value. According to Fick's second law, the chloride content $[C(x, t)]$ with a distance x form concrete surface at time t can be simplified as (Stewart and Rosowsky, 1998),

$$C(x, t) = C_0 \left[1 - \operatorname{erf} \left(\frac{x}{2\sqrt{tD}} \right) \right] \quad (4.2)$$

where C_0 is the surface chloride concentration (kg / m^3 or % weight of concrete),

D is the chloride diffusion coefficient ($cm^2 / year$) and erf is the error function.

Based on Equation 4.2, the corrosion initiation time can be formulated by (Thoft-Christensen, 1998):

$$T_i = \frac{X^2}{4D} \left[\operatorname{erf}^{-1} \left(\frac{C_o - C_{cr}}{C_o} \right) \right]^2 \quad (4.3)$$

where X is the concrete cover (cm), C_{cr} is the critical chloride concentration at which corrosion begins (kg/m^3 or % weight of concrete).

The corrosion initiation time can be determined based on the distribution of four random variables (X, D, C_o, C_{cr}). In fact, the distribution and descriptors of the distribution are extremely diverse for different bridge structures and exposed environments. Field conditions seldom agree with that assumed with Fick's law, some studies point out that it is not a good model to illustrate chloride penetration. However, it is often used in many cases since it shows agreement with some laboratory and field data (Stewart and Rosowsky, 1998).

Many studies have focused on improving the corrosion initiation models based on numerical calculation and empirical expressions for main random variables mentioned in Equation 4.3. Following sections will identify the models and data used in this research.

4.2.1.1.1 Surface chloride concentration-- C_o

For structural components affected by de-icing salts typically deck, surface chloride concentration may be vary for different amounts of de-icing salts, location of

de-icing salts, efficiency of drainage, quality of expansion joints, etc. Hoffman and Weyers (1994) concluded that the mean of surface chloride concentration is $3.5 \text{ kg} / \text{m}^3$ with a lognormal distribution and the coefficient of variation is 0.5. This data was obtained based on studies in samples taken from 321 concrete bridge decks in USA.

For marine structures, the surface chloride concentration depends mainly on the proximity to seawater. Corrosion risk is low for structures in submerged zone where oxygen is not available. However, in splash and tidal zones, chlorides accumulated on the surface of concrete cover results in extreme high values of the surface chloride concentration. Based on data from onshore structures in Victoria, Australia, Collins and Grace (1997) suggested a lognormal distribution for the surface chloride concentration with mean equals $7.35 \text{ kg} / \text{m}^3$. In this research, the coefficient of variation is assumed to be 0.5. It is applicable for substructures of onshore bridges such as pier columns and pilecaps.

For offshore structures with influence from marine atmosphere, chloride ions carried by wind can accumulate on the surface of concrete. After examining corrosion in sample bridges from Tasmanian, Australia, McGee (2000) expressed the surface chloride concentration as a function of distance from the coast:

$$C_o(d) = \begin{cases} 2.95 \text{ kg} / \text{m}^3 & d < 0.1 \text{ km} \\ 1.15 - 1.81 \cdot \log_{10}(d) & 0.1 \text{ km} < d < 2.84 \text{ km} \\ 0.03 \text{ kg} / \text{m}^3 & d > 2.84 \text{ km} \end{cases} \quad (4.4)$$

where d is the distance from the coast (km). The coefficient of variation was 0.49 for those structures with distances exceed 0.1 km from the coast. The height above

seawater level is not an important consideration. For this research, the surface chloride concentration is modeled as a lognormal distribution with the mean value determined by equation 4.4 and a 0.5 coefficient of variation.

4.2.1.1.2 Diffusion coefficient-- D

The chloride diffusion coefficient has a close relationship with the permeability of concrete, which is influenced by water-cement ratio, cement type, curing, compaction and relative humidity, etc. It is not affected significantly by the source of chloride ions. Papadakis et al. (1996) modeled the diffusion coefficient as:

$$D = D_{H_2O} \cdot 0.15 \cdot \frac{1 + \rho_c \frac{w}{c}}{1 + \rho_c \frac{w}{c} + \frac{\rho_c}{\rho_a} \cdot \frac{a}{c}} \left(\frac{\rho_c \frac{w}{c} - 0.85}{1 + \rho_c \frac{w}{c}} \right)^3 (cm^2 / s) \quad (4.5)$$

where,

$\frac{a}{c}$ is the aggregate-to-cement ratio,

ρ_c is the mass density of cement,

ρ_a is the mass density of aggregates

D_{H_2O} is the chloride diffusion coefficient in an infinite solution, which equals

$1.6 \times 10^{-5} cm^2 / s$ for NaCl,

$\frac{w}{c}$ is the water-cement ratio, estimated from Bolomey's formula, namely

$$\frac{w}{c} = \frac{27}{f'_{cyl} + 13.5} \quad (4.6)$$

f'_{cyl} is the concrete compressive strength of a standard test cylinder in MPa .

The result of diffusion coefficient for an ordinary concrete mix is approximately $2.8 \times 10^{-12} m^2 / s$. This model has the best fit to available literature and laboratory data (Vu and Stewart, 2000). However, it is only efficient if sufficient experimental data is available because it is not straightforward to obtain data of concrete properties (e.g., $\frac{w}{c}, \frac{a}{c}, \rho_c, \rho_a$) of existing structures. In this research, ρ_c , ρ_a and $\frac{a}{c}$ is assumed to be 3.16, 2.6 and 2 respectively (Papadakis et al., 1996).

4.2.1.1.3 Critical chloride concentration-- C_{cr}

As mentioned in previous sections, the corrosion of reinforcement is initiated when the chloride content exceeds a threshold value with sufficient moisture and oxygen. The critical chloride concentration is one of the most important parameters to determine the corrosion initiation time. Critical chloride concentration can be influenced by concrete properties such as mix proportions, water-cement ratio, and environmental factors such as temperature and relative humidity. Many studies have suggested the value and distribution of critical chloride concentration based on experimental data. Alonso et al. (2000) compiled numerous data from different studies and concluded that the critical chloride concentration may lie in a range from $0.5-10 kg/m^3$ with few values above $3 kg/m^3$. In this research, a uniform distribution within the range of $0.6-1.2 kg/m^3$ for the critical chloride concentration is used based on recommend data by Stewart and Rosowsky (1998).

4.2.1.1.4 Comparison of chloride concentration

After identifying all the variables related to the chloride concentration, a deterministic approach is initially used here to qualitatively illustrate the effect of different exposure environments and different concrete qualities on the chloride concentration. Following are three typical exposure environments of RC elements considered in this research:

- de-icing salts, $C_0 = 3.5 \text{ kg} / \text{m}^3$
- onshore splash zone, $C_0 = 7.35 \text{ kg} / \text{m}^3$
- offshore with 50m distance from coast, $C_0 = 2.95 \text{ kg} / \text{m}^3$

Generally, with the same concrete quality, the chloride concentration increase with the increase of the surface chloride concentration, as shown in Figure 4.3. Figure 4.4 compared the chloride concentration under each exposure environment with different concrete qualities. Chloride concentration in poor quality of concrete has the highest value. It can be obviously seen that, use of suitable quality of concrete could reduce up to 50% chloride content, which might be of significance to defer the initiation of corrosion and increase possible service life.

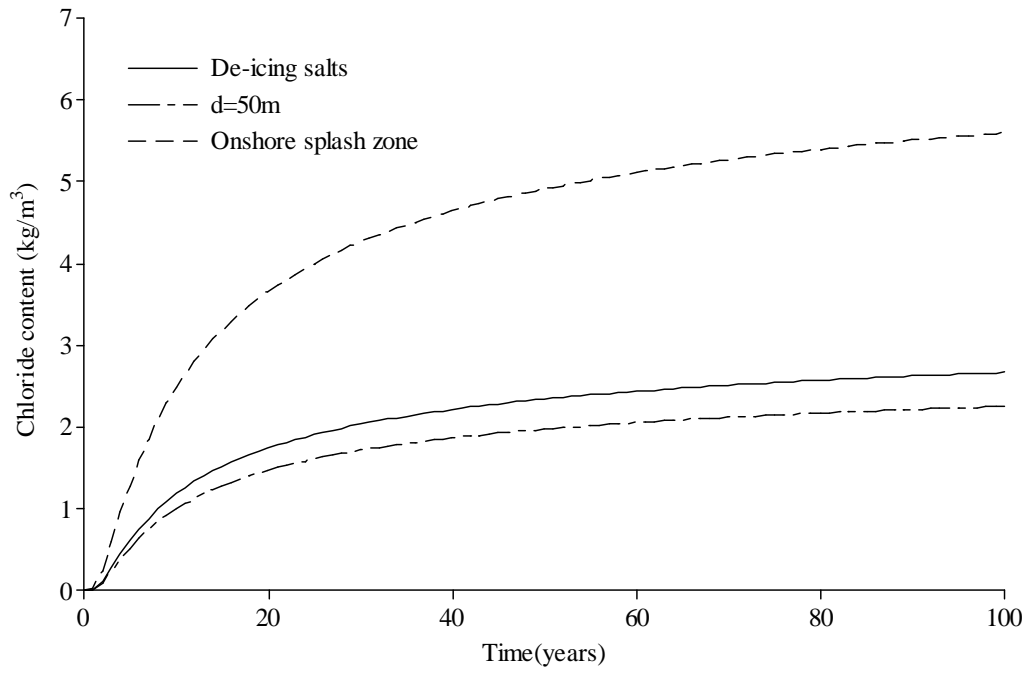


Figure 4.3 Chloride concentrations at a depth 50mm from the surface for ordinary concrete mix.

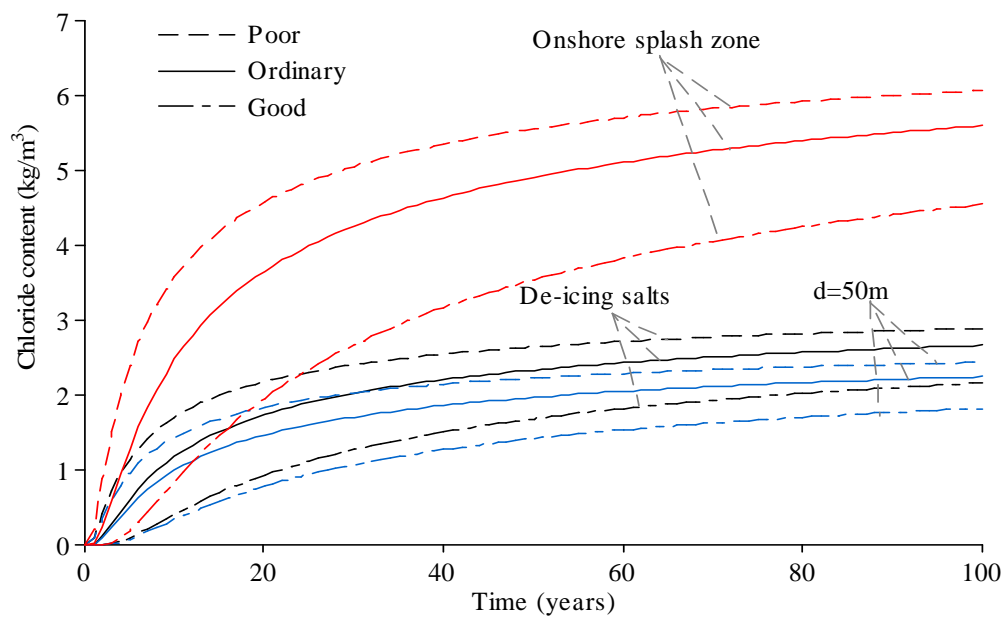


Figure 4.4 Chloride concentrations at a depth 50mm from the surface for coastal zone structures.

4.2.1.1.5 Probabilistic modeling of distribution of corrosion initiation time

Summarizing previous sections, statistical characteristics of all the random variables correlated to corrosion initiation time T_i are shown below in Table 4.1. Monte Carlo simulation is used as the computational procedure. For an example RC element located 50m from the coast with ordinary concrete mix and ordinary concrete cover depth ($w/c = 0.55$ and concrete cover depth=50 mm), the modeling result for the probability density function of corrosion initiation time is displayed in Figure 4.5. 10, 000 samples were obtained using Monte Carlo simulation function of software @Risk. As the value of corrosion initiation time is significant only within the service life of the bridge, samples above 100 years are meaningless and were filtered out. Statistical analysis concludes that this group of samples fits a lognormal distribution well and probabilistic properties of corrosion initiation time obtained from filtered samples can better represent its distribution.

Distribution of the corrosion initiation time would be different with varying concrete quality and location of the RC elements. Figure 4.6 to 4.11 illustrates the influence of water-cement ratio and concrete cover depth on the distribution of corrosion initiation time under different exposure environments. Generally, the corrosion begins earlier in a poor concrete quality element (high water-cement ratio or insufficient cover depth). Mean and standard deviation of the corrosion initiation time both increase with the improvement of concrete quality. Moreover, under the same concrete condition, mean and standard deviation of the corrosion initiation time of RC elements located in a splash zone would be extremely early, which is probably due to the high surface chloride concentration of continuous sea water

splash.

However, coefficient of variation (COV) of modeling results of the corrosion initiation time based on data in Table 4.1 is high, which means the results have a high degree of uncertainty. Sensitivity analysis has been conducted using the same example RC element mentioned above, as shown in Figure 4.12, with the COV of surface chloride concentration C_0 varying from 0.5 to 0.1, the mean corrosion initiation time decreases gradually, while the variability of corrosion initiation time drops substantially. More sensitivity analysis results can be found in Enright and Frangopol's (1998b) research in which specific parametric studies have been done to illustrate the sensitivity of the corrosion initiation time to the main descriptors of each input random variable. As the corrosion initiation time is a key parameter in posterior studies, in practical applications, it is better to use more certain inputs to ensure less variable modeling results. Modifications can be made by combining inspection data of particular cases, laboratory data and experiential formulations. Detailed data and calculation for modeling corrosion initiation time is shown in Appendix B.

Variable		Mean	Coefficient of variation	Distribution
$C_0 (kg / m^3)$	de-icing salts	3.5	0.5	Lognormal
	onshore splash zone	7.35	0.5	Lognormal
	coastal zone	Equation 4.4	0.5	Lognormal
$X (mm)$		Specified+6	$\sigma = 11.5$	Normal (Val and Stewart, 2003)
$D (cm^2 / year)$		Equation 4.5	0.2	Normal
$C_{cr} (kg / m^3)$		0.9		Uniform range from 0.6 to 1.2

Table 4.1 Statistical characteristics of chloride concentration variables.

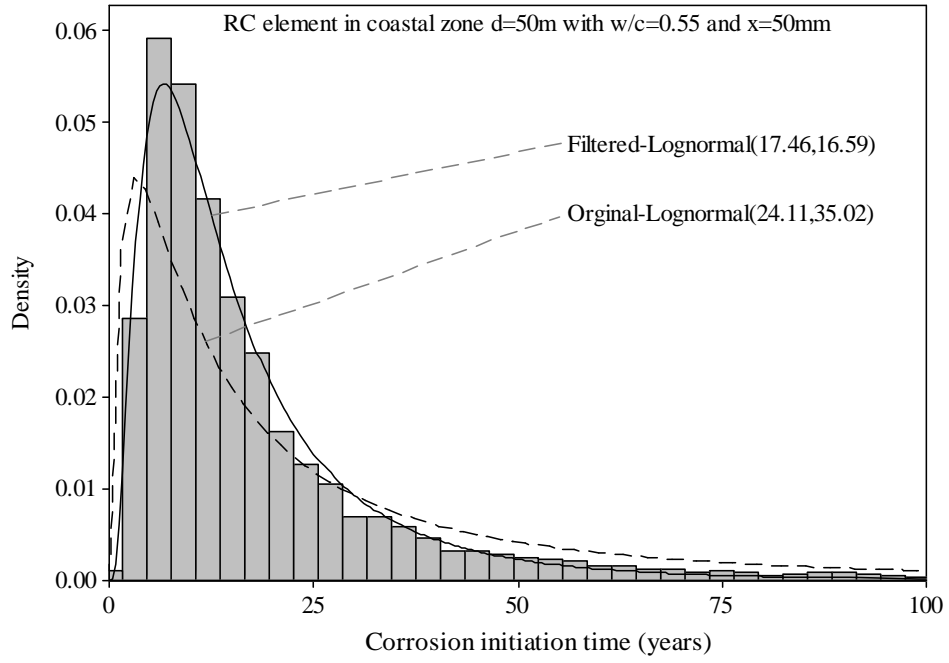


Figure 4.5 Probability density function fit of corrosion initiation time of RC elements located 50m from coast with ordinary concrete mix ($w/c=0.55$) and concrete cover depth $x=50\text{mm}$.

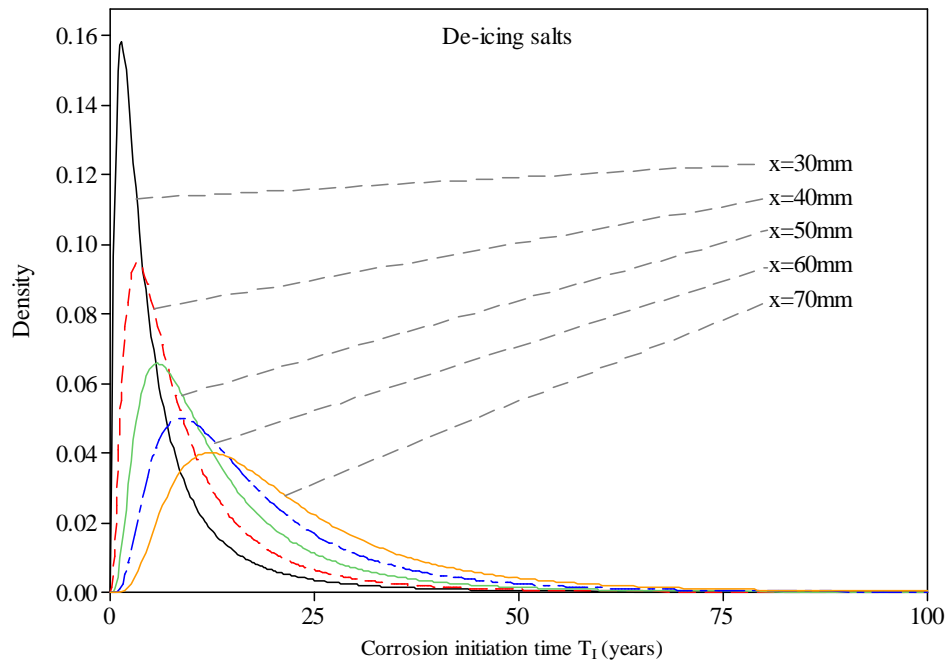


Figure 4.6 Probability density function of corrosion initiation time of de-icing salts affected RC elements with ordinary concrete mix ($w/c=0.55$).

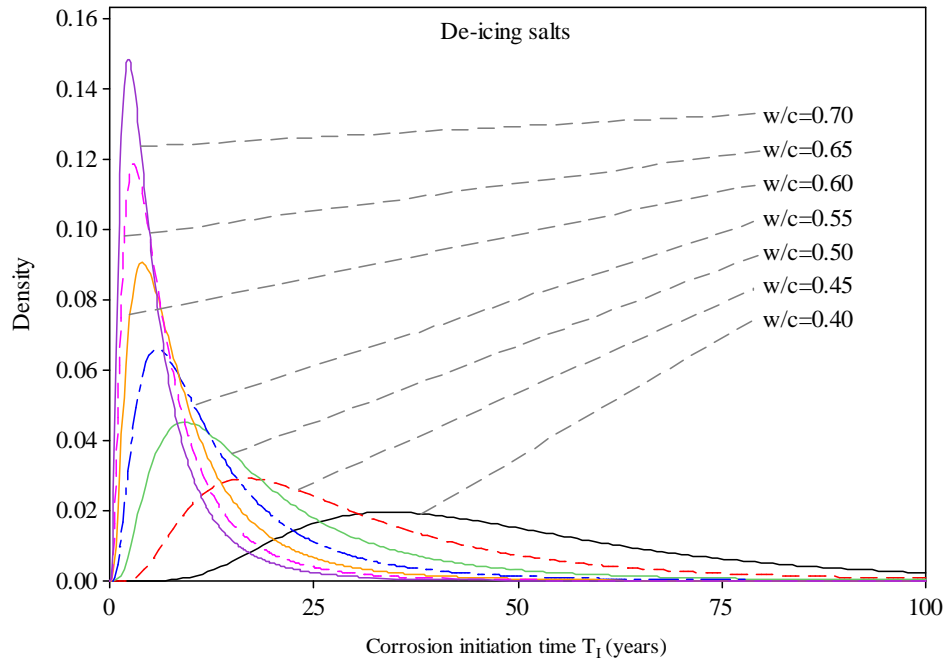


Figure 4.7 Probability density function of corrosion initiation time of de-icing salts affected RC elements with cover depth $x=50\text{mm}$.

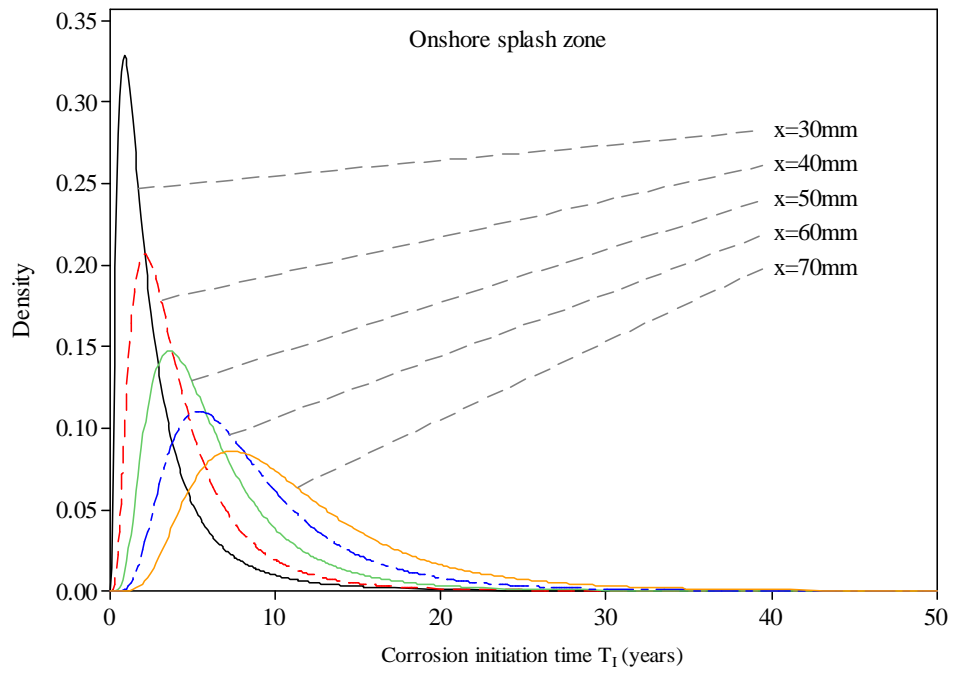


Figure 4.8 Probability density function of corrosion initiation time of onshore splash zone RC elements with ordinary concrete mix ($w/c=0.55$).

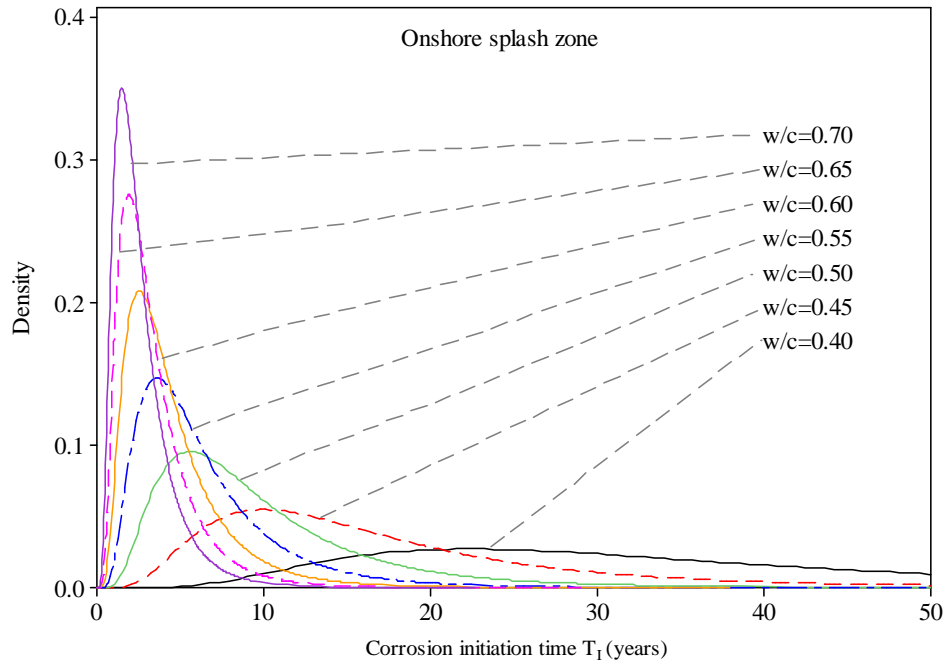


Figure 4.9 Probability density function of corrosion initiation time of onshore splash zone RC elements with cover depth $x=50\text{mm}$.

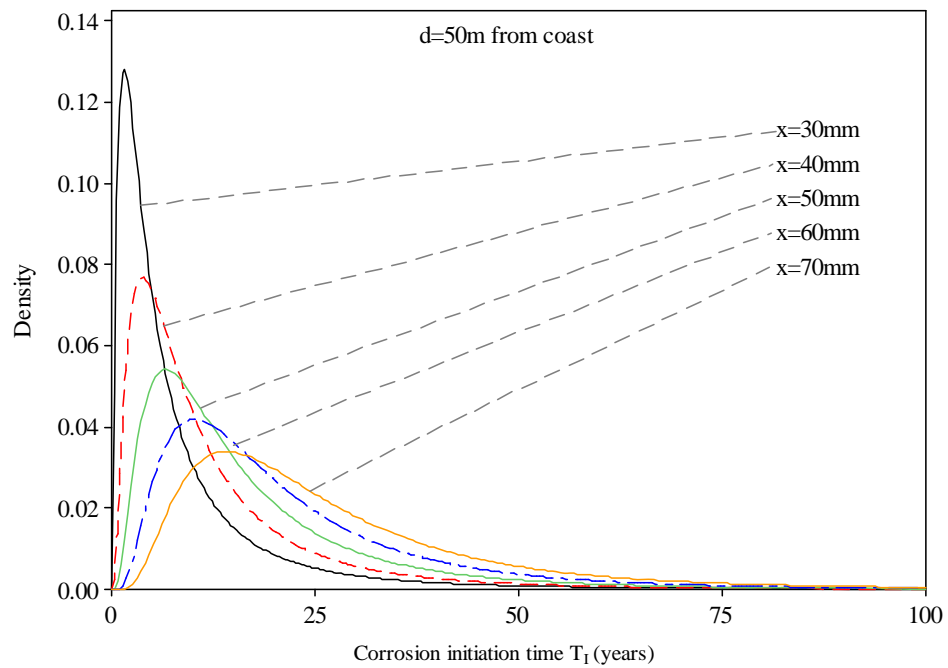


Figure 4.10 Probability density function of corrosion initiation time of RC elements located 50m from coast with ordinary concrete mix ($w/c=0.55$).

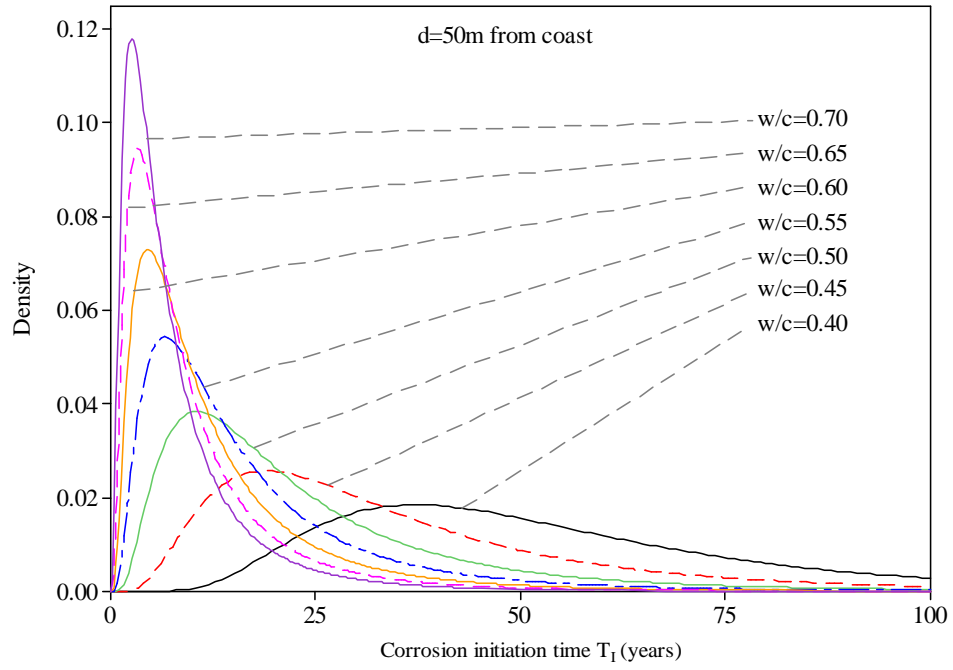


Figure 4.11 Probability density function of corrosion initiation time of RC elements located 50m from coast with cover depth $x=50$ mm.

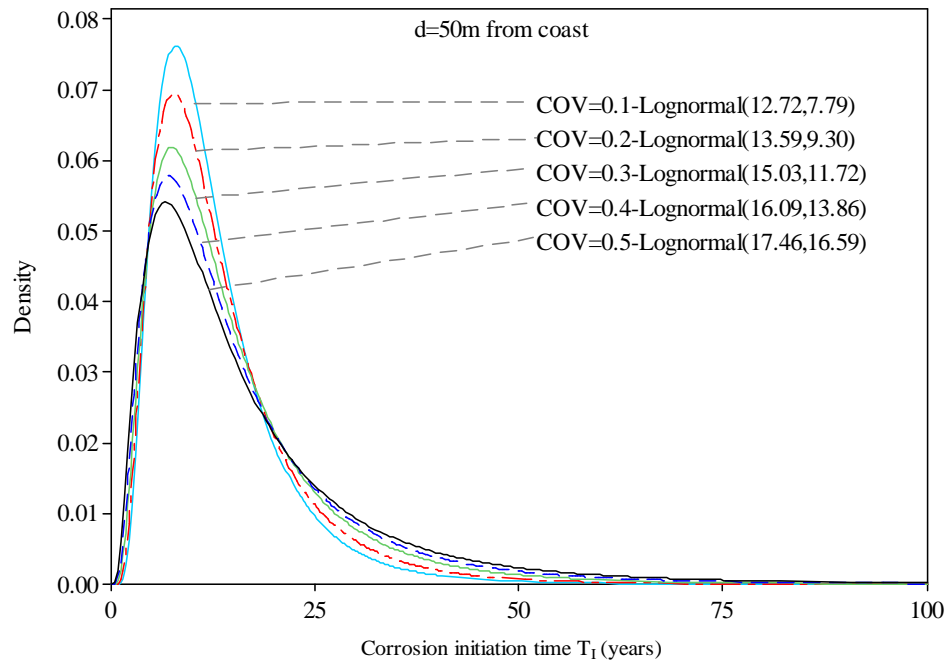


Figure 4.12 Effect of coefficient of variation of surface chloride concentration $COV(C_0)$ on distribution of corrosion initiation time.

4.2.1.2 Corrosion propagation

Corrosion propagation is recognized as an electrochemical process. A parameter to measure the corrosion rate is called corrosion current, i_{corr} . Once the corrosion initiate, the protective oxide layer on the surface of reinforcement has been damaged and the corrosion will be ongoing with a corrosion rate depending on the availability of moisture and oxygen, temperature and resistivity of concrete (Hunkeler, 2005). Vu and Stewart (2000) developed an improved model, that is, for a typical environmental condition: humidity 75%, temperature 20° C ,

$$i_{corr}(1) = \frac{3.78(1 - \frac{w}{c})^{-1.64}}{cover} \quad (\mu A / cm^2) \quad (4.7)$$

where $i_{corr}(1)$ is the corrosion current at the beginning of corrosion propagation, and the cover depth is given in cm. Figure 4.13 shows the effect of concrete quality and depth of concrete cover on the initial corrosion current. Three typical values of water-cement ratio were assigned to be 0.45, 0.55 and 0.65 to represent good, ordinary and poor quality of concrete respectively. Model error of the initial corrosion current can form to a normal distribution with mean equals 1.0 and the coefficient of variation equals 0.2.

It has been suggested that the corrosion rate will reduce with time. The reduction rate would be rapid during the first few years after initiation and then much more slow the next years. Liu and Weyers (1998) had developed a formulation to estimate the reduction of corrosion current over time, which is

$$i_{corr}(t_p) = i_{corr}(1) \cdot 0.85t_p^{-0.29} \quad (4.8)$$

where t_p is the time since corrosion initiated. (See Figure 4.14)

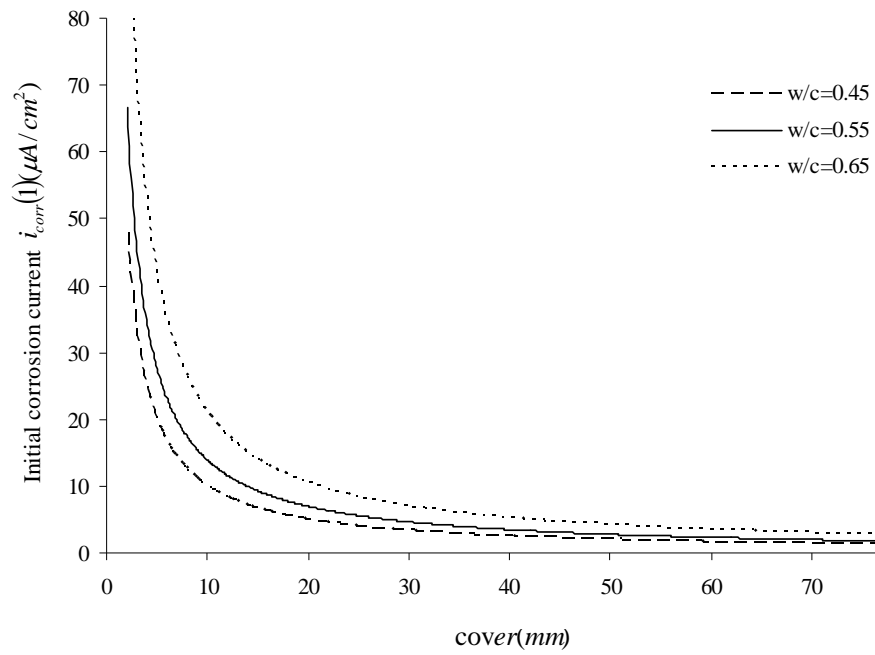


Figure 4.13 Influence of water-cement ratio and cover on initial corrosion current.

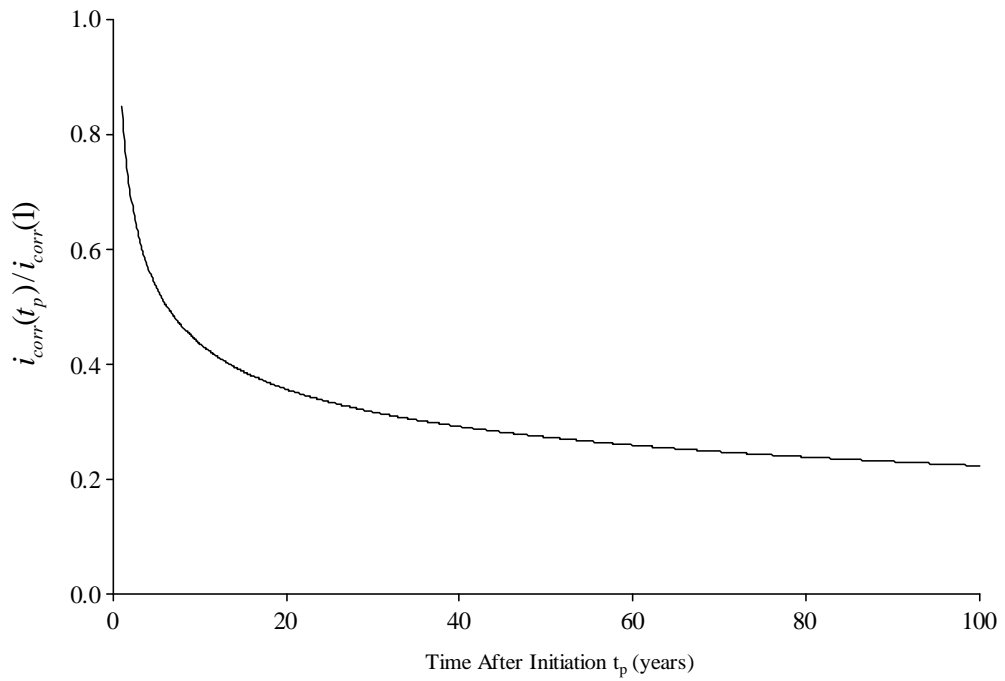


Figure 4.14 Reduction of corrosion current over time.

General corrosion represents that the corrosion causes approximately uniform area loss over the surface of the steel bars. In this case, according to Faraday's law, a corrosion current of $i_{corr} = 1\mu A/cm^2$ equals to an area loss of steel section of $11.6\mu m/year$ (Val and Melchers, 1997). The penetration depth (mm) in a steel bar after corroded t_p years can be formulated as,

$$\begin{aligned} p(t_p) &= 0.0116 \times \left[1 + \int_1^{t_p} i_{corr}(t) \cdot dt \right] = 0.0116 i_{corr}(1) \left[1 + \int_1^{t_p} t^{-0.29} \cdot dt \right] \\ &= 0.0116 i_{corr}(1) \left[1 + \frac{t_p^{0.71} - 1}{0.71} \right] \end{aligned} \quad (4.9)$$

There is another type of corrosion which localized to a small area on the surface of a rebar but could result in severe area loss of the cross-section. It is often found in chloride induced corrosion. Observed pits can be in various forms. A hemispherical form is assumed here for simplicity. For localized corrosion, the maximum penetration depth p_{max} is significantly higher than the general situation. Val and Melchers (1997) assumed the ratio $R = p_{max} / p(t_p)$ to be a uniform distribution from 4 to 8. Gonzalez et al. (1995) found the value of the ratio is varied from 2.8 to 8.9 based on experimental results. So the radius of the pit for localized corrosion can be expressed as,

$$p_{max}(t_p) = 0.0116 i_{corr}(1) \left[1 + \frac{t_p^{0.71} - 1}{0.71} \right] R \quad (4.10)$$

A uniform distribution between 3.5 and 8.5 is taken here for R .

4.2.1.2.1 Area loss of steel reinforcement

Based on formulations presented in previous sections, the area loss of steel reinforcement cross section under general corrosion and localized corrosion can be concluded as Equation 4.11 and 4.12, shown in Table 4.2 and 4.3. t is the time since the structure was exposed to the chloride environment and t_p is the time since the corrosion initiation. In practice, both general corrosion and localized corrosion occur simultaneously. So it is necessary to have a combination model, see Table 4.4. For the sake of simplicity, it is assumed that at any time point, localized corrosion occurs immediately after general corrosion has been initiated.

Corrosion Type	General Corrosion
Cross Section Configuration	
Time-dependent Area of A Steel Bar	$A(t) = \frac{\pi}{4} [D(t)]^2 \quad (4.11)$ <p>where,</p> $D(t) = \begin{cases} D_0 & t < T_I \\ D_0 - 2p(t_p) & t \geq T_I \end{cases}$ $t_p = t - T_I \quad (\text{Enright and Frangopol, 1998b})$ $p(t_p) = 0.0116i_{corr}(1) \left[1 + \frac{(t_p)^{0.71} - 1}{0.71} \right]$

Table 4.2 Calculation of area loss of steel reinforcement cross section under general corrosion.

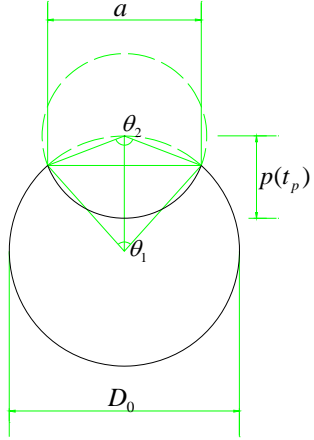
Corrosion Type	Localized Corrosion
Cross Section Configuration	
Time-dependent Area of A Steel Bar	$A(t) = \begin{cases} \frac{\pi D_0^2}{4} - A_1 - A_2 & p(t_p) \leq \frac{D_0}{\sqrt{2}} \\ A_1 - A_2 & p(t_p) \geq \frac{D_0}{\sqrt{2}} \end{cases} \quad (4.12)$ <p>where,</p> $A_1 = \frac{1}{2} \left[\theta_1 \left(\frac{D_0}{2} \right)^2 - a \left \frac{D_0}{2} - \frac{p(t_p)^2}{D_0} \right \right]$ $A_2 = \frac{1}{2} \left[\theta_2 p(t_p)^2 - a \frac{p(t_p)^2}{D_0} \right]$ $a = 2p(t_p) \sqrt{1 - \left[\frac{p(t_p)}{D_0} \right]^2}$ $\theta_1 = 2 \arcsin \left(\frac{a}{D_0} \right) \quad ; \quad \theta_2 = 2 \arcsin \left[\frac{a}{2p(t_p)} \right]$ <p>(Val and Melchers, 1997)</p> $t_p = t - T_I$ $p(t_p) = 0.0116 i_{corr} (1) \left[1 + \frac{(t_p)^{0.71} - 1}{0.71} \right] R$

Table 4.3 Calculation of area loss of steel reinforcement cross section under localized corrosion.

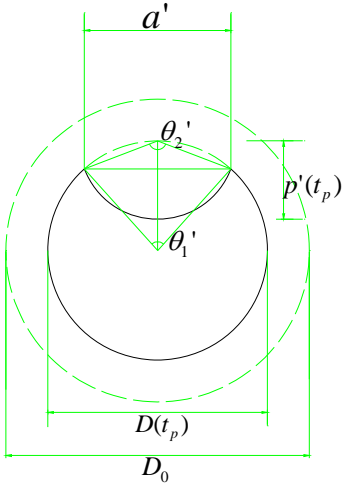
Corrosion Type	Combination Corrosion
Cross Section Configuration	
Time-dependent Area of A Steel Bar	$A(t) = \begin{cases} \frac{\pi D(t_p)^2}{4} - A_1' - A_2' & p'(t_p) \leq \frac{D(t_p)}{\sqrt{2}} \\ A_1' - A_2' & p'(t_p) \geq \frac{D(t_p)}{\sqrt{2}} \end{cases} \quad (4.13)$ <p>where,</p> $D(t_p) = D_0 - 0.0232i_{corr}(1) \left[1 + \frac{(t_p)^{0.71} - 1}{0.71} \right]$ $p'(t_p) = 0.0116i_{corr}(1) \left[1 + \frac{(t_p)^{0.71} - 1}{0.71} \right] R$ $A_1' = \frac{1}{2} \left[\theta_1' \left(\frac{D(t_p)}{2} \right)^2 - a' \left \frac{D(t_p)}{2} - \frac{p'(t_p)^2}{D(t_p)} \right \right]$ $A_2' = \frac{1}{2} \left[\theta_2' p'(t_p)^2 - a' \frac{p'(t_p)^2}{D(t_p)} \right]$ $a' = 2p'(t_p) \sqrt{1 - \left[\frac{p'(t_p)}{D(t_p)} \right]^2}$ $\theta_1' = 2 \arcsin \left[\frac{a'}{D(t_p)} \right] \quad ; \quad \theta_2' = 2 \arcsin \left[\frac{a'}{2p'(t_p)} \right]$ $t_p = t - T_l$

Table 4.4 Calculation of area loss of steel reinforcement cross section under combination corrosion.

4.2.1.2.2 Comparison of area loss

An example steel bar with initial diameter $D_0 = 32mm$ was initially explored using deterministic inputs. For localized corrosion, the value of R is assigned to be 6. Figure 4.15 compares the rate of area loss of the three forms of corrosion. Generally, localized corrosion has the slowest reduction rate of the cross-sectional area of the steel bar, followed by general corrosion, which can lead to a nearly 15% area loss of the cross-sectional area of steel bar after 100 years corrosion. As combination corrosion is the total effect of general corrosion and localized corrosion, it has the most observable reduction rate. Figure 4.16 and 4.17 illustrates the effect of concrete quality and cover depth on the area loss function. It can be seen that poor quality of concrete and insufficient cover depth could lead to a high corrosion current, which could result in a rapid decrease of the steel reinforcement cross-sectional area.

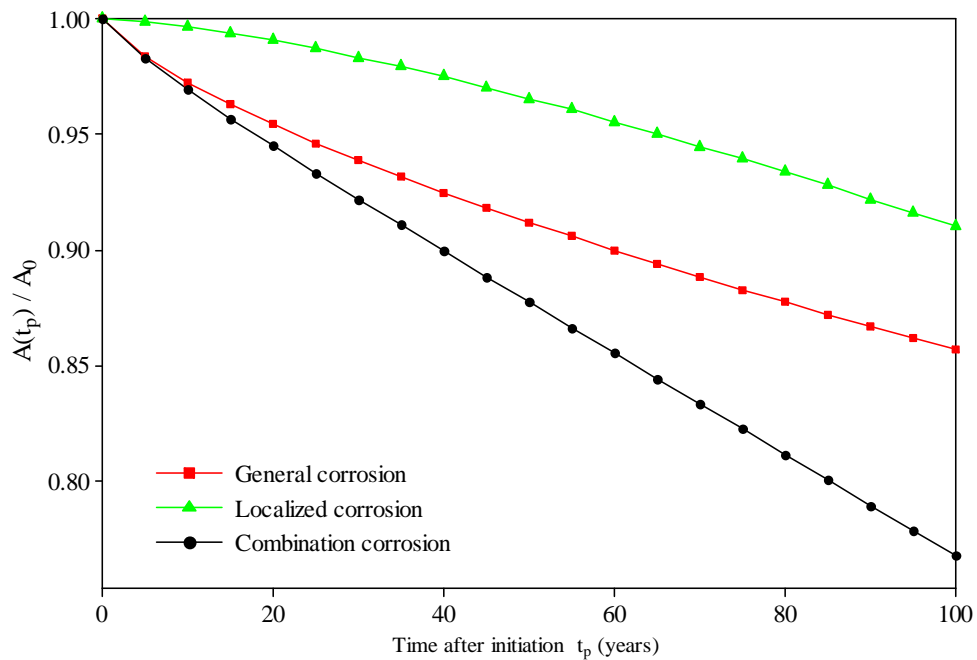


Figure 4.15 Area loss function comparison of different corrosion types for the sample steel bar.

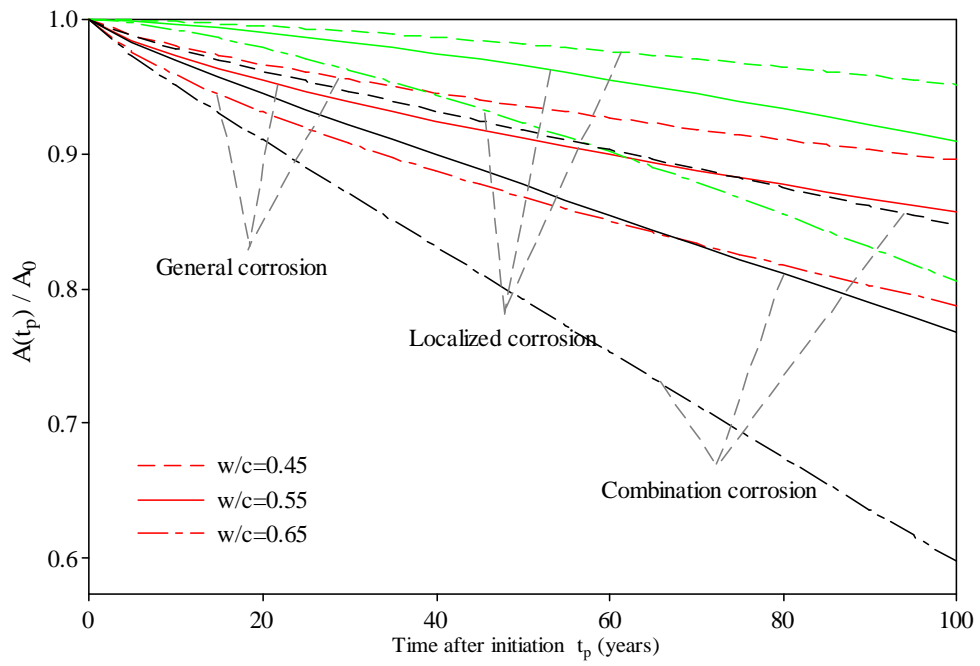


Figure 4.16 Area loss function comparison of different quality of concrete with cover=50mm.

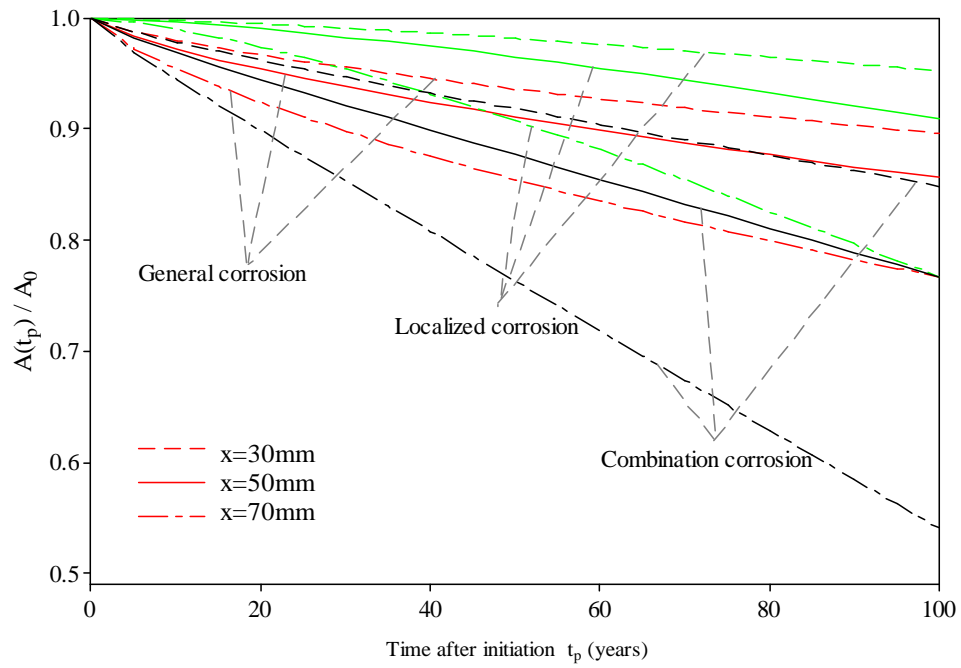


Figure 4.17 Area loss function comparison of different concrete cover depth with ordinary quality of concrete.

4.2.1.2.3 Probabilistic modeling of area loss

Statistical characteristics of all the random variables related to corrosion propagation are shown below in Table 4.5. The analysis chose one sample structural component located in onshore splash zone with $w/c=0.55$ and $x=50\text{ mm}$, the original diameter of reinforced steel was assigned to be 32 mm . Thus, the original area of steel bar is 804.25 mm^2 . All presented corrosion types including general corrosion, localized corrosion and combination corrosion were examined here.

Figure 4.18 to 4.20 are the histograms of samples and distribution fit of the residual area of one steel bar of example structure after 50 years exposure under general corrosion, localized corrosion and combination corrosion respectively. Based on statistical analysis, it can be concluded that the residual area of steel bar under general corrosion fits a normal distribution, while the residual area of steel bar subject to localized corrosion and combination corrosion fits a Weibull distribution. Figure 4.21 to 4.23 shows how the distributions of residual of steel bar change with exposure time. It can be concluded that, with the increase of exposure time, the mean value of the residual area of steel reinforcement decreases while the standard deviation increases. However, compared to general corrosion, the changes of standard deviation of residual area of steel reinforcement under localized corrosion and combination corrosion is more dramatic, which means the variability is much higher.

Variable	Mean	COV	Distribution
$D_0(mm)$	Specified	--	Deterministic
$T_I(year)$	Previous modeling results	Previous modeling results	Lognormal
$i_{corr}(1)$ ($\mu A/cm^2$)	Equation 4.7	0.2	Normal
R	6	0.24	Uniform range from 3.5 to 8.5

Table 4.5 Statistical characteristics of chloride propagation variables.

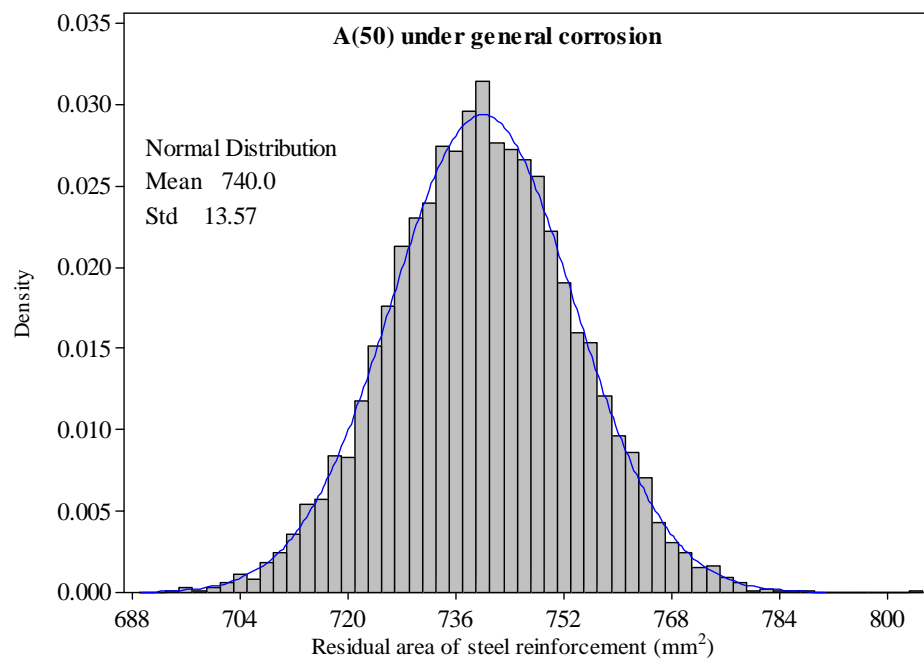


Figure 4.18 Histogram of residual area of steel reinforcement of the sample structural component after 50 years exposure under general corrosion.

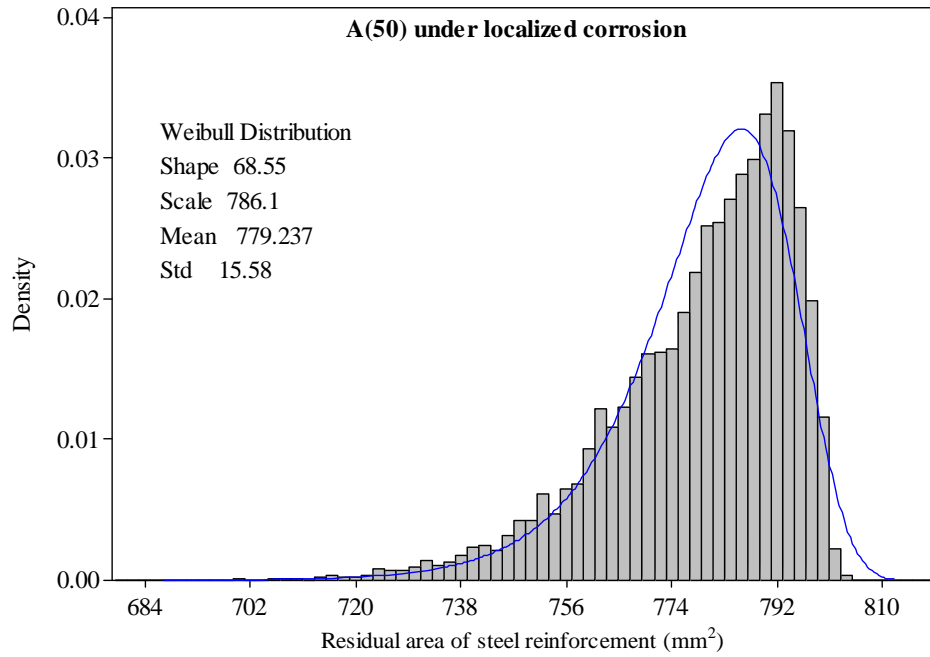


Figure 4.19 Histogram of residual area of steel reinforcement of the sample structural component after 50 years exposure under localized corrosion.

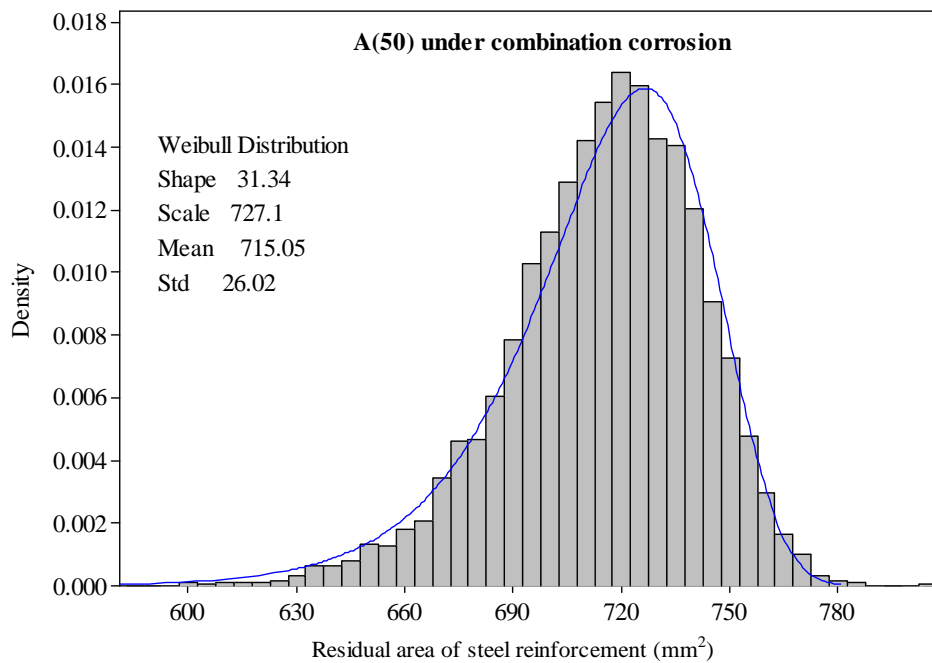


Figure 4.20 Histogram of residual area of steel reinforcement of the sample structural component after 50 years exposure under combination corrosion.

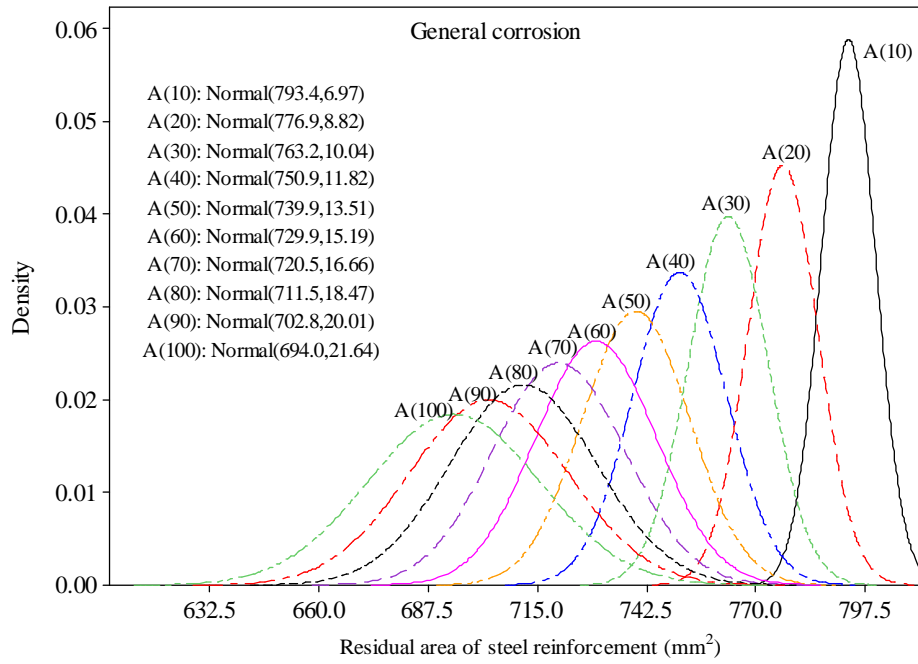


Figure 4.21 Probability density function of residual area of steel reinforcement of the sample structural component under general corrosion.

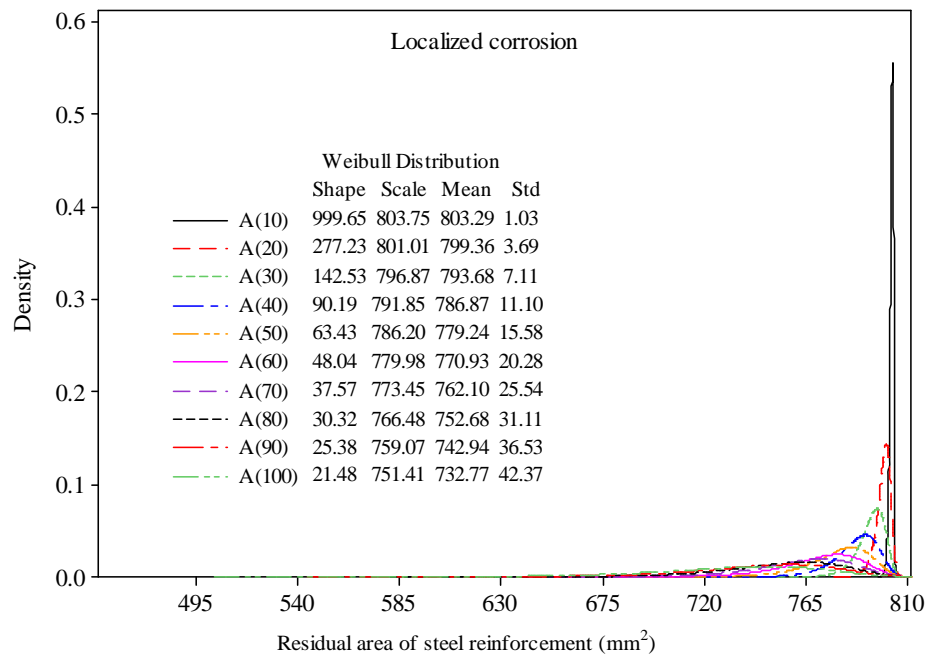


Figure 4.22 Probability density function of residual area of steel reinforcement of the sample structural component under localized corrosion.

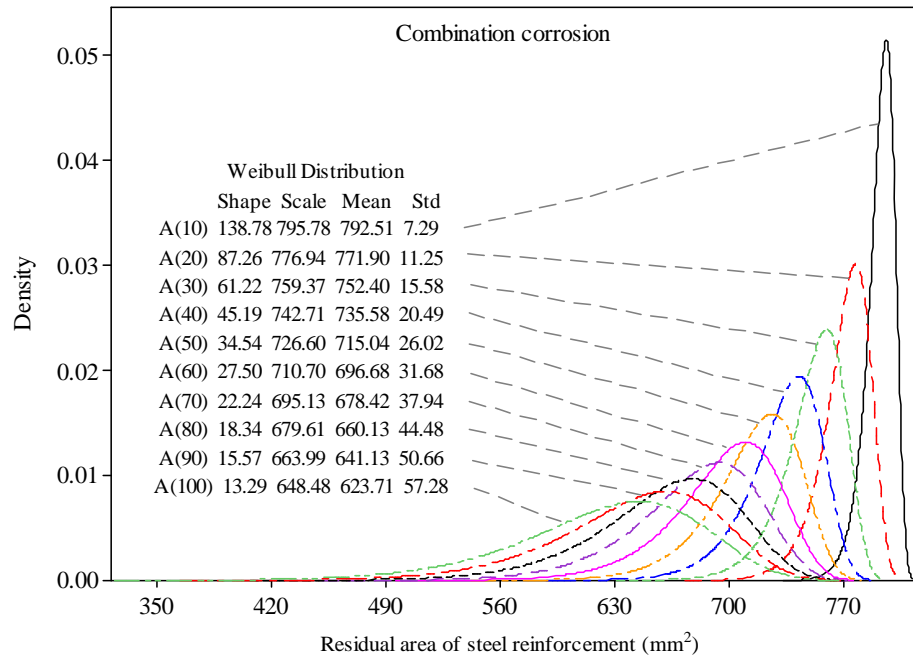


Figure 4.23 Probability density function of residual area of steel reinforcement of the sample structural component under localized corrosion.

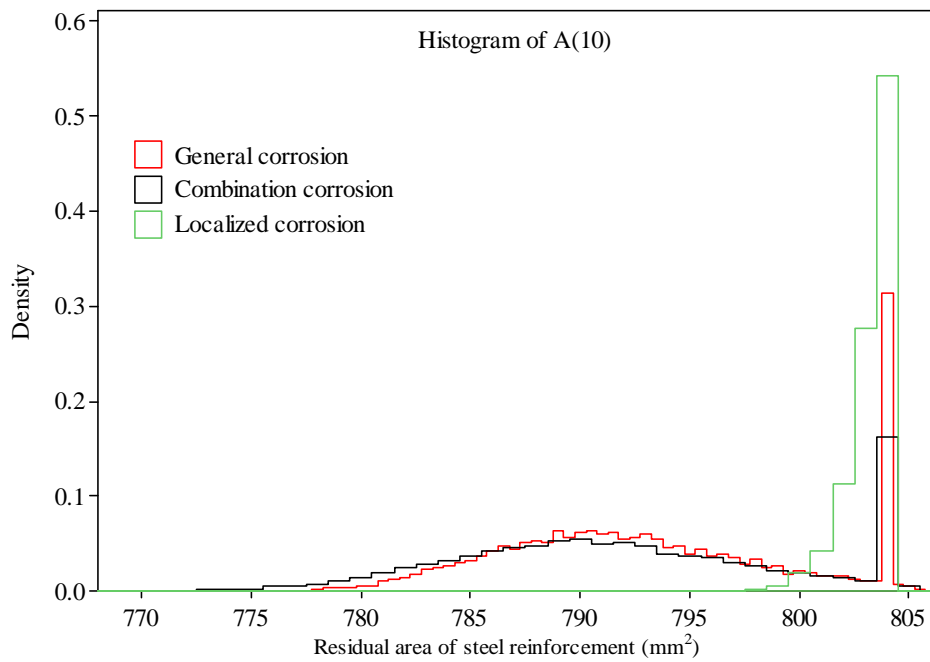


Figure 4.24 Histogram of residual area of steel reinforcement of the sample structural component after 10 years corrosion.

Figure 4.24 shows the histogram of the residual area of steel reinforcement after 10 years corrosion. It can be found that, for all corrosion forms, substantial number of samples lied around 804.25, which means the area of steel bar does not change. Localized corrosion has the same situation as well. This is reasonable because there is a high probability that the corrosion has not been initiated in early stage. If the corrosion initiation time can be specified based on modeling and inspection data, the distribution of residual area could be much more regular. As the residual area is an important indicator of residual resistance, to improve accuracy, it is suggested to use sample values for the residual area directly in latter modeling and analysis. Appendix C shows detailed calculation inputs and findings mentioned in this section.

4.2.2 Resistance degradation

Generally, the time-dependent resistance of an element can be expressed by multiplying the initial resistance and a resistance degradation function (Mori and Ellingwood, 1993),

$$R(t) = R_0 \cdot g(t) \quad (4.14)$$

where R_0 is initial resistance and $g(t)$ is the resistance degradation function.

For rehabilitated structures, changes of resistance of these structures resulting from rehabilitation should be considered. A discrete process is used here for simplification. Assuming all the rehabilitation work can be completed in one year, structural resistance after rehabilitation can be described as:

$$R(t_i + 1) = R(t_i) + \Delta R_i \quad (4.15)$$

where $R(t_i + 1)$ represents the structural resistance after rehabilitation, $R(t_i)$ is the residual resistance before rehabilitation, t_i is the time of the i st rehabilitation and ΔR_i is the expected increase of resistance result from the i st rehabilitation.

However, estimating $R(t_i)$ and ΔR_i is not straightforward. It requires a high expenditure on site survey to obtain reliable data of the actual condition of structure. In this research, $R(t_i)$ is mass estimated based on presented corrosion model. Rehabilitated structure is considered as a new structure, which means presented corrosion model is also adoptable in this situation. So the general description of changes of resistance for rehabilitated structures is (see Figure 4.25),

$$R(t) = \begin{cases} R_0 \cdot g_1(t) & (t \leq t_1) \\ [R_0 \cdot g_1(t) + \Delta R_1] \cdot g_2(t) & (t_1 < t \leq t_2) \\ \{[R_0 \cdot g_1(t) + \Delta R_1] \cdot g_2(t) + \Delta R_2\} \cdot g_3(t) & (t_2 < t \leq t_3) \\ \vdots & \vdots \end{cases} \quad (4.16)$$

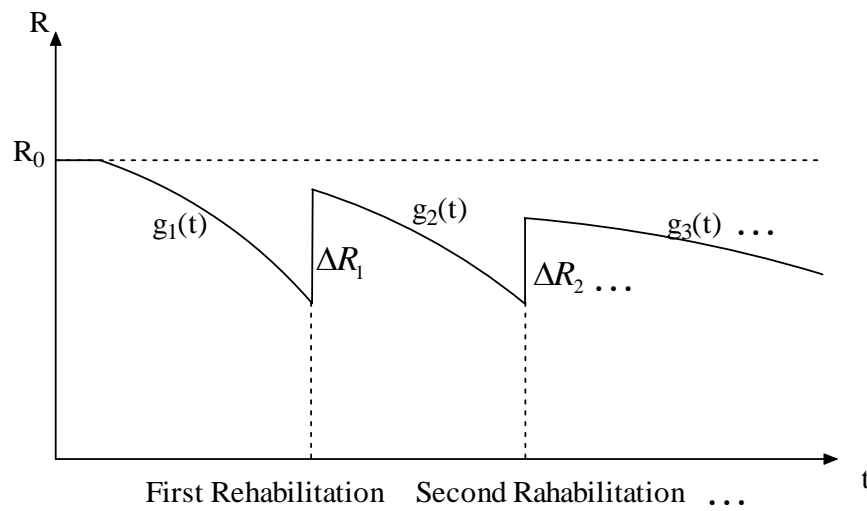


Figure 4.25 General description of changes of resistance of rehabilitated structure.

4.3 Time-dependent structural reliability

4.3.1 Time-dependent live load model

For single lane bridges, the maximum load effect is caused by a single truck or two trucks following behind each other, and for multiple-lane bridges, the critical load effect occurs when heavily loaded trucks are side-by-side and have fully correlated weights (Nowak and Szerszen, 1998). Val and Melchers (1997) suggested that the load from a single truck can be modeled as a normal random variable with mean $\mu_w = 287.5kN$ and a coefficient of variation of 0.412. The load of one truck of two side-by-side trucks is assumed to be normally distributed with a mean $\mu_w = 275kN$ and a coefficient of variation of 0.408.

Considering the increase in traffic volume, the time-dependent distribution of the weight of the heaviest truck (annually) can be formulated as (Vu and Stewart, 2000):

$$F_n(w, t) = \left[\Phi \left(\frac{w - \mu_w \cdot (1 + \lambda_m)^t}{\sigma_w \cdot (1 + \lambda_m)^t} \right) \right]^{N \cdot (1 + \lambda_v)^t} \quad (4.17)$$

where λ_m is the annual increases in trucks loads, λ_v is the annual increases in heavy traffic (truck) volume, N is the number of crossings of heavily loaded fully correlated trucks per year, μ_w and σ_w are statistical parameters for the live load of a single truck and Φ is the cumulative function for the standard normal distribution. The maximum live load for multiple lane bridges is calculated by superposition truck load in each lane. Statistical parameters of live load,

including $\mu_w, \sigma_w, \lambda_m$ and λ_v , can be estimated based on historical traffic records of the bridge to be analyzed if such information is available.

4.3.2 Probability of failure and reliability index

The reliability of existing bridge structures can decrease in service due to the degradation of resistance and the increase of traffic loads. The cumulative probability of failure and reliability index over the bridge's service life can be calculated by:

$$p_f(t) = P\{R(t) < S(t)\} \quad (4.18)$$

$$\beta(t) = \Phi^{-1}[1 - p_f(t)] \quad (4.19)$$

For existing bridge structures, it is more significant to assess the conditional probability which indicates the future performance trend of the structure based on current performance level. The condition probability that the structure will fail in $(t_i - t_{i-1})$ subsequent years given that it has survived t_{i-1} years can be expressed as (Vu and Stewart, 2000):

$$p_f'(t_i) = p_f(t_i | t_{i-1}) = \frac{p_f(t_i) - p_f(t_{i-1})}{1 - p_f(t_{i-1})} \quad (4.20)$$

Therefore, the probability that failure will occur within the period $[t_{i-1}, t_i]$ or the failure-time probability can be formulated as (Radojicic et al., 2001),

$$p^{LT}(t_i) = (1 - p_f(t_{i-1})) \cdot p_f'(t_i) \quad (4.21)$$

Failure-time probability is suggested to be used in calculation of expected failure cost which feeds into life cycle cost.

4.3.3 Service life prediction

Over the service life of a structure, it should be ensured that the reliability index is always above a target reliability index which indicates a critical condition.

$$\beta(t) \geq \beta^* \quad (4.22)$$

where $\beta(t)$ is the time-dependent reliability index and β^* is the minimum allowed reliability index. β^* can be determined based on the design target reliability index, which is selected to provide a consistent and uniform safety margin bridges. In Canada and the USA, the notional value for the target reliability index chosen was 3.5 (Ryall, 2001). The importance of the structure element in the system and the specific service scenario could also be considered. Thus, possible service life can be mass predicted.

4.4 Illustrative example

4.4.1 Example description

The structural component considered in this study is a typical pier column. Figure 4.26 shows the design dimensions and the allocation of steel reinforcement. All bars are Y20. Statistical parameters for the dimensions, material properties,

exposure environment and loads for this structure are given in Table 4.6. These values and distributions were identified based on existing structures and other research studies (Vu and Stewart, 2000, Stewart and Rosowsky, 1998, Val and Melchers, 1997, Thoft-Christensen, 1998).

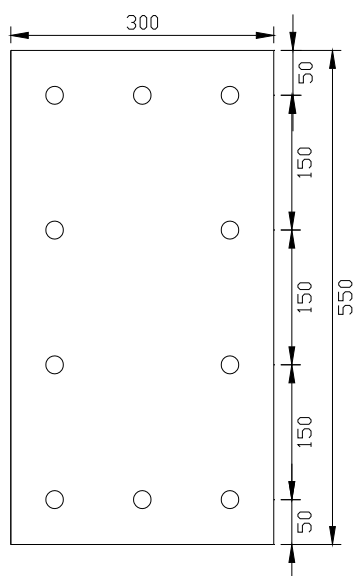


Figure 4.26 Cross-section of case pier column.

Variable	Mean	Coefficient of variation	Distribution
$b(mm)$	300	$\sigma = 5mm$	Normal
$h(mm)$	550	$\sigma = 10mm$	Normal
Yield stress $f_{sy} (MPa)$	400	0.1	Normal
Dead load $G(kN)$	840	0.1	Normal
Truck load per lane(kN)	275	0.408	Normal
Concrete strength $f'_c (MPa)$	25.75 (when $w/c = 0.7$) 32.96 (when $w/c = 0.6$) 41.2 (when $w/c = 0.5$)	0.18	Normal
Concrete cover depth $X(mm)$	36 56 76	$\sigma = 11.5$	Normal
Surface chloride concentration $C_0(kg/m^3)$	2.95(Coastal zone d=50m) 3.5 (De-icing salts) 7.35(Onshore splash zone)	0.5	Lognormal

Table 4.6 Statistical characteristics of resistance and load variables of case column.

In order to compare the effect of different durability design on the time-dependent reliability, several mean values were selected for concrete strength, concrete cover depth and surface chloride concentration. The values in bold font in Table 4.6 are the baseline values for this case. The distribution of maximum live load is evaluated according to Equation 4.17 assuming this column is a part of a double lane bridge with $\lambda_m=0.5\%$, $\lambda_v=0.5\%$ and $N=600$. Probabilistic analysis concludes that maximum live load generally approaches an extreme value distribution. In this research, the reliability index and probability of failure of case pier column was calculated every five years over design service life using Monte Carlo Simulation (see Appendix D).

In this research, time-dependent resistance was estimated under several assumptions:

- The case column is considered as short and it is subjected to pure axial compression. The load-carrying capacity of a short, axially loaded column can be calculated by:

$$N_{uo} = 0.85 f'_c A_g + f_{sy} A_s \quad (4.23)$$

- All sides of the structure are exposed to an aggressive environment and subjected to the same degree of corrosion.
- Resistance loss due to concrete cracking and spalling is ignored.
- In practice, the corrosion of steel bars tends to be a complicated combination of general corrosion and localized corrosion. It is clear that bond strength loss could more or less affect the resistance capacity of a structure (Val et al., 1998). However, in classical structural analysis models, perfect bond strength between steel and concrete was assumed. For coherence and simplicity, bond strength

loss is not considered here.

- Since it is an element level analysis, system effects are ignored such as collapse mechanisms and load redistribution.

4.4.2 Structural resistance

Mean structural resistance as a function of time of the case pier column with baseline inputs is shown in Figure 4.27. In this case, it can be observed that chloride induced corrosion can cause an approximately 12% decrease in mean structural resistance over a 100 year period. Figure 4.28 shows the probability density function of structural resistance. Generally, structural resistance fits a normal distribution. Compared to the mean value, the standard deviation of structural resistance only slightly increased over time.

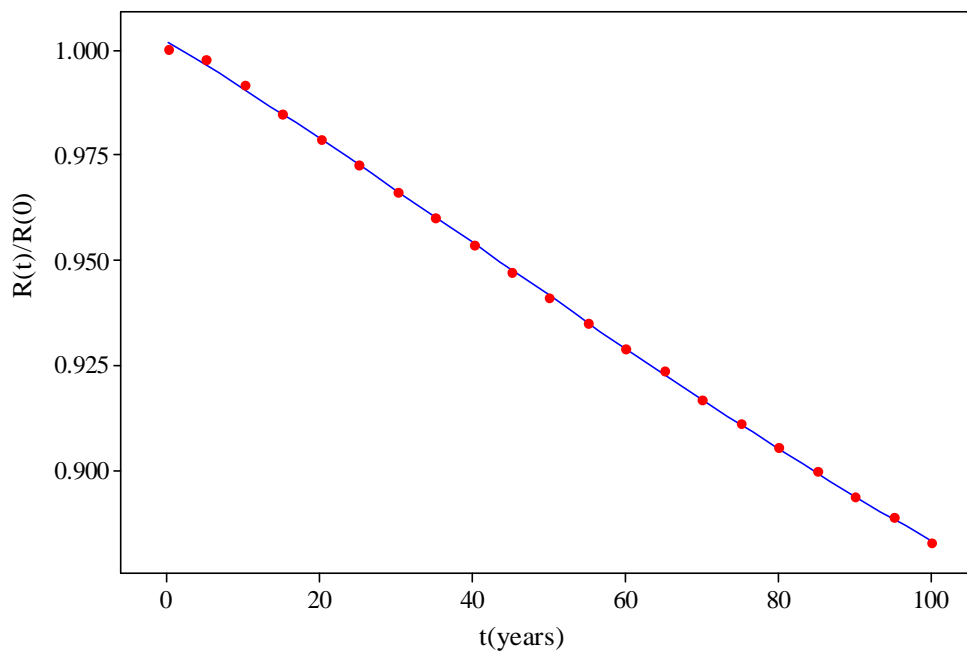


Figure 4.27 Mean structural resistances as a function of time.

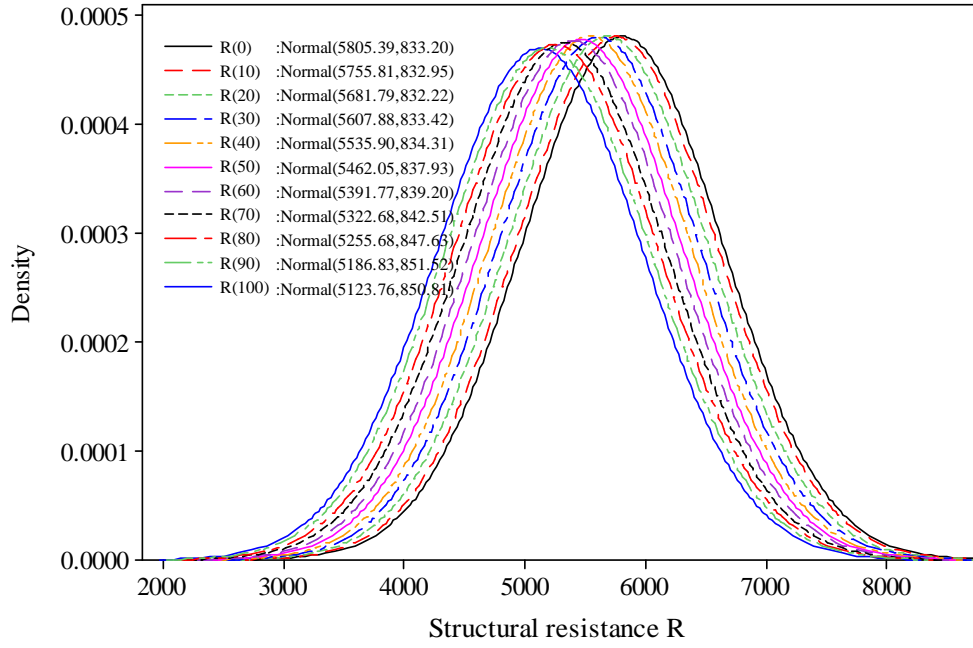


Figure 4.28 Probability density function of structural resistance.

4.4.3 Structural reliabilities

4.4.3.1 Basic results

Figure 4.29 and 4.30 show the probability of failure and reliability index of the case pier column with baseline inputs. It can be seen that the failure-time probability is lower than the cumulative probability of failure, however, they have a similar increase rate over time. After 100 years exposure and service, the cumulative probability of failure reaches 0.6%. Assuming the minimum reliability index $\beta^* = 3.2$, the structure tends to be at high failure risk around year 67.

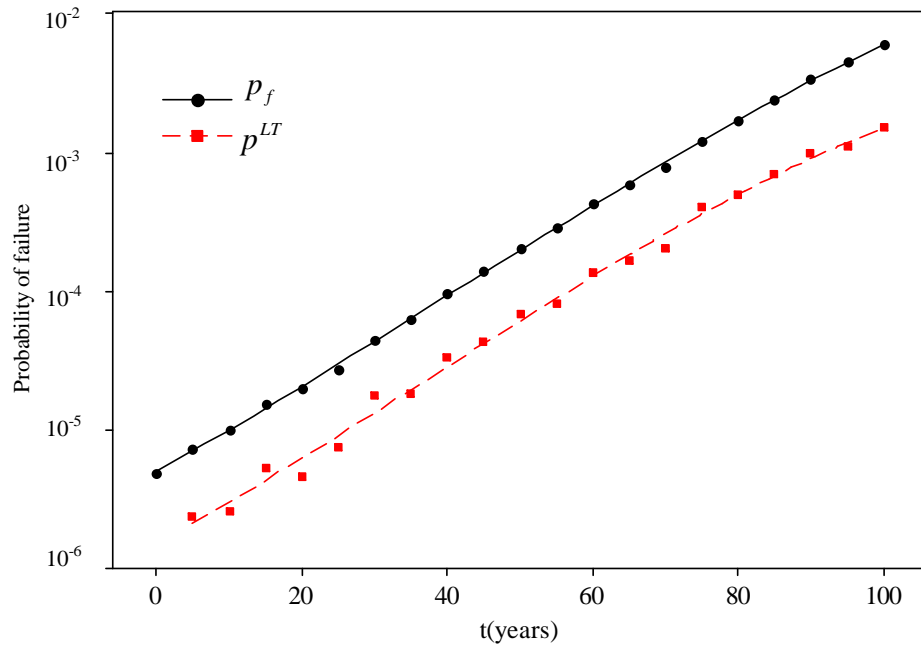


Figure 4.29 Probability of failure as a function of time.

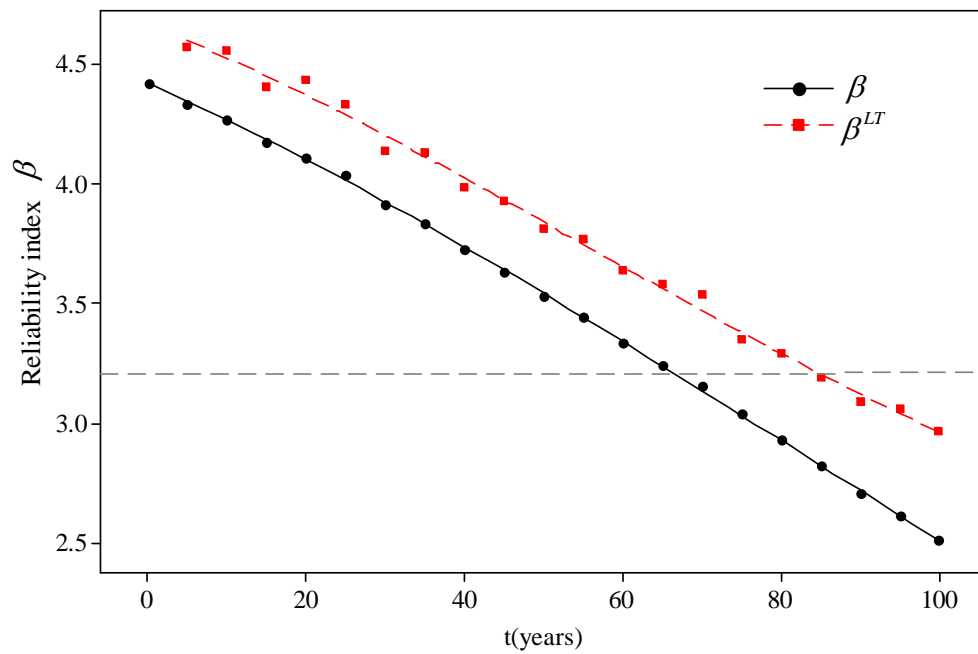


Figure 4.30 Reliability index as a function of time.

4.4.3.2 Comparative results

Time-dependent cumulative reliability index was selected as the indicator of the structural reliability. The results of the analysis are presented in several figures. For comparison purposes, in each figure, only one input parameter is varied.

Figure 4.31 shows the changes in the time-dependent reliability index under the following situations: (1) assuming the load is constant; (2) assuming the resistance is constant; (3) assuming both load and resistance are a function of time. The figure shows that, for this case pier column, the effect of changes of both load and resistance are visible and they both should be taken into account. Figure 4.32 shows the effects of different corrosion types on the reliability index. It can be seen that the reliability index under combination corrosion has the fastest decrease rate. Comparing general corrosion and localized corrosion, the changes of reliability index under general corrosion is slightly more than localized corrosion at first several decades. However, after that, localized corrosion causes a more severe loss of reliability than general corrosion. This is compatible with the area-loss function under each corrosion type. As combination corrosion has the most similarity with the corrosion in practice, the case was calculated under combination corrosion in later analysis. Figure 4.33 illustrates how the time-dependent reliability index changes with different exposure environment. Generally, the decrease rate for the reliability index has a direct ratio with the surface chloride concentration C_0 .

Figure 4.34 and 4.35 shows the time-dependent reliability index of different concrete durability design. Generally, concrete properties have more notable effects

on the time-dependent reliability index than other parameters mentioned above. The effect of varying the concrete cover depth on the time-dependent reliability index is showing in Figure 4.34. After 100 years exposure and service, the reliability index with 30mm concrete cover is 2.03 and the cumulative probability of failure is about 10 times as the one with 70mm as concrete cover depth. Changing water-cement ratio can induce a larger variety of the time-dependent reliability index, which is shown in Figure 4.35. Since concrete strength is associated with the water-cement ratio, the reliability index differs with different water-cement ratio even at the beginning of service life. The difference tends to be more intensive during later service. The reliability index with $w/c=0.7$ at 100 years is about 1.14 and it has more than 400 times the probability of failure than the one with $w/c=0.5$.

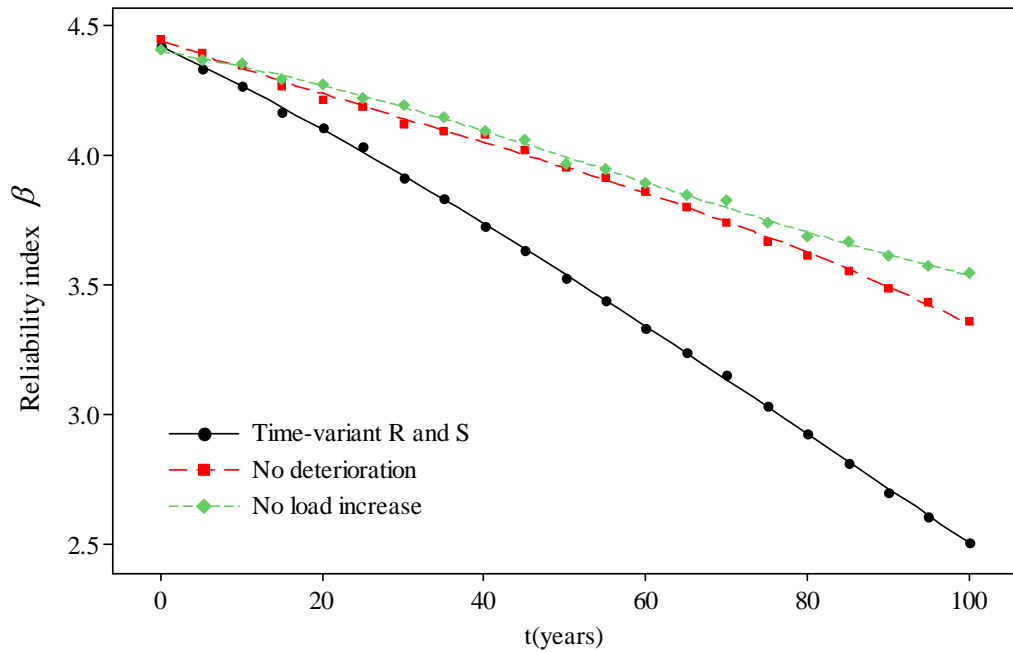


Figure 4.31 Variations of reliability index for different load and resistance scenarios.

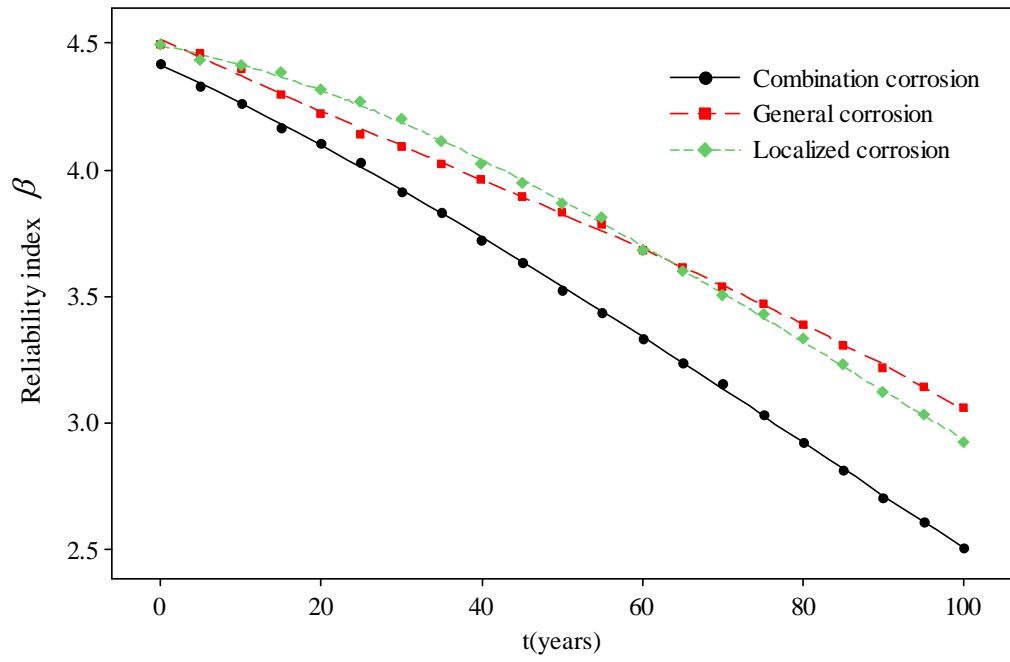


Figure 4.32 Variations of reliability index for different corrosion types.

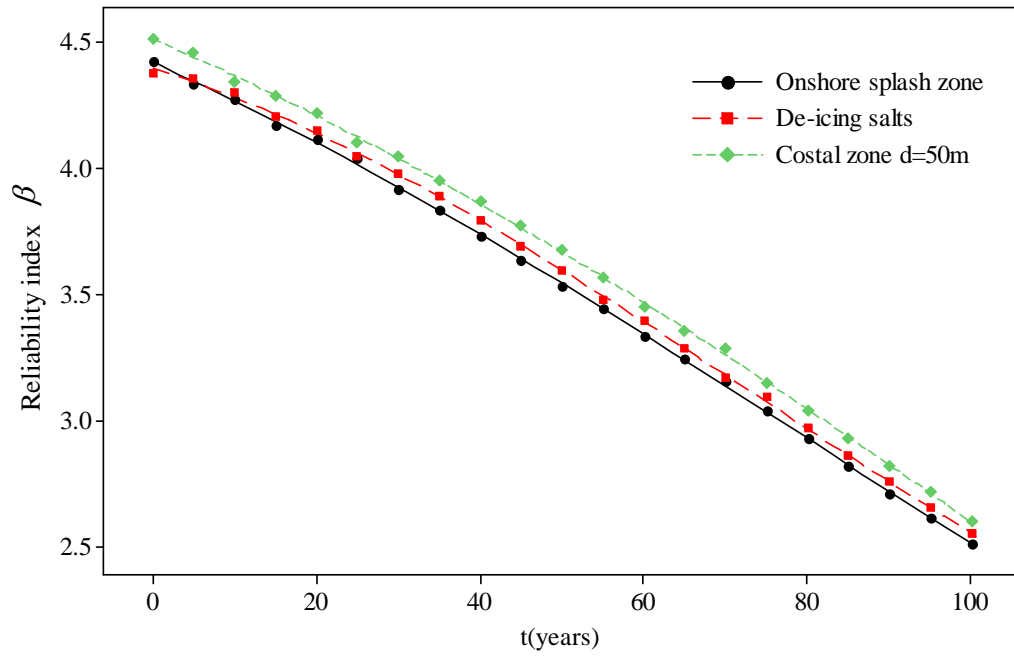


Figure 4.33 Variations of reliability index for different exposure environment.

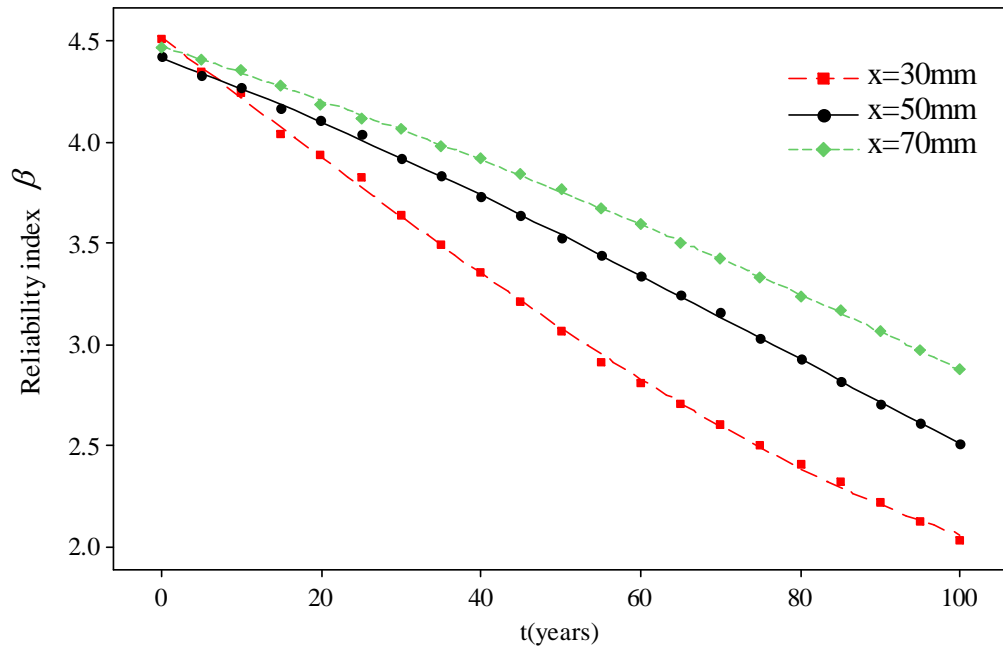


Figure 4.34 Variations of reliability index for concrete cover depth.

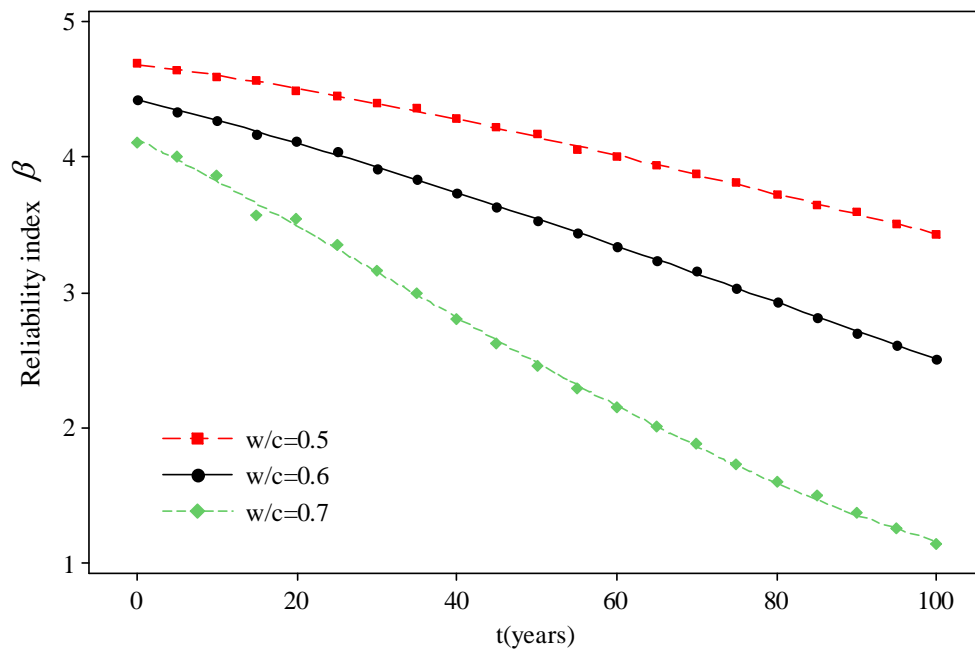


Figure 4.35 Variations of reliability index for different water-cement ratio.

4.4.4 Analysis of rehabilitation options

It can be seen that the case pier column should be rehabilitated before year 67. Two rehabilitation options are considered here, externally bonded concrete jacket and externally bonded fiber reinforced polymer composite sheets.

External bonding using concrete jacket is one of the traditional techniques available in rehabilitation of existing reinforced concrete structures. This method is effective and economical for increasing the capacity of reinforced concrete structural members. As strengthened structural member is still exposed to aggressive environments, corrosion needs to be considered. FRP materials have a high strength to weight ratio and good resistance to corrosion and have been identified as an ideal material for external retrofitting. However, long-term field data of FRP materials are not yet available. The case pier column was analyzed based on the following inputs and assumptions:

- The rehabilitation began and accomplished in the period of time from year 50 to 55.
- For option 1, external bonding using concrete jacket, the jacket depth was assumed to be $50mm$, water cement ratio and strength of concrete is $w/c = 0.5$ and $f'_c = 40MPa$ respectively. That meant the mean resistance of the case pier column was expected to increase by approximately $3000kN$. There would be resistance degradation after rehabilitation due to chloride concentration and propagation.
- For option 2, external bonding using FRP, it was assumed that the mean resistance can be increased by $1500kN$ with a 10% increase of the standard

deviation. FRP was assumed to be non-corrosive in future services.

Figure 4.36 shows the reliability indexes of the rehabilitation options as a function of time. It can be seen that option 2 is more effective in increasing structural reliability although the mean resistance increase is only half of that for option 1. This is because in option 1, concrete property and corrosion related variables are highly uncertain and result in a high coefficient of variation. However, compared to the original performance, both rehabilitation options have a significant effect on prolonging the service life of the structure.

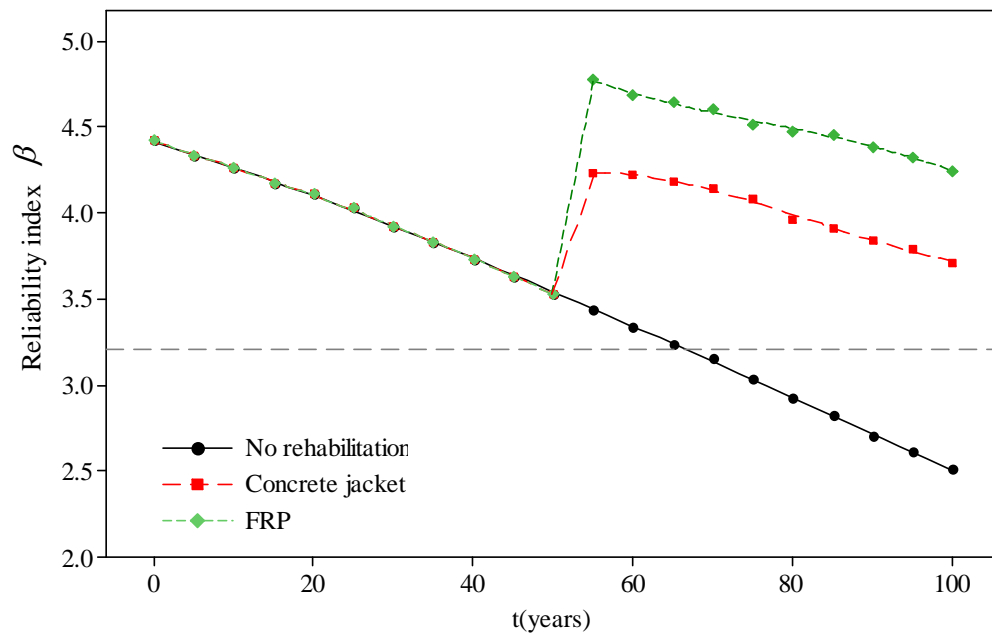


Figure 4.36 Time-dependent reliability indexes for rehabilitation options.

4.5 Conclusion

In this chapter, a probabilistic method to evaluate the time-dependent reliability and the probability of failure of reinforced concrete bridge components has been presented. Based on existing corrosion models, a combination corrosion model has been developed which could better represent the actual area loss of steel bars. In the analysis of time-dependent reliability, uncertainties associated with resistance degradation, expected increase of resistance due to rehabilitation, load effects and environmental variables was considered. The probabilistic distribution of the surface chloride concentration, diffusion coefficient, critical chloride concentration and material variables were identified from literature. Monte Carlo simulation is employed in modeling the increasing live load and the degradation to obtain the time-dependent reliability during design service life. A case pier column was selected as an illustrative example. The results show that under ordinary conditions, corrosion of steel reinforcement could result in an approximately 12% reduction of resistance after 100 years exposure to a onshore splash environment, and the structure would be at a high failure risk around year 67. In comparative studies, it was found that the concrete cover depth and water cement ratio have a large influence on the time-dependent probability of failure and reliability index. Possible performance trend after rehabilitation is also studied by comparing two rehabilitation options, external bonding using concrete jacket and external boning using FRP. The results show that the using FRP is more effective in enhancing the reliability index of case pier column and ensuring the structure last longer under increasing load and aggressive environment.

CHAPTER 5 LIFE CYCLE COST ANALYSIS AND INTEGRATION MODEL

In the service life of a bridge, there are a number of costs and benefits occurring from time to time. Improving durability of new structures can reduce future maintenance costs but increase the initial costs. Design and management of bridges should be aimed at determining and implementing the best possible strategy that insures an adequate level of reliability and serviceability at the lowest possible cost during whole service life. Thus, costs associated with essential maintenance and possible failure should be taken into account in addition to initial cost of construction/rehabilitation of new and old structures.

This chapter will introduce the concept of life cycle cost analysis and the model of each costs components. An additional model will be demonstrated to integrate the qualitative and quantitative methods presented in previous chapters to acquire a quantitative overall probability of failure of a bridge or a bridge sub-system, which is required to estimate the expected failure cost.

5.1 Life cycle cost analysis

Life cycle cost analysis is an evaluation method, which uses an economic analysis technique that allows comparison of investment alternative having different cost streams. It evaluates each alternative by estimating the costs and timing of the cost over a selected analysis period and converting these costs to economically comparable values considering time-value of money over predicted whole of life cycle.

Making a decision for selection of the rehabilitation method will be done by minimizing the life cycle costs. Cost elements associated in a rehabilitation project may include four major categories:

- Initial cost
- Maintenance, monitoring and repair cost
- Costs associated with traffic delays or reduced travel time (Extra user cost)
- Failure cost

For simplicity, if monitoring, repair, extra user cost are considered as the maintenance cost then the cash flow for any rehabilitation method can be shown as in Figure 5.1. In order to be able to add and compare cash flows, these costs should be made time equivalent. It can be presented in several different ways, but the most commonly used indicator in road asset management is net present value of the investment option. The net present value of an investment alternative is equal to the sum of all costs and benefits associated with the alternatives discounted to today's values.

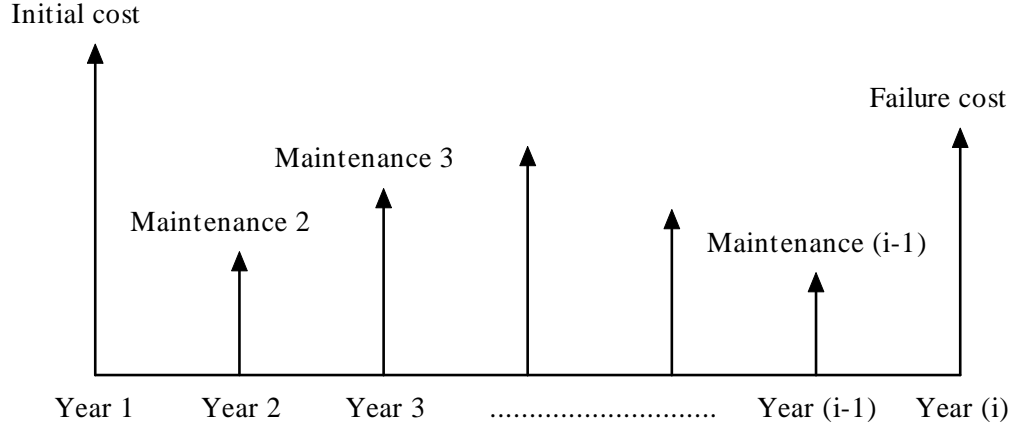


Figure 5.1 Cash flow for the rehabilitation of bridges.

Objective function for the optimal bridge rehabilitation can be formulated as the maximization of,

$$W = B_{lifecycle} - C_{lifecycle} \quad (5.1)$$

where $B_{lifecycle}$ is the benefit which can be gained from the existence of the bridge after rehabilitation and $C_{lifecycle}$ is the cost associated with the bridge during its whole life. Assuming the benefit from the bridge will be the same irrespective of the rehabilitation method considered, it is possible to consider only the cost components. Therefore the new objective function will be the minimization of the total cost during its whole life cycle subjected to reliability and other constraints. The whole of life cycle cost can be estimated as,

$$C_{lifecycle} = C_{initial} + C_{repair} + C_{user} + C_{failure} \quad (5.2)$$

5.1.1 Modeling of the initial cost

Initial rehabilitation cost will include preliminary design cost, start up, material and

labour costs (supervisors, skilled and unskilled). All these costs will incur in the base time of the project.

5.1.2 Modeling of the maintenance (repair) cost

Modeling of the future maintenance cost is complicated. Thoft-Christensen (2000) divided this cost into three categories namely, functional repair cost $C_1(t_{r,i})$, fixed repair cost $C_2(t_{r,i})$, and unit dependent repair cost $C_3(t_{r,i})$, if a repair is to be taken place at the time $t_{r,i}$. r is the discount rate and i is the number of occurrence of repair. Therefore the corresponding maintenance cost may be defined as (Thoft-Christensen, 2000),

$$C_{maintenance}(t_{r,i}) = C_1(t_{r,i}) + C_2(t_{r,i}) + C_3(t_{r,i}) \quad (5.3)$$

The expected repair cost discounted to the time $t = 0$ is the summation of the single repair cost.

$$C_{repair} = \sum_{i=1}^n (1 - P_f(t_{r,i})) \cdot C_{maintenance}(t_{r,i}) \frac{1}{(1+r)^{t_{r,i}}} \quad (5.4)$$

where n is the number of failures during the life cycle of the bridge and P_f is the updated failure probability at each failure time.

5.1.3 Modeling of user cost

User cost may be of two folds, during initial rehabilitation and during the next periodic rehabilitation. User cost may be calculated in terms of costs associated with traffic delay, and in case of using alternate routes wear and tear of user vehicle.

The expected user cost may be formulated as,

$$C_{user} = \sum_{i=1}^n C_{user}(t_{r,i}) \frac{1}{(1+r)^{t_{r,i}}} \quad (5.5)$$

5.1.4 Modeling of expected failure costs

Expected failure costs $C_{failure}$ include all money expended as a result of a structural collapse of the bridge, or a situation in which such collapse is imminent and the bridge must be closed to traffic. Failure cost can be estimated by (Branco and Brito, 2004b, Nezamian et al., 2004):

$$C_{failure} = P_f \cdot C_F \quad (5.6)$$

where P_f is the probability of failure, C_F is the total estimated cost of the bridges actual collapse (or the end of its service life before expected) including bridge replacement costs C_{FR} , lost lives and vehicle and equipment costs C_{FL} and architectural/cultural/historical costs C_{FH} , see Equation 5.7 (Branco and Brito, 2004b).

$$C_F = C_{FR} + C_{FL} + C_{FH} \quad (5.7)$$

Activity	Deaths per 100 million hours of exposure
Travel by helicopter	500
Travel by airplane	120
Walking beside a road	20
Travel by car	15
Construction (average)	5
Building collapse	0.002
Bridge collapse	0.000002

Table 5.1 Loss of lives in everyday life.

It is not easy to assess the loss of lives and vehicle and equipment costs C_{FL} . However, when such loss can be avoided, the cost of failure C_F can be better estimated. Table 5.1 shows the deaths due to bridge collapse compares to other fatality accident (Ryall, 2001). Wen and Kang (1998) points out that the minimum expected life cycle cost is not sensitive to the costs associated with human death and injury because of the inappreciable probability of its occurrence. Also, it is difficult to evaluate the architectural/cultural/historical costs (Branco and Brito, 2004b). Thus, costs result from actual failure approximately equal to replacement costs, the costs associated with life and vehicle loss and architectural/cultural/historical costs are ignored.

5.2 An integrated model

A qualitative methodology based on fault tree model to analysis the probability of failure (likelihood or frequency) and the risk of failure of serviceability of

reinforced concrete bridges has been presented in Chapter 3. The method is capable to obtain the relative severity of likelihood and the risk of occurrence of distress mechanisms of bridge components, ranking the overall risk of failure of serviceability of among different components in a bridge or a group of bridges. Since this method does not need to rely on actual data and probabilistic analysis, it is simple and easy to perform. But the result is subjective and fuzzy to some extent. Chapter 4 has discussed a quantitative methodology to analyze the time-dependent reliability and the probability of failure of bridge components due to initiation of distress mechanisms. However, since most bridges are redundant structures, failure of an individual component does not imply the system failure (Enright and Frangopol, 1998a). In this situation, VOTING gate, which has been mentioned in Table 3.1, can be used to roughly estimate the probability of failure of a parallel system which is made up with several same components, such as piles or columns.

5.2.1 VOTING gate model

VOTING gate means once M of N combinations of inputs occur, the output event occurs, see Figure 5.2 (Ericson, 2005). Figure 5.3 shows another way to understand the VOTING gate, it is actually the simplification of combination of C_N^M AND gates with M inputs and OR gates with C_N^M inputs. Assume that all components has the same probability of failure, system probability of failure can be expressed as:

$$p_{f_s} = 1 - (1 - p_{f_c}^M)^{C_N^M} \quad (5.8)$$

where p_{f_s} is the system probability of failure, p_{f_c} is the components probability of failure, M is the number of failure of components that indicate the system failure, N is the total number of parallel components. p_{f_c} can be estimated using the methodology presented in Chapter 4, using corresponding resistance and load effects for individual components.

Figure 5.4 and 5.5 shows the effect of M and N on the system probability of failure. It is clear that system probability of failure changes intensively when varying M . N is easy to determine and only has modulate effect on the system probability of failure. Thus, M is a crucial factor for the accuracy of the calculation. M can be obtained by analyzing the system load effect and components load capacity. However, it is not straightforward because the system effects and load redistribution are supposed to be considered. Moreover, once one or more component failure occurs, the load effects for rest of the components suddenly enhance and result in the increase of the probability of failure. For the sake of simplicity, all the component probability of failure is assumed to have the same initial value and increment over time until system failure occurs. This assumption would lead to an overlook of the system probability of failure, but provides a reasonable result and relative severity.

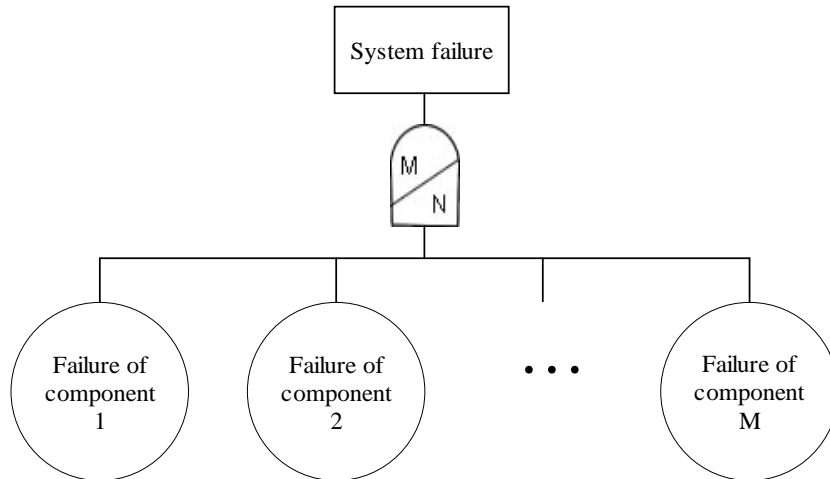


Figure 5.2 VOTING gate.

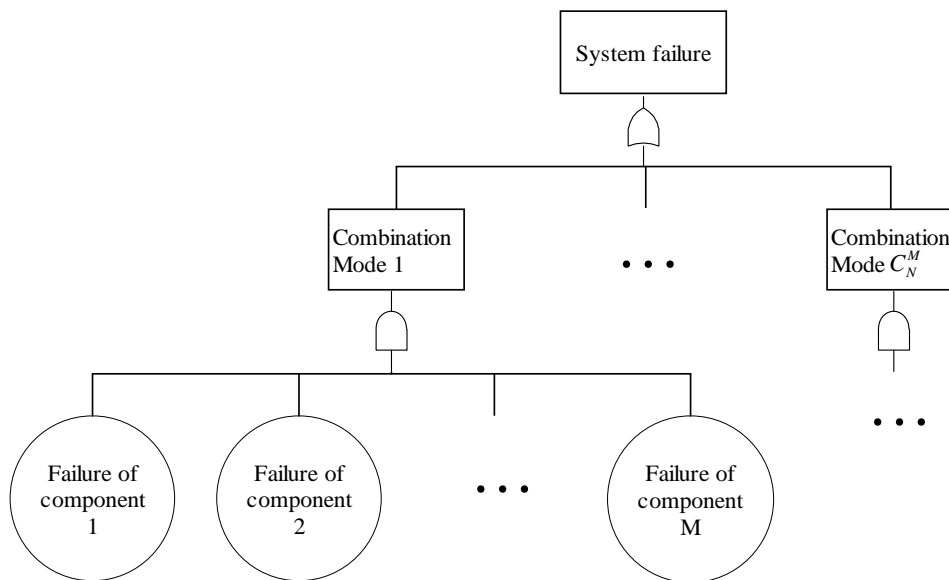


Figure 5.3 Illustrate the meaning of VOTING gate.

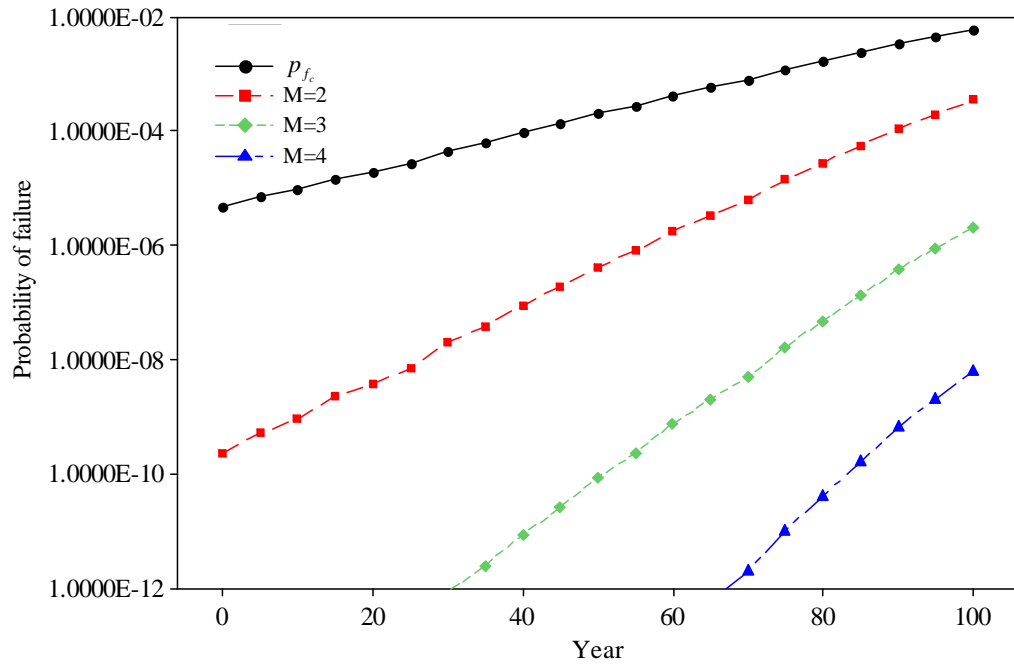


Figure 5.4 Changes of system probability of failure with M ($N=5$).

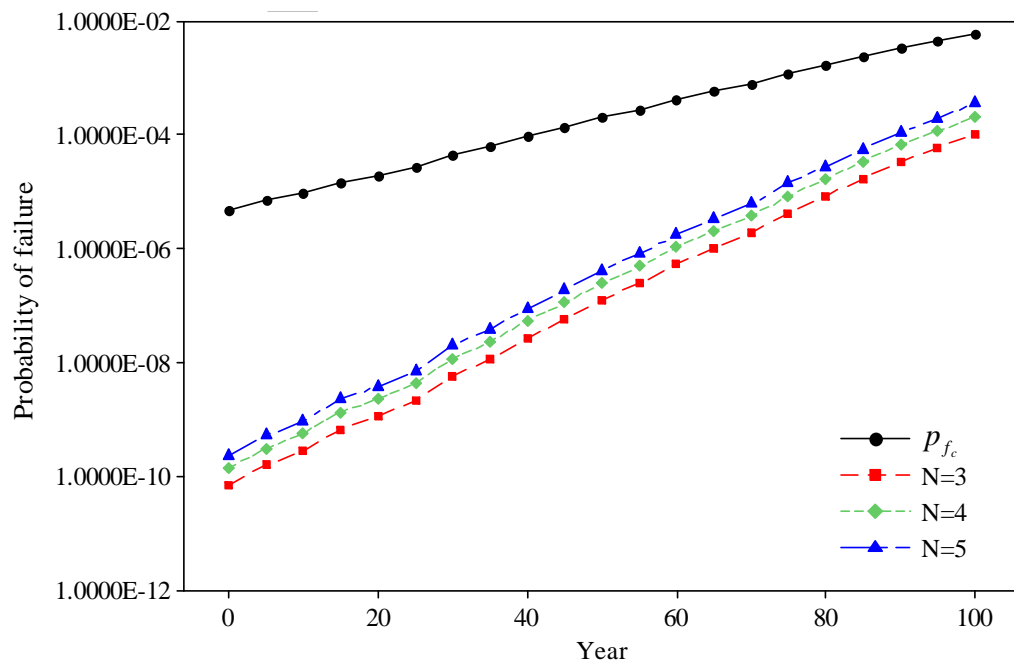


Figure 5.5 Changes of system probability of failure with N ($M=2$).

5.2.2 Integration

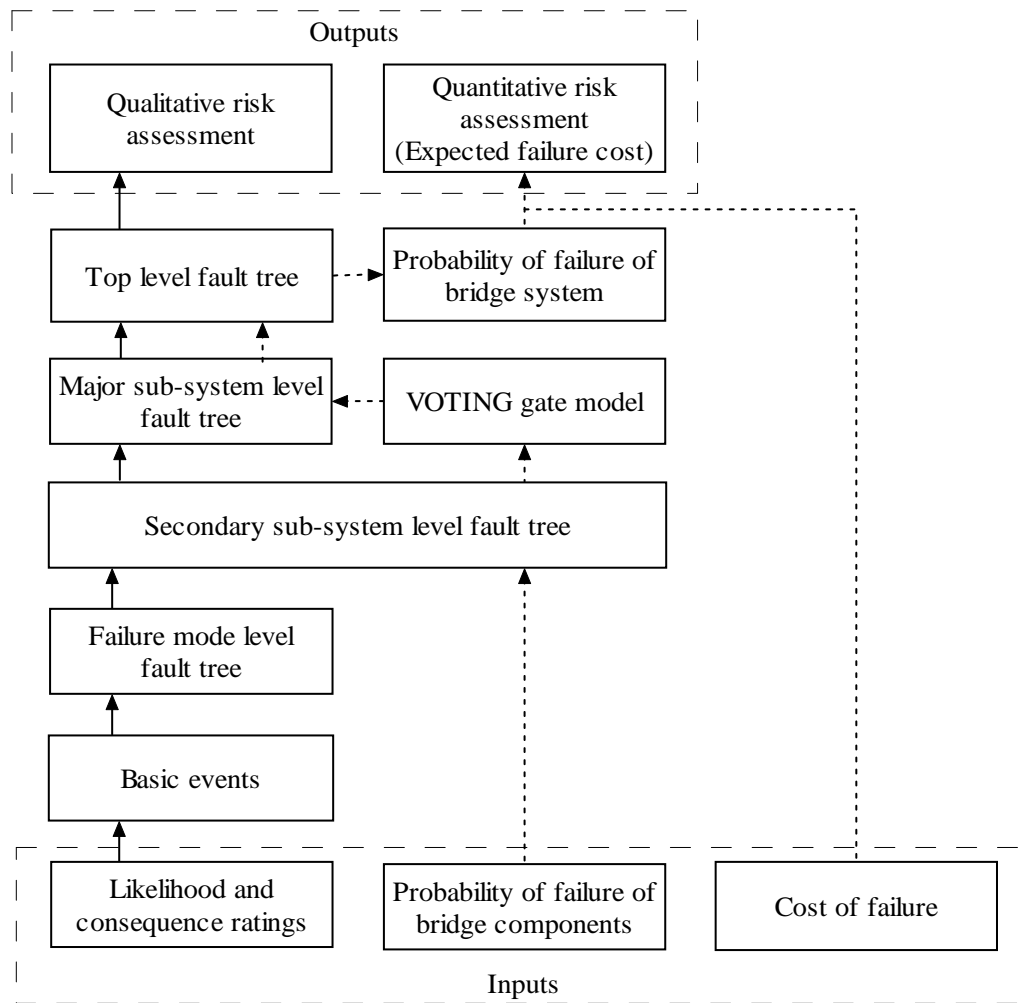


Figure 5.6 Flow chart of qualitative and quantitative risk assessment of bridge system.

The VOTING gate model can provide a connection of the quantitative results of component probability of failure due to initiation of a distress mechanism and the previous fault tree model, see Figure 5.6. The main flow in the chart connected by real line arrows is the major steps of the qualitative risk assessment of bridges based on fault tree model with likelihood and consequence ratings as inputs. When sufficient data are available and quantitative probability of failure of bridge components can be calculated, there is a better alternative to acquire quantitative

probability of failure of bridges, see the dashed flow in Figure 5.5. The probabilities of failure due to each distress mechanisms are combined to get the component probability of failure of individual components. Then the VOTING gate is employed to calculate the sub-system probabilities of failure of certain parallel systems which are used as inputs for major sub-system fault tree. An example to calculate the probability of failure of a bridge system according to the integration procedure will be given in following sections. Time-variant probability of failure of bridge system is then converted into the failure-time probability (see Equation 4.21) and combined with the cost of failure to acquire a quantitative failure cost.

5.3 Illustrative example

The selected example is the pier of a bridge shown in Figure 5.7. The superstructure of the bridge rests on a headstock and three columns. The columns stand on a pilecap, which in turn rests on four piles. Here pier is at the major sub-system level while headstocks, columns, pilecaps and piles are at secondary sub-system level, individual columns and piles are at component level.

Table 5.2 shows the hypothetic inputs for the calculation including the probability of failure of each component due to initiation of four major distress mechanisms and the value of M and N. The probability of failure here is the cumulative probability of failure at year 50.

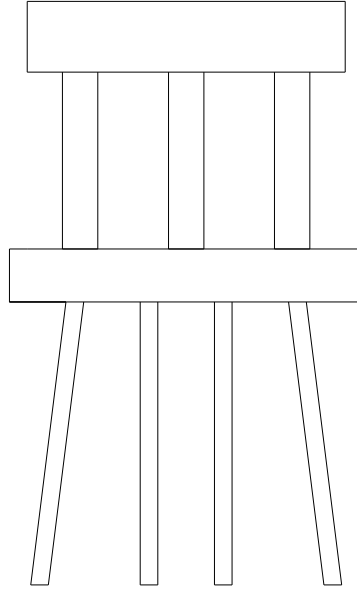


Figure 5.7 Overview of case pier.

Components	p_{f_c}				N	M
	Chloride Attack	Alkali-Silica Reaction	Carbonation	Plastic Shrinkage		
Headstocks	0.0002	0.00003673	0.000004573	0	1	1
Columns	0.00207	0.000391	0.000005562	0	3	2
Pilecaps	0.007875	0.00009573	0.000005323	0	1	1
Piles	0.002275	0.0001472	0	0	4	2

Table 5.2 Case inputs.

Based on the inputs, the calculation contains following steps:

- According to the secondary sub-system fault tree shown in Figure 3.5 to 3.8, calculate the component probability of failure p_{f_c} for headstocks, columns, pilecaps and piles (see Figure 5.8 to 5.11).
- Using the VOTING Gate model to calculate the probability of failure p_{f_s} of parallel systems, in this case the columns and piles:

$$P_{f_s}(\text{columns}) = 1 - (1 - 0.002465739^2)^{C_3^2} = 0.0000182395 \quad (5.9)$$

$$P_{f_s}(\text{piles}) = 1 - (1 - 0.002421865^2)^{C_4^2} = 0.0000703829 \quad (5.10)$$

- Calculate the probability of failure of pier based on the major sub-system fault tree in Figure 3.4, see Figure 5.12. If the inputs for other bridge components such as deck, girder, bearing and abutments are available, the probability of failure of the entire bridge can be estimated according to the overall fault tree frame presented in Figure 3.3.

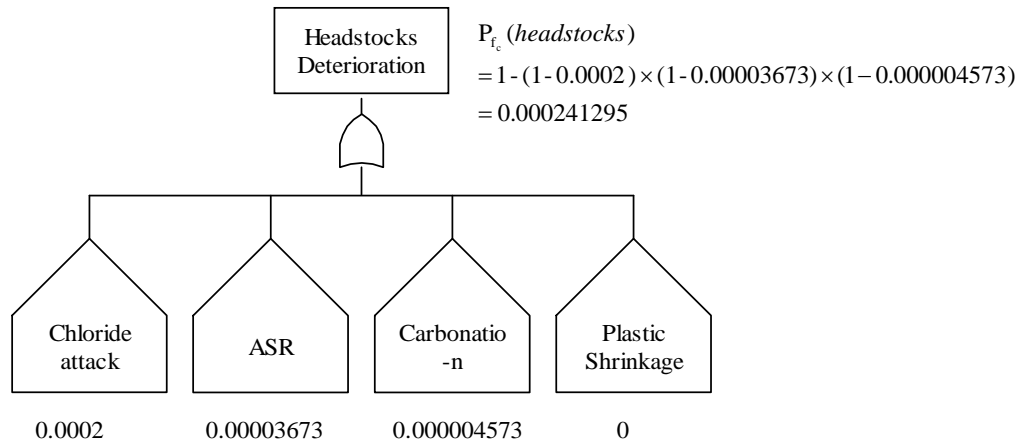


Figure 5.8 Calculation of components probability of failure of case headstocks.

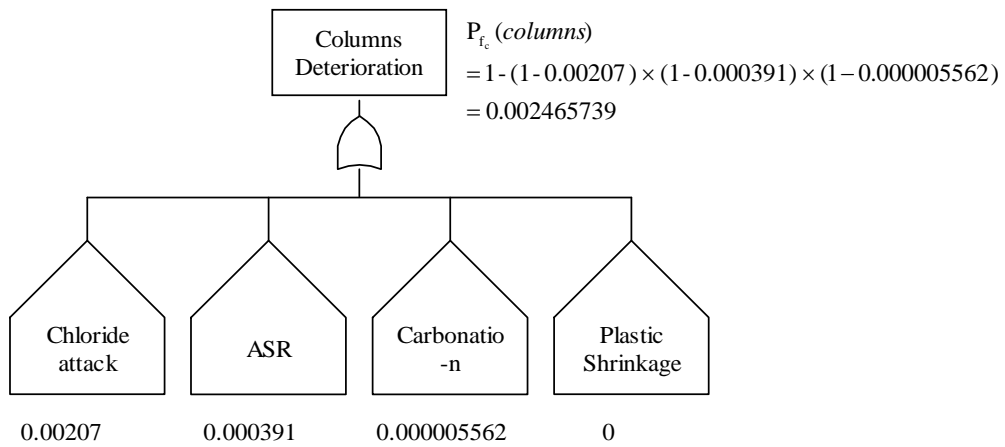


Figure 5.9 Calculation of components probability of failure of case columns.

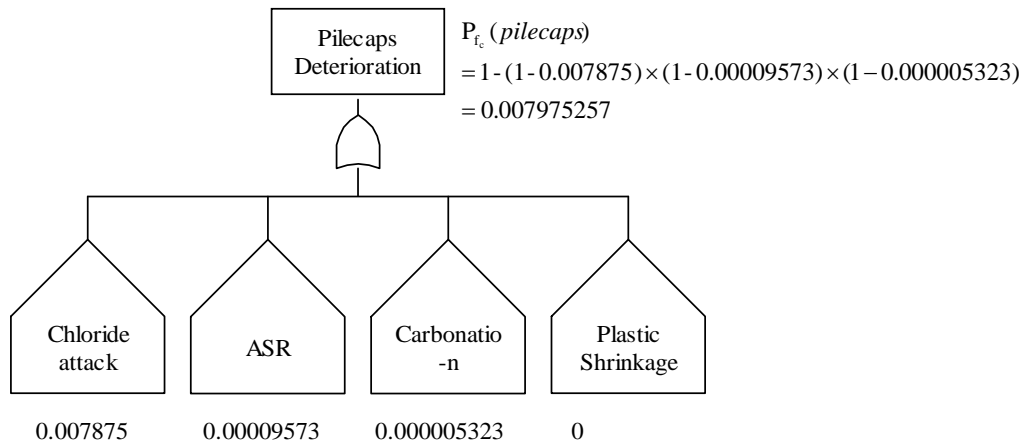


Figure 5.10 Calculation of components probability of failure of case pilecaps.

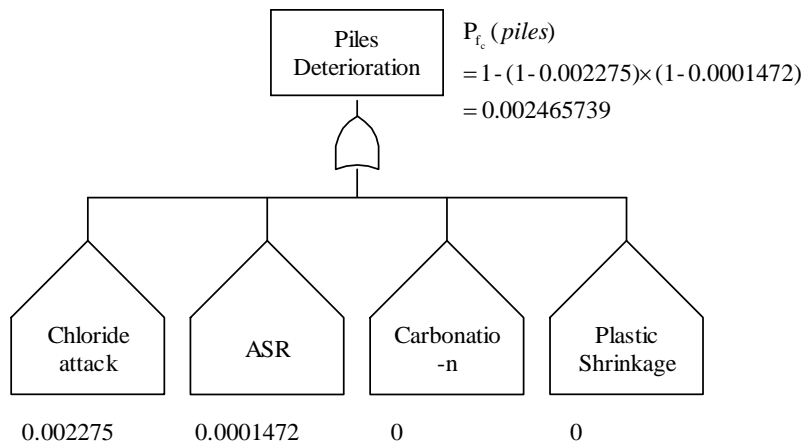


Figure 5.11 Calculation of components probability of failure of case piles.

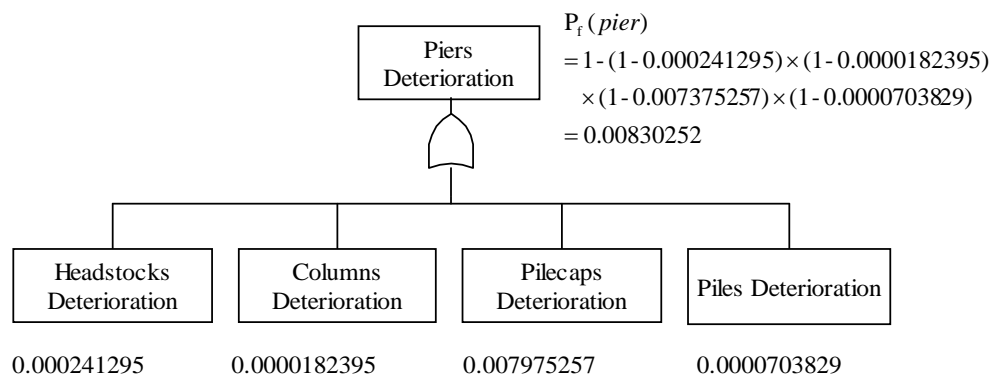


Figure 5.12 Calculation of probability of failure of case pier.

	P_{f_c}	P_{f_s}	P_f of pier	β of pier
Headstocks	0.000241295	0.000241295	0.00830252	2.40
Columns	0.002465739	0.0000182395		
Pilecaps	0.007975257	0.007975257		
Piles	0.002421865	0.0000703829		

Table 5.3 Case outputs.

The outputs are showing in Table 5.3. The probability of failure and reliability index of major sub-system of the case bridge pier is 0.0083 and 2.40 respectively. The result refers to the cumulative probability of failure of the pier at year 50. Repeating the calculation using the inputs component failure probabilities at different time points, the time-dependent cumulative probability of failure and failure-time probability can be calculated.

5.4 Conclusion

This chapter demonstrates basic concepts and models of life cycle cost analysis of bridge rehabilitation. An additional model named VOTING gate model is presented in this chapter, which can be used to integrate the quantitative probability of failure due to initiation of a distress mechanism and the system risk assessment model using fault tree analysis. It provides alternatives for the users to qualitative or quantitative assessment of the risk of failure depending on availability of detailed data. Parameters M and N are introduced. It is found that the results of the system probability of failure are sensitive to the value of M . An illustrative example has also been presented to show the procedures of using the model. The integrated

model can lead to a quantitative analysis of the probability of failure of an entire bridge or major bridge sub-systems and provides inputs for estimating the expected failure cost in life cycle cost analysis.

CHAPTER 6 CONCLUSION AND RECOMMENDATIONS

6.1 Conclusion

Work presented in this thesis demonstrates that it is possible to estimate risk of failure of reinforced concrete bridges qualitatively and quantitatively. A risk assessment model using fault tree analysis of reinforced concrete bridges has been developed. A probabilistic time-dependent reliability analysis of reinforced concrete bridge components is presented based on existing corrosion models and reliability analysis methodologies. These models are then integrated to obtain the time-dependent system reliability and probability of failure which is a crucial parameter in life cycle cost analysis.

6.1.1 Qualitative risk assessment based on fault tree analysis

Chapter 3 has demonstrated a structured method to qualitatively assess the system risks of failure of reinforced concrete bridges. This model can be used to identify the important risks for particular bridge components and their relative severity, and to rank the performance trends of bridges, or rank the risk of failure among a group of bridges to determine maintenance priorities. Conclusions regarding the methodology of qualitative risk assessment of reinforced concrete bridges using

fault tree analysis are shown below.

- Fault tree analysis can be used in risk assessment of overall, generalized system. The general process of using fault tree analysis in risk assessment is shown in Figure 3.1. In this work, fault tree analysis has been used to estimate the likelihood of occurrence of major distress mechanisms: chloride induced corrosion, alkali-silica reaction, carbonation and plastic shrinkage, and only the sub-tree of pier was examined in detail.
- Fault tree model of failure of reinforced concrete bridges are constructed by analysis the possible events that causing the occurrence of top event until all the events are basic or easy to evaluate. Fault tree models developed in this research include top level fault tree, major sub-system fault trees, secondary sub-system fault trees and fault trees of each distress mechanisms. The fault tree model has the ability to consider various parameters related to load, material, design, environmental and construction variables.
- Inputs of the fault tree risk assessment model are the likelihoods of occurrence of each basic event and the consequences of each distress mechanism. It can be analyzed both qualitatively and quantitatively depending on the inputs. In this work, three scale ratings from “High”, “Medium” to “Low” are used for both likelihood and consequences. These ratings are converted into numerical values using logarithmic scales for calculation. Model outputs risks of failure are also scaled in ratings from “High”, “Moderate” to “Low”.
- A case study was carried out to illustrate the application of the methodology on a major sub-system, pier. The results have shown that the methodology is capable for estimating the risk rankings and the relative severities. Sensitivity

analysis concluded that the total scaled risk ratings is sensitive to the consequence ratings, water-cement ratio and the variables related to moisture in external environment.

- Inevitably this method is not perfectly correct because it relies on subjective judgment to some extent. However, it presents a methodology to minimize subjectivity and to provide a logical consistent approach to the problem of risk assessment.

6.1.2 Probabilistic time-dependent reliability analysis

A model of probabilistic evaluation of the time-dependent reliability and probability of failure of deteriorated bridge components has been developed in Chapter 4. The methodology presented is a component level model of the time-dependent reliability of bridge components subjected to initiation of a distress mechanism. Chloride induced corrosion is selected as the example mechanism. The result of residual capacity and time-dependent probability of failure can be applied to performance assessment and life cycle cost analysis for both new structures and existing structures. Major achievements in Chapter 4 are shown below.

- A methodology of time-dependent reliability analysis of reinforced concrete bridges has been developed and the application was demonstrated for one failure mechanism, chloride induced corrosion.
- This research has identified all environmental variables, load effects, material variables, construction variables and established probability distribution for them based on literature as the inputs for time-dependent reliability analysis,

as shown in Table 4.1, 4.5 and 4.6.

- A combination corrosion model (see Table 4.4) has been developed based on existing general corrosion and localized corrosion model. The differences among these three types of corrosion were studied. Generally, localized corrosion has the slowest reduction rate of the cross-sectional area of steel bars. Followed by general corrosion which could result in an up to 15% area loss of the cross-sectional area of steel bars after 100 years exposure. Combination corrosion could lead to the most observable reduction in cross-sectional area loss of steel bars.
- Probabilistic analysis has been carried out on modeling the corrosion initiation time, time-dependent cross-sectional area loss of steel bars, time-dependent resistance and time-dependent reliability under various exposure environment and design variables. The modeling results show that based on the distribution of inputs identified previously, the distribution of important variables associated with corrosion initiation and propagation can be concluded as shown in Table 6.1.

Variables	Notation	Distribution
Corrosion initiation time	T_i	Lognormal
Time-dependent cross-sectional area loss	$A(t)$	Normal (General corrosion) Weibull (Localized corrosion) Weibull (Combination corrosion)
Time-dependent live load	$S(t)$	Extreme value
Time-dependent resistance	$R(t)$	Normal

Table 6.1 Distribution of modeling results of important variables associated with chloride induced corrosion.

- A typical calculation has been performed for a hypothesis pier column to

illustrate the whole process, typical outcomes of a reliability analysis concludes that there will be an approximately 12% decrease in the mean structural resistance of the case pier column with ordinary concrete quality under combination corrosion exposed to an onshore splash zone. Assuming the minimum reliability index $\beta^* = 3.2$, the structure could be at high risk around year 67.

- The sensitivity of time-dependent reliability to important uncertain variables has been examined. The most influencing variables are water-cement ratio and concrete cover depth.

6.1.3 Life cycle cost analysis and integrated model

Major issues discussed in Chapter 5 is life cycle cost analysis and an integrated model, which is shown as follows:

- A review of the life cycle cost concept and general models for cost elements correlated to bridge rehabilitation has been presented, together with the reliability analysis and risk assessment, it can offer prominent improvements in selecting the most suitable rehabilitation strategy.
- A VOTING gate model is introduced to capture the effect of redundancy of bridge structures on probability of failure. Sensitivity analysis concludes that parameter M affects the system probability of failure intensively.
- VOTING gate model is further used in integrating the components probability of failure result from models presented in Chapter 4 and the system risk assessment fault tree model. The integrating process provides alternatives for

modeling system risk of failure and probability of failure depending on whether there are sufficient detailed data for quantitative probabilistic analysis, as shown in Figure 5.5. The process is illustrated by an example calculation. The integrated model can lead to a quantitative analysis of the probability of failure of entire bridge or major bridge sub-systems and the expected failure cost.

6.1.4 Summary

In general, this research refers to important aspects related in risk and reliability analysis area of deteriorating reinforced concrete bridges. It provides qualitative and quantitative risk assessment and time-dependent reliability analysis models considering of both component and system level. Interactions between components and various factors related in design, construction and exposed environment that induce the deterioration of reinforced concrete bridges are considered. It presents establishment of the probabilistic distributions of important variables related in chloride induced corrosion and includes an improved corrosion model. This study also links with life cycle cost analysis model of bridge rehabilitation by providing one of the most important inputs, the probability of failure. It enables probabilistic estimation of the expected failure cost and offers crucial criterion of reliability-based life cycle cost decision making model of deteriorated reinforced concrete bridges. With the aid of fault tree analysis and probabilistic time-dependent reliability analysis, the proposed method effectively overcame the difficulty of data unavailability in risk assessment of existing reinforced concrete

bridges.

6.2 Recommendations

Since there are many assumptions and limitations involved in this study, several aspects may be addressed in future work to improve the quality and accuracy of the model. These include:

- A study of important distress mechanisms not mentioned in Chapter 3 such as sulfate attack, freeze-thaw action and those which are not examined in detail in Chapter 4, will widen the application of the model and increase its capacity to model more interactions and complexity.
- The accuracy of the model can be greatly improved by using five point scales or more. Accordingly, more specific and authoritative rules for assigning the likelihood and consequences ratings need to be established. This will lead to much less sensitive total scaled risk ratings.
- Since there are various laboratory and mathematical models of corrosion mechanisms and the probabilistic distributions of uncertain variables, and majority of them are not consistent, it is necessary to review more recent literature and find the most appropriate models for each mechanism which not only satisfy the accuracy requirement but also are easy to apply.
- In this research, the effects of cracking, spalling, bond strength loss, load redistribution and moment capacity are all ignored in structural analysis of the case pier column. Models to include these influences need to be added. This might result in the consideration of more functional ultimate limit states.

- FRP is a relative new material with high strength and good resistance to corrosion which is currently increasingly used in rehabilitation of structures. However, it is much more expensive compared to traditional rehabilitation materials and the long-term performance data are not available. More research should be aimed at addressing in the properties and the performance of FRP and cost related issues. Thus, life cycle cost of rehabilitation options using FRP can be better evaluated.
- There are many life cycle cost models for design, maintenance and rehabilitation decisions considering different limit states for new bridges and existing bridges. However, cost elements for design of new bridges and maintenance of existing bridge are not exactly the same. It would be valuable to conclude a standard and detailed model to capture the cost characteristics of reinforced concrete bridges.
- In the VOTING gate model, M is crucial parameter for the calculation. However, it is not easy to determine its value. This study only assumes some value for M and studies its effects on system probability of failure. Further modeling of M is essential.

REFERENCES

AS/ NZS 4360 (2004) *Risk management*, Standards Australia.

Alonso, C, Andrade, C, Castellote, M & Castro, P (2000) 'Chloride threshold values to depassivate reinforcing bars embedded in a standardized OPC mortar', *Cement and Concrete Research*, vol. 30, no. 7, pp. 1047-1055.

Branco, FA & Brito, JD (2004a) 'Design for durability', in *Handbook of Concrete Bridge Management*, ASCE, pp. 65-93.

Branco, FA & Brito, JD (2004b) 'Failure cost', in *Handbook of Concrete Bridge Management*, ASCE, pp. 374-410.

Cheung, MS & Kyle, BR (1996) 'Service life prediction of concrete structures by reliability analysis', *Construction and Building Materials*, vol. 10, no. 1, pp. 45-55.

Collins, FG & Grace, WR (1997) 'Specifications and testing for corrosion durability of marine concrete: the Australian perspective (ACI SP 170-39)', in *Proceedings of the 4th CANMET/ACI International Conference on durability of concrete*, Sydney, American Concrete Institute, pp. 757-776.

Creagh, MS, Wijeyakulasuriya, V & Williams, DJ (2006) 'Fault tree analysis and risk assessment for the performance of unbound granular paving materials', *22nd ARRB Conference-Research into Practice*. Canberra, Australia.

Enright, MP & Frangopol, DM (1998a) 'Failure time prediction of deteriorating fail-safe structures', *Journal of Structural Engineering*, vol. 124, no. 12, pp. 1448-1457.

Enright, MP & Frangopol, DM (1998a) 'Probabilistic analysis of resistance degradation of reinforced concrete bridge beams under corrosion', *Engineering Structures*, vol. 20, no. 11, pp. 960-971.

Ericson, CA (2005) 'Fault tree analysis', in *Hazard analysis techniques for system safety*, Hoboken, NJ, Wiley, pp. 183-222.

Estes, AC & Frangopol, DM (1999) 'Repair optimization of highway bridges using system reliability approach', *Journal of Structural Engineering*, vol. 125, no. 7, pp. 766-775.

FABER, MH (2006) 'Logical trees', in *Risk and safety in civil, surveying and environmental engineering*, <http://www.ibk.ethz.ch>, pp. 133-140.

Gonzalez, J, Andrade, C, Alonso, C. & Feliu, S. (1995) 'Comparison of rates of general corrosion and maximum pitting penetration on concrete embedded steel reinforcement', *Cement and Concrete Research*, vol. 25, no. 2, pp. 257-264.

Guiguis, S (1980) *Durability of concrete structures*, Cement and Concrete Association of Australia.

Hoffman, P & Weyers, RE (1994) 'Predicting critical chloride levels in concrete bridge decks', in *Structural Safety and Reliability: Proceedings of ICOSSAR'93*. Balkema, Rotterdam, pp. 957-959.

Hunkeler, F (2005) 'Corrosion in reinforced concrete: processes and mechanisms', in Bohni H *Corrosion in reinforced concrete structures*, Cambridge, England, Woodhead; Boca Raton, pp. 1-42.

Johnson, PA (1999) 'Fault tree analysis of bridge failure due to scour and channel instability', *Journal of Infrastructure Systems*, vol. 5, no. 1, pp. 35-41.

Lebeau, KH & Wadia-Fascetti, SJ (2000) 'A fault tree model of bridge deterioration', *8th ASCE Specialty Conference on Probabilistic Mechanics and Structural Reliability*, Notre Dame, Indiana.

Leira, BJ & Lindgard, J (2000) 'Statistics analysis of laboratory test data for service life prediction of concrete subjected to chloride ingress', *International Conference on Applications of Statistics and Probability*, Sydney, Rotterdam : Balkema, pp. 291-295.

Liu, T & Weyers, RW (1998) 'Modeling the dynamic corrosion process in chloride contaminated concrete structures', *Cement and Concrete Research*, vol. 28, no. 3, pp. 365-379.

Mahar, DJ & Wilbur, JW (1990) *Fault tree analysis application guide*, Rome, Reliability Analysis Center.

Maheswaran, T, Sanjayan, JG & Taplin, G (2005) 'Deterioration modeling and prioritizing of reinforced concrete bridges for maintenance', *Australian Journal of Civil Engineering*, vol. 2, no. 1, pp. 1-12.

Mcgee, RW (2000) 'Modeling of durability performance of Tasmanian bridges', in *Proceedings of ICASP8 Applications of Statistics and Probability in Civil Engineering*, Sydney, A.A. Balkema, pp.297-306.

Modarres, M (2005) 'Introduction and basic definitions', in *Risk analysis in engineering: techniques, tools, and trends*, Boca Raton Taylor & Francis, pp. 1-12.

Morcous, G, Lounis, Z & Mirza, MS (2003) 'Identification of environmental categories for Markovian deterioration models of bridge decks', *Journal of Bridge Engineering*, vol. 8, no. 6, pp. 353-361.

Mori, Y & Ellingwood, BR (1993) 'Reliability-based service-life assessment of aging concrete structures', *Journal of Structural Engineering*, vol. 119, no. 5, pp. 1600-1621.

Nezamian, A, Setunge, S, Lokuge, W & Fenwick, JM (2004) 'Reliability based optimal solution for rehabilitation of existing bridge structures', *Clients Driving Innovation International Conference*. Queensland, Australia, Surfers Paradise.

Nowak, AS & Szerzen, MM (1998) 'Bridge load and resistance models', *Engineering Structures*, vol. 20, no. 11, pp. 985-990.

Papadakis, V, Roumeliotis, A, Fardis, M & Vagenas, C (1996) 'Mathematical modeling of chloride effect on concrete durability and protection measures'. in Dhir R & Jones M *Concrete repair, rehabilitation and protection*. London, E&F Spon, pp. 165-174.

Patev, RC, Schaaf, DM & James, RM (2000) 'Time-dependent reliability for structures subjected to Alkali-Aggregate Reaction', in *Proceedings of 9th United Engineering Foundation Conference* California Reston: ASCE, pp. 152-163.

Radojicic, A, Bailey, SF & Bruhwiler, E (2001) 'Probabilistic models of cost for the management of existing structures', in Frangopol, DM & Furuta, H *Life-Cycle Cost Analysis and Design of Civil Infrastructure Systems*. ASCE, pp. 251-270.

Rendell, F, Jauberthie, R. & Grantham, M (2002) 'Deterioration of concrete', *Deteriorated concrete: inspection and physicochemical analysis*, London, Thomas Telford, pp. 29-54.

Ropke, JC (1982) 'Concrete repairs', *Concrete problems: causes, and cures*, New York, McGraw-Hill, pp. 99-100.

Ryall, MJ (2001) 'Durability and protection', *Bridge management*, Oxford, Butterworth-Heinemann, pp. 331-377.

Sharabah, A. Setunge, S & Zeephongsekul, P (2006) 'Use of Markov chain for deterioration modeling and risk management of infrastructure assets', *International Conference on Information and Automations*. Colombo, Sri Lanka.

Sianipar, PRM & Adams, TM (1997) 'Fault-tree model of bridge element deterioration due to interaction', *Journal of Infrastructure Systems*, vol. 3, no. 3, pp. 103-110.

Stewart, MG (2001) 'Reliability-based assessment of ageing bridges using risk ranking and life cycle cost decision analyses', *Reliability Engineering & System Safety*, vol. 74, no. 3, pp. 263-273.

Stewart, MG & Melchers, RE (1997a) 'Risk-based decision process', *Probabilistic risk assessment of engineering systems*, London, Chapman & Hall, pp. 5-11.

Stewart, MG & Melchers, RE (1997b) 'System evaluation', *Probabilistic risk assessment of engineering systems*, London, Chapman & Hall, pp. 154-201.

Stewart, MG & Rosowsky, DV (1998) 'Structural safety and serviceability of concrete bridges subject to corrosion', *Journal of Infrastructure Systems*, vol. 4, no. 4, pp. 146-155.

Thoft-Christensen, P (1998) 'Assessment of the reliability profiles for concrete bridges', *Engineering Structures*, vol. 20, no. 11, pp. 1004-1009.

Thoft-Christensen, P (2000) 'On reliability based optimal design of concrete bridges', *2000 Structures Congress*. Philadelphia, pp. 1-8.

Tonias, DE & Zhao, JJ (2007) 'The structure', *Bridge Engineering: Design, Rehabilitation and Maintenance of Modern Highway Bridges*, New York, Mcgraw-hill, pp. 1-16.

Val, DV & Melchers, RE (1997) 'Reliability of deteriorating RC slab bridges', *Journal of Structural Engineering*, vol. 123, no. 12, pp. 1638-1644.

Val, DV & Stewart, MG (2003) 'Life-cycle cost analysis of reinforced concrete structures in marine environments', *Structural Safety*, vol. 25, no. 4, pp. 343-362.

Val, DV, Stewart, MG & Melchers, RE (1998) 'Effect of reinforcement corrosion on reliability of highway bridges', *Engineering Structures*, vol. 20, no. 11, pp. 1010-1019.

Venkatesan, S, Setunge, S, Molyneaux, T & Fenwick, J (2006) 'Evaluation of distress mechanisms in bridges exposed to aggressive environments', *Second International Conference of the CRC for Construction Innovation*. Australia.

Vick, SG (2002) 'Reliability, risk and probabilistic methods', *Degrees of belief: subjective probability and engineering judgment*. Reston, ASCE Press, pp. 105-180.

Vu, KAT & Stewart, MG (2000) 'Structural reliability of concrete bridges including improved chloride-induced corrosion models', *Structural Safety*, vol. 22, no. 4, pp. 313-333.

Wen, YK & Kang, YJ (1998) 'Optimal seismic design based on life-cycle cost', in Frangopol DM *Optimal performance of civil infrastructure systems*. Reston, ASCE, pp 194-210.

Willams, DJ, Gowan, M & Golding, B (2001) *ACARP Project C8039 Final Report, Risk assessment of Bowen Basin Spoil rehabilitation*. Brisbane, University of Queensland.

Zhang, Z, Sun, X & Wang, X (2003) 'Determination of bridge deterioration matrices with state national bridge inventory data', *9th International Bridge Management Conference*. Orlando, Florida Transportation Research Board.

APPENDIX A SPECIFIC RULES FOR ASSIGN LIKELIHOOD RATINGS

Basic events	Description	Rules for assign likelihood
A1	Reactive aggregate	If the concrete mix contains ASR sensitive elements shown in Table A.2, A1=High; if not, A1=Low; if unknown, A1=Medium.
A2	Presence of excessive moisture	See Table A.3.
A4	Improper concrete mix in design	Check whether fly ash has been used in concrete mix. If yes, A4=Low; if no, A4=High; if unknown, A4= Medium
A7	Improper water cement ration design	Refer to relevant design codes and specifications (e.g. Table A.4 and Table A.5)
A8	Improper construction and curing	Same as PS2
CHL1	High chloride environment	See Table A.6
CHL2	Moisture and oxygen	See Table A.7
CHL7	Insufficient depth of concrete cover in design	Refer to relevant design codes and specifications (e.g. Table A.4 and Table A.5)
CHL9	Improper water cement ratio design	Refer to relevant design codes and specifications (e.g. Table A.4 and Table A.5)
CHL10	Improper construction and curing	Same as PS2
C1	High carbon dioxide	If bridge is located in urban area with high traffic capacity, C1= High
C2	High relative humidity	If $50\% < \text{Relative Humidity} < 75\%$, C2=High
C5	Improper concrete mix in design (water cement ratio)	Refer to relevant design codes and specifications (e.g. Table A.4 and Table A.5)
C6	Improper construction and curing	Same as PS2
PS2	Improper curing	Proper curing methods including: protecting the concrete with temporary coverings or applying a fog-spray during any appreciable delay between placing and finishing; providing sunshades to reduce the temperature at the surface of the concrete, etc. If those works haven't been done, PS2=High.
PS3	High wind velocity (in plastic stage of concrete)	If wind velocity 0-10(mph), PS3=Low 10-20 (mph), PS3= Medium 20-30 (mph), PS3= High
PS4	Low relative humidity (in plastic stage of concrete)	Relative Humidity $< 30\%$ PS4=High $30\% < \text{Relative Humidity} < 70\%$ PS4= Medium Relative Humidity $> 70\%$ PS4=Low.

Table A.1 Rules for assign likelihood ratings of each basic events.

ASR Sensitive Coarse Aggregates Element	ASR Sensitive Fine aggregate
Tuff	Quartz
Andesite	Feldspar
Trachyte	Granite
Quartz	Quartzite
Feldspar	Chert
Granite	
Chert	
Sand stone	
Slate	
Greenstone	
Ferniginous rock	
Quartzite	
Meta-greywacke	

Table A.2 ASR sensitive aggregates.

No.	Pattern Definition	Likelihood of A2
1	Below low water level (submerged)	High
2	In tidal zone (also wetting and drying zone)	Medium
3	In Splash Zone	Medium
4	In Splash - Spray zone (also wetting and drying zone)	Medium
5	In splash-tidal zone	Medium
6	Above Splash zone	Low
7	Well above splash zone (nearly top deck)	Low
8	Benign Environment	Low

Table A.3 Likelihood of A2 according to exposure classification.

Environmental Category	Specification		Detailing Requirements
Category 1 <ul style="list-style-type: none"> – Low humidity (25-50% throughout year) – Temperature range 10-35 °C – Large daily temperature range – Low rainfall – Low atmospheric pollution 	Maximum w/c	0.6	Minimum cover 30 mm
	Minimum cement content	280 kg / m ³	
Category 2 <ul style="list-style-type: none"> – High humidity throughout year – High rainfall – Moderate atmospheric pollution – Running water (not soft) 	Maximum w/c	0.55	Minimum cover 40 mm
	Minimum cement content	300 kg / m ³	
Category 3 <ul style="list-style-type: none"> – Wind driven rain – 1-5km of coast – Heavy condensation – Soft water action – Freeze-thaw action – High atmospheric pollution 	Maximum w/c	0.5	Minimum cover 50 mm
	Minimum cement content	330 kg / m ³	
Category 4 <ul style="list-style-type: none"> – Abrasion – Corrosive atmosphere – Corrosive water – Marine conditions: wetting and drying sea spray within 1km of sea coast – Application of de-icing salt 	Maximum w/c	0.45	Minimum cover 65 mm
	Minimum cement content	400 kg / m ³	

Table A.4 Concrete details in marine conditions.

	Submerged concrete	Concrete in tidal or splash zone	Concrete in atmosphere
Portland cement type	A	D	A
Max w/c ratio	0.45	0.45	0.45
Min cement content (kg/m ³)	400	400	360
Min concrete cover (mm)	65	65	65

Table A.5 Concrete details in marine conditions category 4.

No	Definition	Likelihood of CHL1
1	Salt water containing chlorides (> 15 g/l)	High
2	Water containing sulfate ions (> 1 g/l)	High
3	Water with pH > 7.5	High
4	Aggressive soils with pH < 4	High
5	Humid / Temperate / Dry environments	High
6	Aggressive pollutants	High
7	Aggressive soils (rich in nitrates)	High
8	Salt deposits (e.g. due to water evaporation)	Medium
9	Salt water retention (e.g. hollow spun piles cast with saline water mix)	Medium
10	Added during construction (e.g. Calcium Chloride added as accelerator)	Medium
11	Running or Standing water (e.g. in culverts)	Medium
12	Abrasion / Scouring / Water current effects	Medium

Table A.6 Likelihood of CHL1 according to environment classification.

No	Pattern Definition	Likelihood of CHL2
1	Below low water level (submerged)	Low
2	In tidal zone (also wetting and drying zone)	High
3	In Splash Zone	High
4	In Splash - Spray zone (also wetting and drying zone)	High
5	In splash-tidal zone	Medium
6	Above Splash zone	Medium
7	Well above splash zone (nearly top deck)	Low
8	Benign Environment	Low

Table A.7 Likelihood of CHL7.

APPENDIX B MODELING CORROSION INITIATION TIME

1. Inputs

Parameter		Mean	COV	Distribution
$C_0 (kg / m^3)$	de-icing salts	3.5	0.5	Lognormal
	onshore splash zone	7.35	0.5	Lognormal
	coastal zone	Equation (4.5)	0.5	Lognormal
$X (cm)$		Specified+0.6	$\sigma = 1.15$	Normal
$D (cm^2 / year)$		Equation (4.6)	0.2	Normal
$C_{cr} (kg / m^3)$		0.9	--	Uniform range from 0.6 to 1.2

Table B.1 Statistics characteristics of inputs for modeling corrosion initiation time.

2. Results

Generally, corrosion initiation time fits lognormal distribution, the probabilistic characteristic of the distribution are showing in following tables (see Figure 4.5 to 4.10).

T_i (w/c=0.55)	De-icing salts			Onshore splash zone			Coastal zone d=50m		
	Mean	Std	Correlation	Mean	Std	Correlation	Mean	Std	Correlation
x=3	7.13	9.91	0.985	2.99	3.28	0.996	9.29	13.90	0.965
x=4	10.29	10.91	0.997	4.49	3.65	0.998	12.99	14.59	0.995
x=5	14.23	12.86	0.997	6.42	4.40	0.998	17.46	16.59	0.998
x=6	18.56	15.01	0.997	8.76	5.46	0.997	22.21	18.37	0.997
x=7	23.32	17.04	0.997	11.49	6.71	0.997	27.51	20.53	0.997

Table B.2 Statistics characteristics of modeling results of corrosion initiation time of ordinary quality of concrete structures with different concrete cover depth.

T_i (x=5cm)	De-icing salts			Onshore splash zone			Coastal zone d=50m		
	Mean	Std	Correlation	Mean	Std	Correlation	Mean	Std	Correlation
w/c=0.40	51.07	27.76	0.977	35.81	21.72	0.971	54.61	28.83	0.995
w/c=0.45	32.06	23.56	0.995	17.35	11.59	0.993	36.26	26.56	0.999
w/c=0.50	20.65	17.44	0.998	9.91	6.76	0.998	24.36	21.04	0.999
w/c=0.55	14.23	12.86	0.997	6.42	4.40	0.998	17.46	16.59	0.998
w/c=0.60	10.45	9.88	0.995	4.53	3.12	0.996	13.22	13.51	0.998
w/c=0.65	8.01	7.34	0.993	3.41	2.37	0.994	10.36	11.05	0.997
w/c=0.70	6.42	6.35	0.991	2.68	1.85	0.993	8.39	9.19	0.997

Table B.3 Statistics characteristics of modeling results of corrosion initiation time of x=5cm concrete structures with different concrete qualities.

3. Sensitivity analysis

Varying COV of surface chloride concentration ($COV(C_0)$) from 0.1 to 0.5, the modeling results for a RC element located 50m from coast with ordinary concrete mix(w/c=0.55) and ordinary concrete cover depth (x=5cm) are as (refer to Figure 4.11):

$COV(C_0)$	T_i (w/c=0.55, x=5cm)		
	Mean	Std	Correlation
0.1	12.72	7.79	0.997
0.2	13.59	9.30	0.999
0.3	15.03	11.72	0.999
0.4	16.09	13.86	0.997
0.5	17.46	16.59	0.998

Table B.4 Sensitivity of Statistics characteristics of modeling result of corrosion initiation time with $COV(C_0)$.

APPENDIX C MODELING TIME-DEPENDENT AREA LOSS OF A STEEL BAR

1. Inputs

(1) General conclusion of statistical characteristics of corrosion variables

Parameter	Mean	COV	Distribution
$D_0(mm)$	Specified	--	Deterministic
$T_l(year)$	Previous modeling results	Previous modeling results	Lognormal
$i_{corr}(1) (\mu A/cm^2)$	Equation (4.6)	0.2	Normal
R		0.24	Uniform range from 3.5 to 8.5

Table C.1 Probabilistic characteristics of corrosion variables.

(2) Mean of $i_{corr}(1)$ according to Equation (4.6)

$$i_{corr}(1) = \frac{3.78(1 - \frac{w}{c})^{-1.64}}{cover} (\mu A/cm^2)$$

$i_{corr}(1) (\mu A/cm^2)$		w/c						
		0.4	0.45	0.5	0.55	0.6	0.65	0.7
X(cm)	3	2.91	3.36	3.93	4.67	5.66	7.05	9.08
	4	2.18	2.52	2.95	3.50	4.25	5.29	6.81
	5	1.75	2.02	2.36	2.80	3.40	4.23	5.45
	6	1.46	1.68	1.96	2.33	2.83	3.52	4.54
	7	1.25	1.44	1.68	2.00	2.43	3.02	3.89

Table C.2 Mean values of initial corrosion current.

(3) Modeling results of distribution of corrosion initiation time T_i see Appendix

A.

2. Outputs

The analysis chose one example structure element located in onshore splash zone with $w/c=0.55$ and $X=5\text{cm}$, the original diameter of reinforced steel was assigned to be 32mm.

(1) General Corrosion

- Modeling result and statistics characteristics for residual area of each year, t means the time since the structure was built. The results of every 5 years in 100 years service time are shown below.

A(t)	Minimum	Maximum	Mean	Std Dev
Area(0)	804.2476807	804.2476807	804.2476807	0
Area(5)	787.9973755	805.934082	801.9029387	3.330639403
Area(10)	772.7432251	805.5770264	793.4748021	6.836793018
Area(15)	760.8905029	805.7592773	784.6803134	8.19741549
Area(20)	744.8383789	805.1825562	776.7940691	8.798379428
Area(25)	733.5720825	805.315918	769.5760774	9.457900938
Area(30)	728.2871094	804.4627075	762.9589413	10.23138118
Area(35)	714.8706055	804.2476807	756.7605758	11.00518805
Area(40)	709.1749878	804.2476807	750.9209643	11.78536491
Area(45)	698.1865845	804.8932495	745.3486622	12.65235058
Area(50)	689.1233521	804.2476807	739.9798879	13.57352605
Area(55)	680.1604004	800.006897	734.8422062	14.367835
Area(60)	662.6408081	804.2476807	729.8559939	15.26124554
Area(65)	662.0369873	800.2047729	725.0314704	16.0827538
Area(70)	653.1646729	801.9112549	720.331146	16.94448686
Area(75)	649.1297607	793.4943848	715.7596841	17.74420725
Area(80)	643.9008789	783.7592163	711.3186702	18.46701732
Area(85)	632.2446899	794.4733887	706.9507864	19.30799415
Area(90)	624.180481	781.2797852	702.691712	20.02100711
Area(95)	622.6675415	778.2516479	698.5154138	20.76178026
Area(100)	607.7827148	781.1063843	694.4257818	21.49003878

Table C.3 Modeling result of time-dependent cross-sectional area of case steel bar under general corrosion.

- Distribution fit (take *Area*(50) for example): The residual area of steel bar generally fits normal distribution, see Figure C.1.

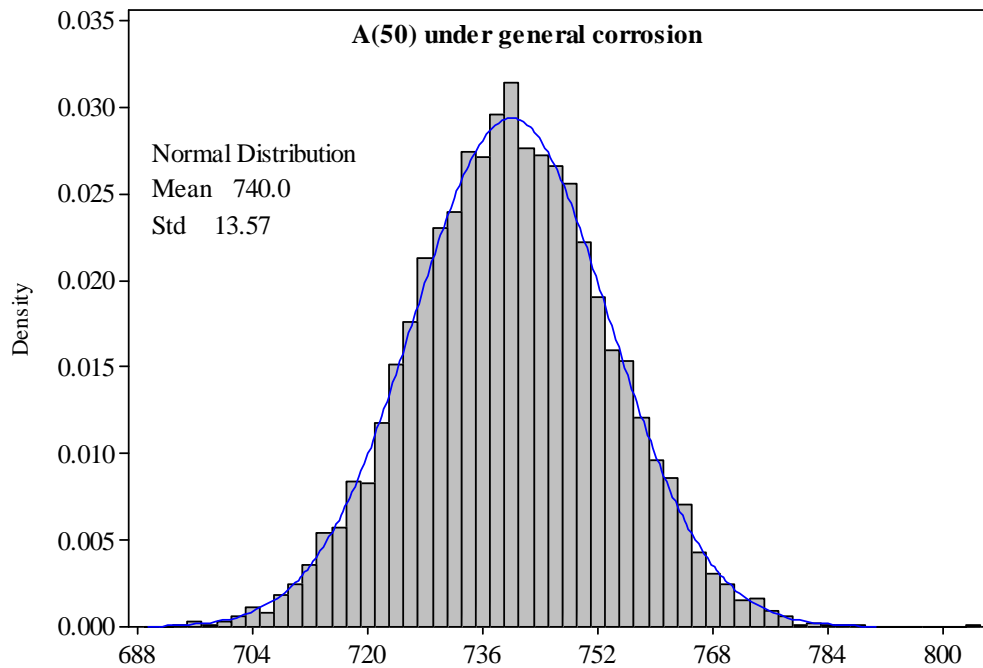


Figure C.1 Distribution of A(50) under general corrosion.

(2) Localized corrosion

- Modeling result and statistics characteristics for residual area of each year, t means the time since the structure was built. The results of every 5 years in 100 years service time are shown in the table below.

A(t)	Minimum	Maximum	Mean	Std Dev
Area(0)	804.2476807	804.2476807	804.2476807	0
Area(5)	801.9077148	804.2476807	804.1491038	0.209058219
Area(10)	793.835083	804.2476807	803.2896395	1.047719336
Area(15)	786.6506348	804.2476807	801.6116103	2.260072853
Area(20)	778.4899292	804.2476807	799.357088	3.700966882
Area(25)	768.9797974	804.2476807	796.6816805	5.30544075
Area(30)	752.3262939	804.2476807	793.6842491	7.122153393
Area(35)	734.8835449	804.2476807	790.369812	9.076569863
Area(40)	722.5448608	804.2476807	786.8757243	11.12723314
Area(45)	708.9033203	804.2476807	783.1470599	13.4177191
Area(50)	688.8182983	804.2476807	779.2387531	15.60545697
Area(55)	683.2276001	804.1743164	775.1675316	17.98782784
Area(60)	652.1546631	804.2476807	770.9367043	20.32847871
Area(65)	617.4414063	804.1300049	766.6117417	22.85819082
Area(70)	621.8325806	804.2331543	762.1030584	25.55301382
Area(75)	604.6831055	803.7747803	757.452636	28.3158307
Area(80)	570.0836182	801.9466553	752.6906693	31.12963547
Area(85)	529.4793701	803.614502	747.8756689	33.87897947
Area(90)	539.7609253	802.8283691	742.9443331	36.53373549
Area(95)	534.1951294	802.765564	737.9673679	39.31593543
Area(100)	498.6390076	801.5526123	732.7767397	42.37107772

Table C.4 Modeling result of time-dependent cross-sectional area of case steel bar under localized corrosion.

- Distribution fit (take *Area(50)* for example): The residual area of steel bar under localized corrosion generally fits weibull distribution.

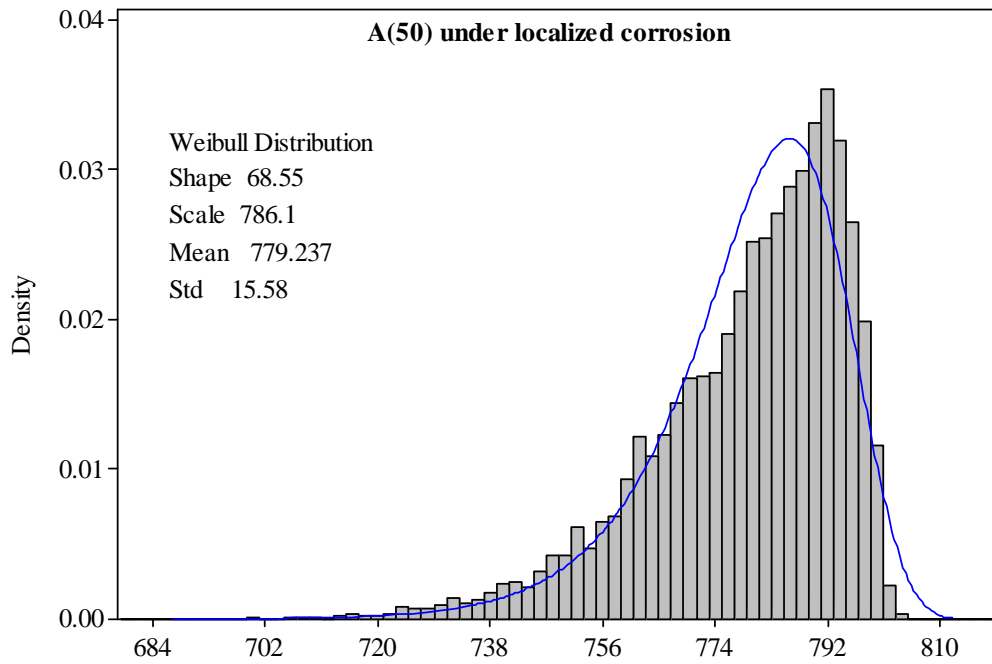


Figure C.2 Distribution of A(50) under localized corrosion.

(3) Combination corrosion

- Modeling result and statistics characteristics for residual area of each year, t means the time since the structure was built. The results of every 5 years in 100 years service time are shown below.
- Distribution fit (take $Area(50)$ for example): The residual area of steel bar under combination corrosion generally fits weibull distribution with 0.996 as correlation.

Output Name	Minimum	Maximum	Mean	Std Dev
Area(0)	804.2476807	804.2476807	804.2476807	0
Area(5)	785.6577759	805.9046631	801.8043541	3.506166199
Area(10)	762.3381348	805.5652466	792.5169016	7.684239498
Area(15)	743.6143188	805.7383423	782.0452089	9.975991675
Area(20)	723.5170288	805.1801758	771.9065961	11.70946823
Area(25)	707.0757446	805.3112793	762.0173422	13.6248899
Area(30)	680.4177856	804.4623413	752.4096422	15.88302159
Area(35)	654.1191406	804.2476807	742.9071053	18.28292645
Area(40)	628.0790405	804.2476807	733.5874989	20.76454775
Area(45)	612.1134033	804.8892822	724.3056335	23.56658497
Area(50)	585.288147	804.2476807	715.0524844	26.29228417
Area(55)	574.9091797	799.9334717	705.8738353	29.17333005
Area(60)	521.4235229	804.2476807	696.6931101	32.00996074
Area(65)	480.1575317	800.0870361	687.5874856	35.00249765
Area(70)	483.0906067	801.8966675	678.4312393	38.18960684
Area(75)	465.6013184	793.0215454	669.2710925	41.41617121
Area(80)	424.1028748	780.2393799	660.1397964	44.68569481
Area(85)	366.8240356	793.84021	651.0372632	47.83257285
Area(90)	384.9334106	778.9431152	641.9373864	50.86634193
Area(95)	378.6016846	776.7697754	632.8858559	53.98625097
Area(100)	330.8067322	778.4119873	623.7241087	57.43929645

Table C.5 Modeling result of time-dependent cross-sectional area of case steel bar under combination corrosion.

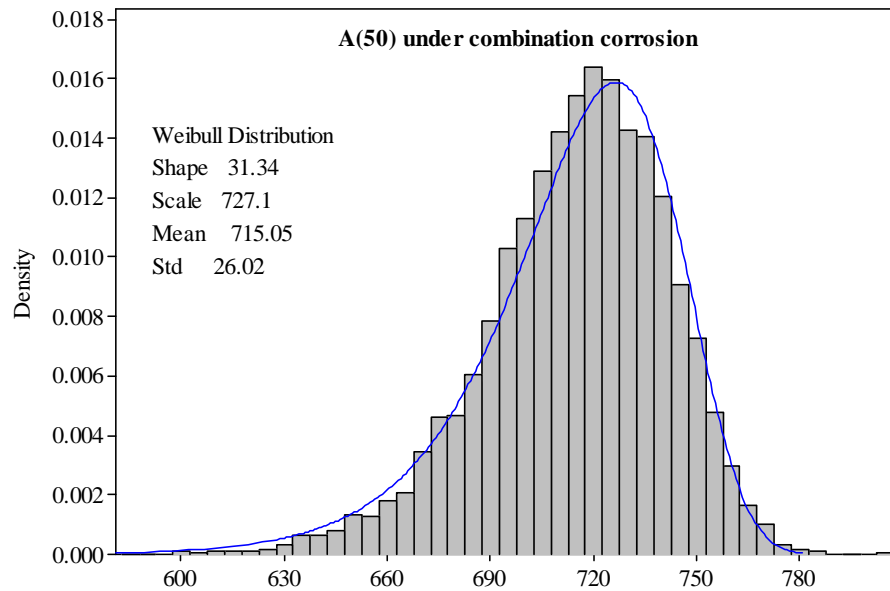


Figure C.3 Distribution of A(50) under combination corrosion.

APPENDIX D ILLUSTRATIVE EXAMPLE

CALCULATION OF TIME-DEPENDENT RELIABILITY ANALYSIS

1. Live load distribution

Considering the increase of traffic volume, the time-dependent distribution of the weight of heaviest truck (annually) can be formulated as,

$$F_n(w, t) = \left[\Phi \left(\frac{w - \mu_w \cdot (1 + \lambda_m)^t}{\sigma_w \cdot (1 + \lambda_m)^t} \right) \right]^{N \cdot (1 + \lambda_v)^t}$$

where λ_m is annual increases in trucks loads, λ_v is annual increases in heavy traffic (truck) volume, N is the number of crossings of heavily loaded fully correlated trucks per year, μ_w and σ_w are statistical parameters of live load of a single truck and Φ is the cumulative function of standard normal distribution. Assigning $\lambda_m=1\%$, $\lambda_v=1\%$ and $N=600$, live load generally approach extreme value distribution, the probabilistic parameters are showing in the table below:

Year	Live load			
	Mean	Std	a	b
0	1245.934	85.394	1207.503	66.581
5	1279.107	87.38	1239.781	68.13
10	1313.132	89.364	1272.913	69.677
15	1348.087	91.454	1306.928	71.306
20	1383.944	93.572	1341.832	72.958
25	1420.775	95.677	1377.715	74.599
30	1458.55	97.948	1414.468	76.37
35	1497.344	100.265	1452.22	78.176
40	1537.13	102.529	1490.986	79.942
45	1577.918	104.844	1530.732	81.747
50	1619.939	107.346	1571.627	83.698
55	1663.026	109.906	1613.562	85.693
60	1707.171	112.373	1656.597	87.617
65	1752.531	114.997	1700.777	89.663
70	1799.099	117.681	1746.136	91.756
75	1846.835	120.417	1792.641	93.889
80	1895.883	123.231	1840.423	96.083
85	1946.214	126.102	1889.462	98.321
90	1997.88	129.06	1939.8	100.63
95	2050.87	132.1	1991.42	102.99
100	2105.33	135.14	2044.51	105.37

Table D.1 Probabilistic characteristics of live load.

2. Structural resistance distribution

Generally, time-dependent resistance fits normal distribution. Probabilistic parameters of time-dependent resistance under different corrosion types, exposed environments and durability designs are shown in following tables.

Year	Combination corrosion		General corrosion		Localized corrosion	
	Mean	Std	Mean	Std	Mean	Std
0	5805.39	833.2	5809.57	811.53	5809.57	811.53
5	5791.80	833.09	5796.93	811.54	5808.43	811.51
10	5755.81	832.95	5767.87	811.01	5801.8	811.36
15	5717.62	832.88	5741.47	810.7	5790.52	811.29
20	5681.79	832.22	5718.6	810.07	5776.92	811.19
25	5645.43	831.4	5698.34	810.37	5761.74	811.24
30	5607.88	833.42	5679.44	810.54	5743.89	811.7
35	5572.64	834.91	5661.05	808.84	5724.63	811.73
40	5535.90	834.31	5644.56	809.09	5706.25	811.05
45	5499.17	834.94	5627.38	809.77	5683.38	814.46
50	5462.05	837.93	5612.78	809.72	5663.69	814.47
55	5427.47	838.61	5599.44	807.48	5643.88	812.59
60	5391.77	839.2	5584.2	809.4	5618.41	816.96
65	5361.09	840.06	5570.15	809.71	5596.24	819.27
70	5322.68	838.14	5556.7	808.51	5572.02	818.93
75	5288.68	842.51	5544.53	808.86	5552.73	820.44
80	5255.68	847.63	5531.81	808.11	5529.62	822.41
85	5223.51	847.41	5519.58	808.89	5504.77	823.35
90	5186.83	851.52	5506.1	810.29	5475.58	827.9
95	5158.80	852.58	5496.8	808.86	5456.36	829.64
100	5123.76	850.81	5484.71	808.95	5432.43	833.33

Table D.2 Probabilistic characteristics of resistance of structures under combination corrosion, general corrosion and localized corrosion.

Year	Onshore splash zone		De-icing salts		Coastal zone d=50m	
	Mean	Std	Mean	Std	Mean	Std
0	5805.39	833.2	5808.82	832.27	5802.04	817.7
5	5791.80	833.09	5803.89	832.14	5798.21	817.6
10	5755.81	832.95	8782.2	832.21	5780.99	817.46
15	5717.62	832.88	5753.18	833.46	5754.35	818.94
20	5681.79	832.22	5721.68	832.4	5724.29	818.53
25	5645.43	831.4	5686.17	833.04	5692.47	820.99
30	5607.88	833.42	5652.51	833.28	5659.74	821.27
35	5572.64	834.91	5618.62	834.29	5624.64	820.85
40	5535.90	834.31	5578.1	834.27	5591.18	820.12
45	5499.17	834.94	5544.95	837.65	5554.27	819.58
50	5462.05	837.93	5510.8	837.48	5521.24	820.45
55	5427.47	838.61	5473.29	841.57	5486.75	825.6
60	5391.77	839.2	5440.84	839.53	5449.62	828.66
65	5361.09	840.06	5402.97	842.33	5413.21	827.3
70	5322.68	838.14	5366.38	845.97	5384.53	823.07
75	5288.68	842.51	5336.76	846.44	5346.23	831.81
80	5255.68	847.63	5298.66	846.69	5312.24	835.84
85	5223.51	847.41	5259.14	849.88	5274.97	834.47
90	5186.83	851.52	5229.66	853.01	5241.83	837.84
95	5158.80	852.58	5199.81	854.19	5207.49	836.01
100	5123.76	850.81	5160.97	853.35	5176.81	842.05

Table D.3 Probabilistic characteristics of resistance of structures under different exposure environment.

Year	X=3cm		X=5cm		X=7cm	
	Mean	Std	Mean	Std	Mean	Std
0	5810.24	827.77	5805.39	833.2	5811.23	824.91
5	5758.28	827.78	5791.80	833.09	5808.99	824.91
10	5684.09	827.5	5755.81	832.95	5783.18	824.97
15	5609.27	827.28	5717.62	832.88	5769.68	824.96
20	5537.81	827.97	5681.79	832.22	5745.51	824.02
25	5465.9	828.97	5645.43	831.4	5722.04	823.97
30	5391.16	837.82	5607.88	833.42	5699.2	823.64
35	5319.42	842.94	5572.64	834.91	5676.08	824.29
40	5255.54	847.2	5535.90	834.31	5653.1	822.85
45	5182.05	848.77	5499.17	834.94	5628.88	825.27
50	5115.79	855.72	5462.05	837.93	5607.67	824.96
55	5054.45	861.49	5427.47	838.61	5586.09	824.69
60	4997.93	859.82	5391.77	839.2	5564.27	825.71
65	4954.3	859	5361.09	840.06	5539.16	826.6
70	4906.98	856.86	5322.68	838.14	5520.38	826.3
75	4860.44	854.5	5288.68	842.51	5495.66	827.84
80	4822.55	852.59	5255.68	847.63	5475.32	829.21
85	4793.11	848.94	5223.51	847.41	5452.82	826.61
90	4759.72	851.94	5186.83	851.52	5429.49	831.17
95	4732.29	851.15	5158.80	852.58	5406.77	830.63
100	4699.42	845.67	5123.76	850.81	5386.94	832.54

Table D.4 Probabilistic characteristics of resistance of structures with different concrete cover depth.

Year	w/c=0.7		w/c=0.6		w/c=0.5	
	Mean	Std	Mean	Std	Mean	Std
0	4814.77	648.76	5805.39	833.2	6954.2	1032.2
5	4774.59	648.63	5791.80	833.09	6952.3	1032.2
10	4702.85	648.42	5755.81	832.95	6939.2	1032.5
15	4633.62	651.08	5717.62	832.88	6919.3	1031.7
20	4565.55	648.33	5681.79	832.22	6897.4	1032.5
25	4492.9	652.83	5645.43	831.4	6875.5	1032.6
30	4423.87	656.72	5607.88	833.42	6853.1	1032.1
35	4357.53	663.06	5572.64	834.91	6832.1	1032
40	4289.99	665.42	5535.90	834.31	6808.9	1032.1
45	4224.2	671.82	5499.17	834.94	6786.9	1031.6
50	4157.78	674.06	5462.05	837.93	6766.1	1030.4
55	4100.26	681.2	5427.47	838.61	6745.4	1031.9
60	4040.21	677.76	5391.77	839.2	6722	1032.5
65	4001.41	684.02	5361.09	840.06	6701.3	1031.8
70	3945.95	678.83	5322.68	838.14	6680.9	1034
75	3901.87	686.14	5288.68	842.51	6656.9	1033.6
80	3857.71	682.23	5255.68	847.63	6636.7	1031.8
85	3827.32	677.04	5223.51	847.41	6614.7	1035.5
90	3798.39	682.98	5186.83	851.52	6596.1	1033.2
95	3761.88	675.92	5158.80	852.58	6572.4	1037
100	3734.61	672.18	5123.76	850.81	6547.4	1037.9

Table D.5 Probabilistic characteristics of resistance of structures with different water-cement ratio.

3. Calculation of Reliability index and probability of failure

(1) Monte Carlo Simulation

- Calculation of reliability index and probability of failure is simulated using

Matlab program, which shows below:

```
function monte(m1,s1,m2,s2,n) ' m1=Mean of R, s2=Std of R, m2=Mean of live load,  
s2=Std of live load and n=sample size  
r=normrnd(m1,s1,1,n); 'simulating R  
d=normrnd(840,84,1,n); ' simulating dead load  
u=rand(1,n);  
l=m2-0.45*s2-0.7797*s2.*log(-log(u)); 'simulating live load  
z=r-l-d;  
zz=find(z<=0);  
k=length(zz); 'calculation number of failure  
pf=k/n  
beta=norminv(1-pf)
```

- Example inputs and results:

```
>> monte(5805.39,833.2,1245.934,85.394,10e6)  
pf =  
4.9000e-006  
beta =  
4.4215
```

(2) Results table

Year	Combination corrosion				General corrosion				Localized corrosion			
	p_f	β	p_f^*	β^*	p_f	β	p_f^*	β^*	p_f	β	p_f^*	β^*
0	4.90E-06	4.42154	-	-	3.40E-06	4.499854	-	-	3.40E-06	4.499854	-	-
5	7.30E-06	4.334638	2.40E-06	4.573343	4.00E-06	4.465184	6E-07	4.855637	4.60E-06	4.435169	1.2E-06	4.716445
10	9.90E-06	4.267134	2.60E-06	4.556551	5.30E-06	4.404558	1.3E-06	4.700126	5.00E-06	4.417173	4E-07	4.935367
15	1.52E-05	4.170449	5.30E-06	4.404555	8.60E-06	4.298446	3.3E-06	4.506195	5.70E-06	4.388758	7E-07	4.825004
20	1.98E-05	4.109801	4.60E-06	4.435166	1.20E-05	4.224004	3.4E-06	4.499853	7.90E-06	4.317229	2.2E-06	4.591533
25	2.72E-05	4.035871	7.40E-06	4.33164	1.70E-05	4.144874	5E-06	4.417171	9.70E-06	4.271687	1.8E-06	4.633231
30	4.48E-05	3.917155	1.76E-05	4.136913	2.10E-05	4.096193	4E-06	4.46518	1.32E-05	4.202486	3.5E-06	4.493686
35	6.29E-05	3.834539	1.81E-05	4.130474	2.82E-05	4.027388	7.2E-06	4.337667	1.96E-05	4.112145	6.4E-06	4.363494
40	9.63E-05	3.72853	3.34E-05	3.98739	3.68E-05	3.964338	8.6E-06	4.298439	2.79E-05	4.029902	8.3E-06	4.306306
45	1.39E-04	3.634797	4.28E-05	3.928132	4.91E-05	3.894997	1.23E-05	4.21843	3.83E-05	3.954796	1.04E-05	4.256119
50	2.07E-04	3.530612	6.82E-05	3.814572	6.28E-05	3.83493	1.37E-05	4.194053	5.48E-05	3.868293	1.65E-05	4.151701
55	2.89E-04	3.441733	8.17E-05	3.769715	7.70E-05	3.784529	1.42E-05	4.185916	6.82E-05	3.814607	1.34E-05	4.199069
60	4.26E-04	3.335585	1.37E-04	3.639395	1.13E-04	3.687801	3.61E-05	3.968899	1.14E-04	3.68556	4.59E-05	3.911285
65	5.94E-04	3.241602	1.69E-04	3.58464	1.48E-04	3.618776	3.49E-05	3.97694	1.59E-04	3.599851	4.51E-05	3.915518
70	7.97E-04	3.157112	2.03E-04	3.536778	2.00E-04	3.54048	5.17E-05	3.882436	2.24E-04	3.510182	6.47E-05	3.827559
75	0.0012	3.035672	4.04E-04	3.350299	2.59E-04	3.471168	5.94E-05	3.84854	3.00E-04	3.432067	7.56E-05	3.789035
80	0.0017	2.92905	5.01E-04	3.290189	3.49E-04	3.390285	9E-05	3.745484	4.19E-04	3.33973	0.00012	3.673051
85	0.0024	2.820158	7.01E-04	3.19416	4.62E-04	3.3127	0.000113	3.688163	6.15E-04	3.231645	0.000196	3.545167
90	0.0034	2.706483	1.00E-03	3.089519	6.38E-04	3.221279	0.000176	3.57341	8.82E-04	3.127433	0.000266	3.463636
95	0.0045	2.612054	1.10E-03	3.060794	8.24E-04	3.147168	0.000186	3.55874	0.0012	3.035672	0.000319	3.415281
100	0.006	2.512144	1.51E-03	2.966351	0.0011	3.061814	0.000276	3.454236	0.0017	2.92905	0.000501	3.290189

Table D.6 Probabilistic characteristics of probability of failure and reliability index of structures under combination corrosion, general corrosion and localized corrosion.

Year	Onshore splash zone				De-icing salts				Coastal zone d=50m			
	p_f	β	p_f^*	β^*	p_f	β	p_f^*	β^*	p_f	β	p_f^*	β^*
0	4.90E-06	4.42154	-	-	6.10E-06	4.373983	-	-	3.20E-06	4.512725	-	-
5	7.30E-06	4.334638	2.40E-06	4.573343	6.70E-06	4.353469	6E-07	4.855636	4.20E-06	4.454727	1E-06	4.753424
10	9.90E-06	4.267134	2.60E-06	4.556551	8.60E-06	4.298446	1.9E-06	4.62203	7.20E-06	4.337672	3E-06	4.526388
15	1.52E-05	4.170449	5.30E-06	4.404555	1.33E-05	4.200777	4.7E-06	4.430532	9.20E-06	4.283471	2E-06	4.611381
20	1.98E-05	4.109801	4.60E-06	4.435166	1.68E-05	4.147586	3.5E-06	4.493686	1.25E-05	4.2148	3.3E-06	4.506194
25	2.72E-05	4.035871	7.40E-06	4.33164	2.60E-05	4.046451	9.2E-06	4.283467	2.06E-05	4.100645	8.1E-06	4.311703
30	4.48E-05	3.917155	1.76E-05	4.136913	3.53E-05	3.974255	9.3E-06	4.28106	2.66E-05	4.041105	6E-06	4.377583
35	6.29E-05	3.834539	1.81E-05	4.130474	5.14E-05	3.883886	1.61E-05	4.157314	3.93E-05	3.948629	1.27E-05	4.21121
40	9.63E-05	3.72853	3.34E-05	3.98739	7.55E-05	3.789419	2.41E-05	4.064176	5.58E-05	3.86388	1.65E-05	4.151701
45	1.39E-04	3.634797	4.28E-05	3.928132	1.14E-04	3.686231	3.83E-05	3.954778	8.04E-05	3.773768	2.46E-05	4.059382
50	2.07E-04	3.530612	6.82E-05	3.814572	1.63E-04	3.594352	4.88E-05	3.896455	1.18E-04	3.676776	3.77E-05	3.95855
55	2.89E-04	3.441733	8.17E-05	3.769715	2.52E-04	3.478941	8.91E-05	3.74803	1.82E-04	3.565041	6.38E-05	3.831016
60	4.26E-04	3.335585	1.37E-04	3.639395	3.42E-04	3.396154	9E-05	3.745485	2.82E-04	3.447978	0.000101	3.71771
65	5.94E-04	3.241602	1.69E-04	3.58464	5.12E-04	3.283628	0.000171	3.581584	4.01E-04	3.351897	0.000119	3.674981
70	7.97E-04	3.157112	2.03E-04	3.536778	7.64E-04	3.169427	0.000251	3.47923	5.14E-04	3.282859	0.000113	3.689053
75	0.0012	3.035672	4.04E-04	3.350299	0.001	3.090232	0.000236	3.49562	8.32E-04	3.144625	0.000318	3.415895
80	0.0017	2.92905	5.01E-04	3.290189	0.0015	2.967738	0.000501	3.290245	0.0012	3.035672	0.000369	3.375203
85	0.0024	2.820158	7.01E-04	3.19416	0.0021	2.862736	0.000601	3.238452	0.0017	2.92905	0.000501	3.290189
90	0.0034	2.706483	1.00E-03	3.089519	0.0029	2.758879	0.000802	3.155294	0.0024	2.820158	0.000701	3.19416
95	0.0045	2.612054	1.10E-03	3.060794	0.004	2.65207	0.001103	3.060945	0.0033	2.716381	0.000902	3.120682
100	0.006	2.512144	1.51E-03	2.966351	0.0054	2.549104	0.001406	2.987657	0.0047	2.597153	0.001405	2.987872

Table D.7 Probabilistic characteristics of probability of failure and reliability index of structures under different exposure environments.

Year	X=3cm				X=5cm				X=7cm			
	p_f	β	p_f^*	β^*	p_f	β	p_f^*	β^*	p_f	β	p_f^*	β^*
0	3.20E-06	4.512725	-	-	4.90E-06	4.42154	-	-	3.90E-06	4.470601	-	-
5	7.00E-06	4.343861	3.8E-06	4.476152	7.30E-06	4.334638	2.40E-06	4.573343	5.20E-06	4.408685	1.3E-06	4.700126
10	1.08E-05	4.247675	3.8E-06	4.476152	9.90E-06	4.267134	2.60E-06	4.556551	6.70E-06	4.353469	1.5E-06	4.670819
15	2.63E-05	4.043763	1.55E-05	4.165991	1.52E-05	4.170449	5.30E-06	4.404555	9.20E-06	4.283471	2.5E-06	4.564786
20	4.14E-05	3.936148	1.51E-05	4.171947	1.98E-05	4.109801	4.60E-06	4.435166	1.43E-05	4.184337	5.1E-06	4.412888
25	6.51E-05	3.82608	2.37E-05	4.068081	2.72E-05	4.035871	7.40E-06	4.33164	1.91E-05	4.118105	4.8E-06	4.425989
30	1.37E-04	3.63947	7.15E-05	3.802905	4.48E-05	3.917155	1.76E-05	4.136913	2.38E-05	4.067109	4.7E-06	4.43053
35	2.35E-04	3.49741	9.83E-05	3.723311	6.29E-05	3.834539	1.81E-05	4.130474	3.40E-05	3.983177	1.02E-05	4.260462
40	3.89E-04	3.360363	0.000154	3.607911	9.63E-05	3.72853	3.34E-05	3.98739	4.44E-05	3.919318	1.04E-05	4.256118
45	6.57E-04	3.212904	0.000268	3.462185	1.39E-04	3.634797	4.28E-05	3.928132	6.15E-05	3.840068	1.71E-05	4.14352
50	0.0011	3.061814	0.000443	3.324245	2.07E-04	3.530612	6.82E-05	3.814572	8.19E-05	3.769157	2.04E-05	4.102888
55	0.0018	2.911238	0.000701	3.194333	2.89E-04	3.441733	8.17E-05	3.769715	1.22E-04	3.668896	3.99E-05	3.94498
60	0.0025	2.807034	0.000701	3.194131	4.26E-04	3.335585	1.37E-04	3.639395	1.61E-04	3.597088	3.91E-05	3.949821
65	0.0034	2.706483	0.000902	3.120652	5.94E-04	3.241602	1.69E-04	3.58464	2.34E-04	3.498775	7.28E-05	3.798417
70	0.0046	2.604531	0.001204	3.034645	7.97E-04	3.157112	2.03E-04	3.536778	3.03E-04	3.428825	6.94E-05	3.810239
75	0.0062	2.500552	0.001607	2.946417	0.0012	3.035672	4.04E-04	3.350299	4.34E-04	3.330019	0.000131	3.649962
80	0.008	2.408916	0.001811	2.909294	0.0017	2.92905	5.01E-04	3.290189	6.00E-04	3.23869	0.000166	3.588533
85	0.01	2.326348	0.002016	2.875627	0.0024	2.820158	7.01E-04	3.19416	7.77E-04	3.164556	0.000176	3.573225
90	0.0133	2.217338	0.003333	2.713052	0.0034	2.706483	1.00E-03	3.089519	0.0011	3.061814	0.000324	3.410978
95	0.0168	2.12484	0.003547	2.692382	0.0045	2.612054	1.10E-03	3.060794	0.0015	2.967738	0.0004	3.35249
100	0.0209	2.035506	0.00417	2.637981	0.006	2.512144	1.51E-03	2.966351	0.002	2.878162	0.000501	3.290104

Table D.8 Probabilistic characteristics of probability of failure and reliability index of structures with different concrete cover depth.

Year	w/c=0.7				w/c=0.6				w/c=0.5			
	p_f	β	p_f^*	β^*	p_f	β	p_f^*	β^*	p_f	β	p_f^*	β^*
0	2.08E-05	4.098409	-	-	4.90E-06	4.42154	-	-	1.40E-06	4.684971	-	-
5	3.16E-05	4.000533	1.08E-05	4.247671	7.30E-06	4.334638	2.40E-06	4.573343	1.80E-06	4.633232	4E-07	4.935367
10	5.67E-05	3.859972	2.51E-05	4.054686	9.90E-06	4.267134	2.60E-06	4.556551	2.20E-06	4.591534	4E-07	4.935367
15	1.79E-04	3.569253	0.000122	3.667834	1.52E-05	4.170449	5.30E-06	4.404555	2.60E-06	4.556553	4E-07	4.935367
20	2.02E-04	3.537457	2.3E-05	4.075031	1.98E-05	4.109801	4.60E-06	4.435166	3.60E-06	4.487689	2.20E-06	4.591534
25	4.00E-04	3.352864	0.000198	3.542815	2.72E-05	4.035871	7.40E-06	4.33164	4.40E-06	4.444736	8E-07	4.798322
30	7.74E-04	3.165419	0.000375	3.370948	4.48E-05	3.917155	1.76E-05	4.136913	5.40E-06	4.400503	1E-06	4.753423
35	1.40E-03	2.988882	0.000626	3.226676	6.29E-05	3.834539	1.81E-05	4.130474	6.50E-06	4.360105	1.1E-06	4.734126
40	2.50E-03	2.807034	0.001102	3.061395	9.63E-05	3.72853	3.34E-05	3.98739	9.50E-06	4.276329	2.00E-05	4.10748
45	0.0043	2.627559	0.001805	2.910456	1.39E-04	3.634797	4.28E-05	3.928132	1.27E-05	4.211216	3.2E-06	4.512723
50	0.0069	2.462428	0.002611	2.792982	2.07E-04	3.530612	6.82E-05	3.814572	1.57E-05	4.163068	3E-06	4.526387
55	0.0109	2.293835	0.004028	2.649731	2.89E-04	3.441733	8.17E-05	3.769715	2.50E-05	4.055627	9.3E-06	4.281063
60	0.0157	2.151966	0.004853	2.586138	4.26E-04	3.335585	1.37E-04	3.639395	3.09E-05	4.00583	5.9E-06	4.381245
65	0.022	2.014091	0.0064	2.489259	5.94E-04	3.241602	1.69E-04	3.58464	4.24E-05	3.930413	1.15E-05	4.233573
70	0.03	1.880794	0.00818	2.400786	7.97E-04	3.157112	2.03E-04	3.536778	5.36E-05	3.873689	1.12E-05	4.239509
75	0.0418	1.730169	0.012165	2.251879	0.0012	3.035672	4.04E-04	3.350299	7.12E-05	3.803962	1.76E-05	4.136907
80	0.0543	1.604518	0.013045	2.224861	0.0017	2.92905	5.01E-04	3.290189	9.85E-05	3.722833	2.73E-05	4.034993
85	0.0669	1.499284	0.013323	2.216651	0.0024	2.820158	7.01E-04	3.19416	1.36E-04	3.640603	3.75E-05	3.959816
90	0.0853	1.370278	0.019719	2.059583	0.0034	2.706483	1.00E-03	3.089519	1.63E-04	3.593712	2.7E-05	4.037572
95	0.1047	1.255217	0.021209	2.029393	0.0045	2.612054	1.10E-03	3.060794	2.28E-04	3.505238	6.51E-05	3.82604

Table D.9 Probabilistic characteristics of probability of failure and reliability index of structures with different water-cement ratio.